5-20-2005

A Comparative Analysis of the Subsurface Stratigraphic Framework to the Geomorphic Evolution of the Caillou Bay Headland, South-Central Louisiana

Elizabeth Mary Petro
University of New Orleans

A COMPARATIVE ANALYSIS OF THE SUBSURFACE STRATIGRAPHIC FRAMEWORK TO THE GEOMORPHIC EVOLUTION OF THE CAILLOU BAY HEADLAND, SOUTH-CENTRAL LOUISIANA

A Thesis

Submitted to the Graduate Faculty of the
University of New Orleans
in partial fulfillment of the
requirements for the degree of

Master of Science
in
The Department of Geology and Geophysics

by

Elizabeth M. Petro

B.A. LaSalle University, 2002

May, 2005

Table of Contents

List of Figures

Abstract

Studies have documented spatially and temporally variable rates of surface subsidence across the Mississippi River delta plain of Louisiana. Variations in patterns and rates of delta plain subsidence may reflect subsurface distribution of compaction-prone lithosomes.

This research investigates historical changes in the surface geomorphology of the Caillou Bay headland in relation to the distribution of subsurface lithosomes. The stratigraphic framework was developed for the headland, and lithosomes were identified to establish the distribution of different sedimentary units. The geomorphic evolution as indicated by maps was then evaluated in order to locate patterns of shoreline change and wetland loss for the headland. Land loss maps developed were overlain on lithosome contour maps to calculate amounts of land loss overlying each lithosome contour interval. Analysis of results revealed that land loss was not uniform throughout the headland and that land loss patterns for several time periods varied as a function of the thickness of compaction-prone lithosomes.

Chapter 1

Introduction

The modern Mississippi River delta plain of southern Louisiana has been built throughout the last 6,000 years by the deposition of sediments from the Mississippi River and its associated distributaries (Frazier, 1967). During this time the delta plain was deposited as multiple temporally and spatially distinct deltaic progradational events occurred. These progradations successively expanded the deltaic plain and the Holocene sedimentary package. As each delta lobe prograded, the river gradient decreased. Through time this would force the river distributary to avulse and relocate, occupying another channel with a higher basinward gradient. This delta switching cycle created four distinct deltaic complexes, each one consisting of multiple overlapping delta lobes (Penland et al., 1987) (Fig. 1.1). Each of the lobes within a deltaic complex consisted of a network of distributaries that were flanked by natural levees, interdistributary bays, crevasse splays, subdeltas, marsh platforms, and swamps. Progradation is the fundamental process contributing toward the formation of a deltaic headland; once abandoned these headlands became sites of transgressive reworking and are modified by marine processes such as tides and waves. Although some of the processes involved in headland formation and evolution are understood reasonably well (e.g. progradation and marine reworking) there are other contributing factors, such as compaction-driven subsidence, that remain poorly qualified. Previous researchers have suggested that some trends in land loss and change are the result of the distribution of these compactable lithosomes (Roberts et al., 1994).

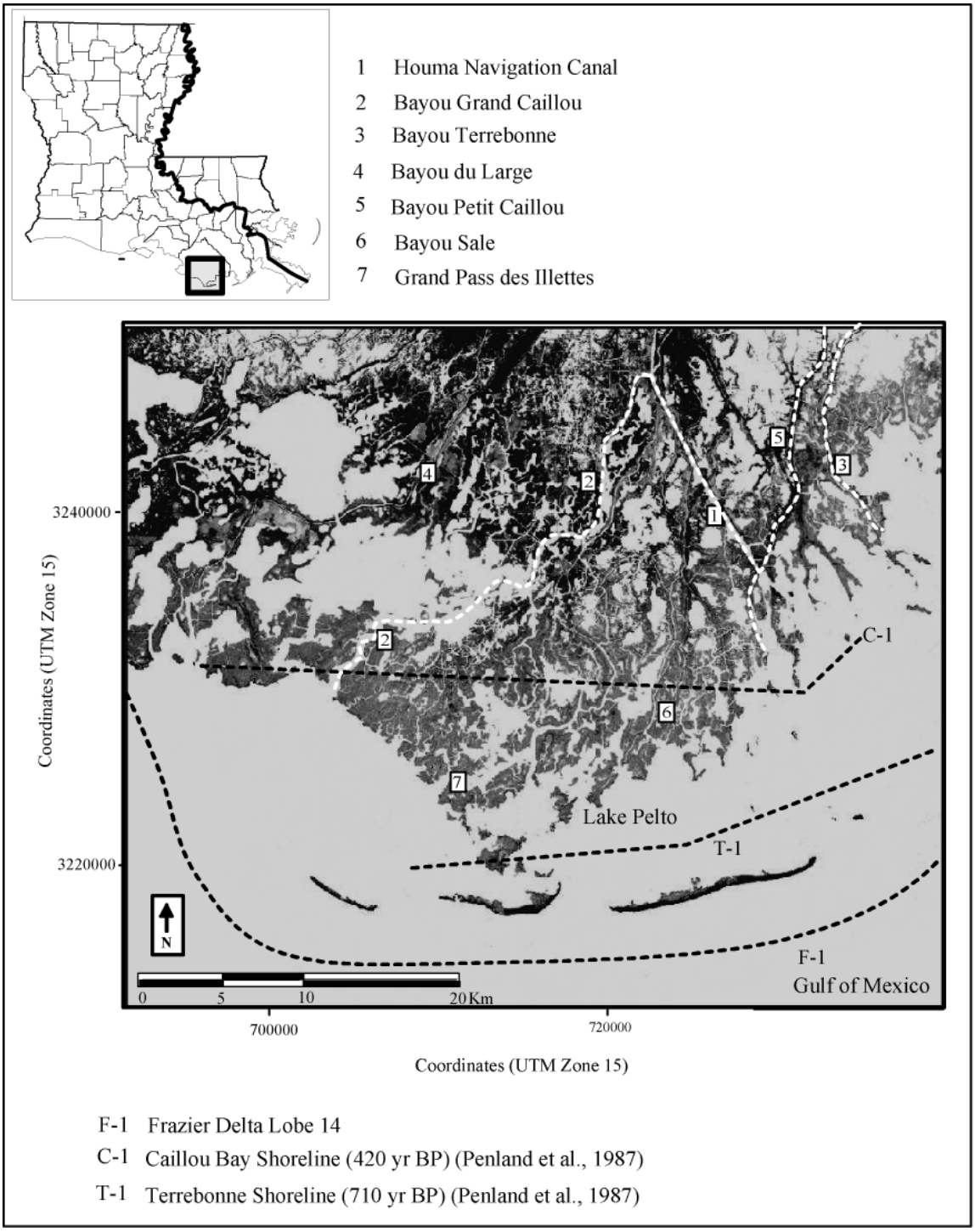

Figure 1.1 – Highlighted area on state map shows the study area for this project. The major ancestral Mississippi River distributaries are shown. Relict shorelines from Penland et al., 1987 and the extent of delta lobe 14 from Frazier, 1967.

The intent of this research is to investigate the role of shallow subsurface compaction in headland geomorphic evolution. The study area for this research is the Caillou Bay headland, located in south-central Louisiana (Figure 1.1). The main objectives of this research are to: 1) determine the patterns of erosion along the southern most extent of the Caillou Bay Headland and, 2) compare these patterns of geomorphic change to the distribution of shallow, subsurface sedimentary bodies.

Significance

The stratigraphic framework and distribution of lithosomes within deltaic headlands reflects variability in the distribution of deltaic subenvironments that are formed during progradation. Because lithosomes may exhibit variation in their sedimentology the expectation is that they will be susceptible to different rates of compaction during burial and dewatering. Conceptually, this implies that areas of the headland may subside at different rates, leading to different rates of relative sea-level rise, inundation, reworking, and the ultimate conversion of marsh platform to open water.

Applied Considerations

Coastal land loss across the delta plain is an issue of particular concern in southeastern Louisiana (Barras et al., 2003). This loss is a result of naturally occurring geologic processes, such as subsidence and sea-level rise, as well as substantial anthropogenic modifications, such as access canal and levee construction. Interior marsh platform loss and shoreline change are both recorded as land loss. Interior marsh platform loss is thought to be due primarily to subsidence and anthropogenic modifications, whereas shoreline change has primarily occurred as a function of sea level rise and subsidence (Roberts, 1994). Current estimates for land loss rates as high as 62

km^2 per year along some sections of the coastal zone have been presented (Barras et al., 2003). Rates of land loss have not remained temporally constant nor are they spatially uniform along the coast (Britsch and Dunbar, 1993). This variability has made determining patterns of erosion difficult. The goal of the work is to provide needed insight into the extent that differential compaction of lithosomes, with varying degrees of compaction potential, influence the geomorphic evolution of a delta headland. A thorough understanding of this has both theoretical and applied importance.

One important aspect of this research is to develop an understanding of the stratigraphic architecture underlying the Caillou Bay Headland. Developing the stratigraphic framework of the headland will aid in determining its transgressive history and evolution. Subsequently, this can help in predicting how coastal restoration projects may perform over time. Differential compaction is one of several variables that affect the evolution of the headland. The utility of establishing a better understanding between the subsurface geology and the surficial geomorphology is that an understanding of the overall transgressive development of the headland will be developed. This will then aid in the development of models that predict future coastal land lost in terms of the nature, rate, and location of headland retreat.

Theoretical Considerations

Determining the distribution of these facies is significant in discerning the influence of delta lithosome distribution on subsequent deltaic sedimentation. For example, Fisk (1955) suggested that variability in thickness, extent, and stratigraphy of deltaic depocenters is influenced by water depths in which deltaic progradation takes place. Limited water depths, or accommodation space, contribute toward the

development of thin, laterally extensive deltaic depocenters. Alternatively, more substantial accommodation space will result in a more laterally restricted but potentially overall thicker depocenter. Because of the overlapping nature of deltaic lobes stratigraphically higher deltaic deposits may have been influenced by the topography of underlying depocenters. Topography of the subjacent depocenter partially develops in response to compaction, which is in turn influenced by the composition of the stratigraphy within the underlying deposit. Consequently, specific knowledge of the processes that control the generation of accommodation space can assist in determining the likely location of subsequent delta depocenters. Developing a detailed picture of the shallow stratigraphy of a deltaic headland may provide insight as to how complex reservoir systems form in response to differential rates of compaction.

Study Focus and Goals

This study investigates the question of whether variable compaction of different sedimentary bodies within the Caillou Bay Headland has influenced the post-progradational evolution of the headland.

Two primary datasets, a subsurface framework geology evaluation and an evaluation of the geomorphic evolution of the headland will be assembled. The first dataset consists of previously acquired cores within a large database of archived core data at UNO, as well as cores that were collected specifically for this study. Collectively, these cores will be used to create cross sections for a variety of locations on the headland and aid in the identification of primary lithosomes. Lithosomes are identified as sedimentary units of uniform character that are bounded by units of distinctly different

character. These characteristics include grain size and distribution, sediment color, and the style of bedding. The intent is to identify the various sedimentary types in order to determine the distribution of compactable lithosomes. These sedimentary units will be used to develop isopach maps depicting unit thickness.

The second dataset is a collection of maps for the time period 1863 to present. The utility of these maps is that they provide a historical record of the headland size and geomorphology; comparison of these maps to one another allows for an evaluation of the geomorphic evolution of the Caillou Bay headland and documentation of the distribution and rate of headland evolution within the historic record that is available. The results constitute a primary component of this research and the ability to identify areas of significant land loss in the study area. The intent is to use these two datasets in conjunction with one another and evaluate whether any correlation exists between the subsurface sediment distributions, as indicated by the core dataset, and the historical geomorphologic evolution that is provided by the comparison of the historic maps.

Chapter 2

Background

This study of the Caillou Bay headland focuses on defining the relationship between the stratigraphic framework and the historical (1895 to 2002) geomorphic evolution. The two main components of the research consist of developing a stratigraphic framework of the headland and compiling a quantitative evaluation of land loss through time across the entirety of the headland.

Study Area

The Caillou Bay headland is located in south-central Louisiana, approximately 75 km south of Houma, Louisiana (Figure 1.1). The study area is bounded along the north by the northern shore of Caillou Lake, in the south by the Isle Dernieres, on the west by the mouth of Oyster Bayou, and along the east by the eastern edge of Timbalier Island. A generally north-to-south network of active and semi-active bayous trend across the study area. Several of these are thought to have been active for at least the last 3,000 yrs BP (Penland et al., 1988), although more recently carrying substantially less flow than at previous times.

Late Holocene Mississippi River Delta Plain Development

The late Holocene Mississippi River delta plain developed during the current sea level high-stand, approximately 6,000 years B.P. (Fisk, 1944; Frazier, 1967; Penland et al., 1988). The delta plain consists of five major delta complexes composed of multiple delta lobes that represent the depocenters of temporally and spatially separate progradational episodes driven by avulsion and delta switching events of the Mississippi

River. The five distinct delta complexes, in order of decreasing age are: Maringouin – Teche, St. Bernard, Lafourche, Plaquemines-Balize, and Atchafalaya complexes (Frazier, 1967).

Caillou Bay Headland Development

The Caillou Bay headland is the third lobe of the Lafourche delta complex and was active between approximately 910 to 420 years B.P. (Penland et al., 1987). The headland was built by deposition from four primary distributaries: Bayou Grand Caillou, Bayou Chauvin, Four Point Bayou, and Bayou Sale (Penland et al., 1987). In general, a deltaic headland consists of a complex assemblage of facies constructed during progradation (Frazier, 1967) (Figure 1.2). Several factors influence deltaic progradation. The sediment load of the river, rates and patterns of subsidence, and sea-level change influence the overall thickness and lateral extent of facies within the headland. Transgressive reworking due to sea level rise and subsidence can alter the sediment distribution post deposition.

Deltaic Cycle

In general the Caillou Bay headland developed within the conceptual framework known as the delta cycle. The delta cycle describes the progradation and subsequent reworking of a deltaic headland that becomes abandoned and starved of river supplied sediment. Delta lobe progradation begins with the entrainment of a distributary system between levees built through time during episodes of river flooding. Progradation proceeds as deltaic facies accumulate on the shelf. Thick units of prodelta silts and clays, at the distal edge of the progradational site, accumulate and compact where the finer grained sediments are present. As compaction decreases, sediment begins to accrete

vertically. A complex network of bayous, natural levees, swamps, and marsh develop through time. Sediment continues to accrete and the vertical gradient decreases. When the gradient decreases sufficiently the river avulses and changes geographic position to where the gradient is steeper, resulting in the initiation of a new delta cycle (Fisk, 1944; Kolb and Van Lopik, 1958, Coleman and Gagliano, 1964). During the Holocene repeated occurrence of these processes has resulted in the formation of the modern Mississippi River delta plain.

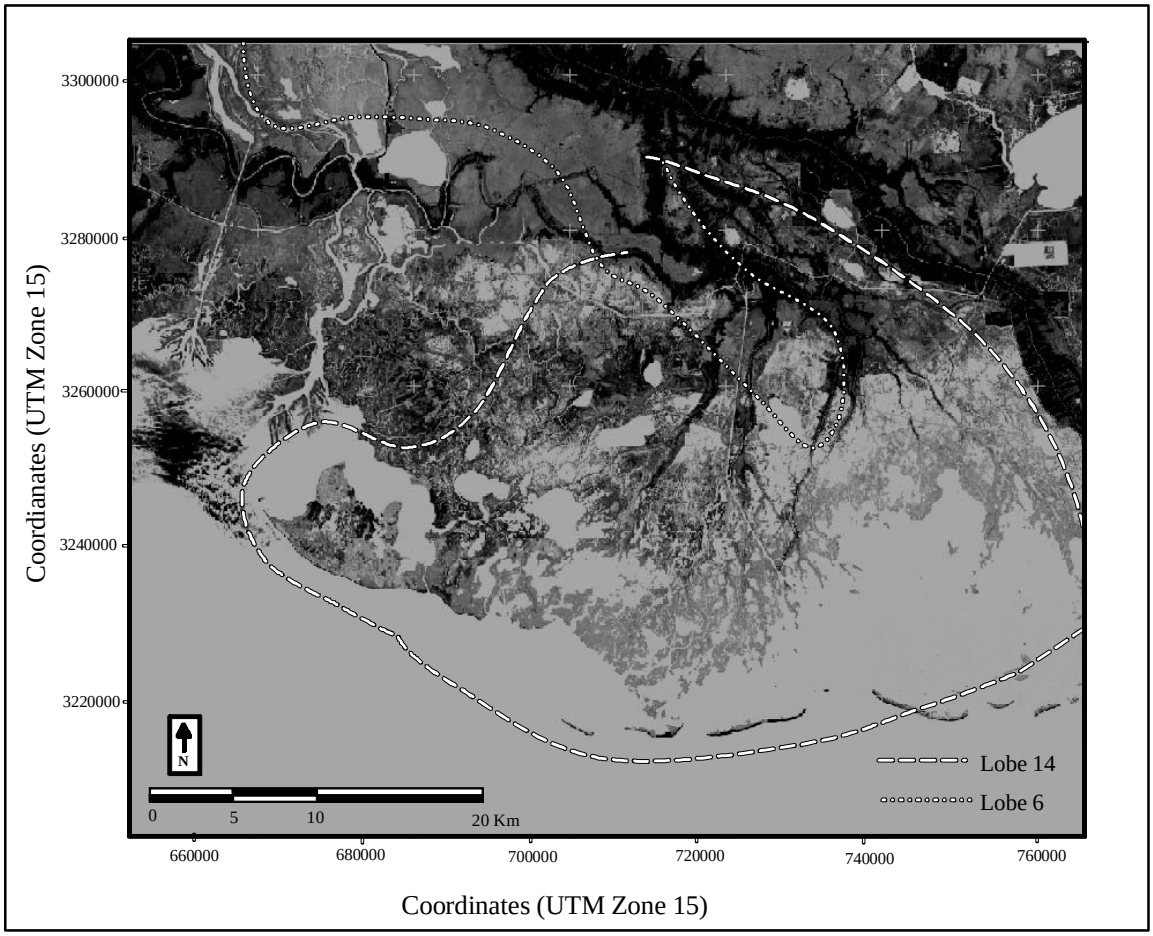

Figure 1.2 – Satellite image (2002) with Frazier's Lafourche delta lobes plotted to show the extent of deposition associated with the progradation of the deltas. Most of the project area is within the area covered by lobe 14, thought to have been deposited between 900-100 B.P. (Frazier, 1967).

Deltaic Depositional Environments

The action of the deltaic cycle has resulted in the construction of the modern Mississippi River delta plain. A cycle is composed of several sedimentary units: prodelta silts and clays, shelf shell and clay beds, delta front silts and clays, interdistributary bay clays and silty clays, natural levee silty clays and sands, and swampy organic clays and peats (Coleman and Gagliano, 1964).

Various researchers have identified and described prodelta deposits. They have been described as silty clays similar to those found within a deltaic-plain complex and form thick, widespread units around the front of the deltaic-plain facies (Fisk and McFarlan, 1955). They have also been described as thick silty clays with burrowed and nonburrowed zones containing rhythmic laminations of silt and clay and colors (Coleman and Gagliano, 1964), and as homogenous fat clay sequence from fine to coarse (Kolb and Van Lopik, 1958).

Interdistributary deposits have been identified and described as bay clays and silty clays with storm debris inclusions, shell fragments, burrows, and plant remains (Coleman and Gagliano, 1964). They have also been described as mostly inorganic fat clays and silt (Kolb and Van Lopik, 1958).

Natural levee deposits are identified and described as silts and clays (Fisk and McFarlan, 1955). They have also been described as fat clay and silt accumulations oxidized to a tan or reddish (Kolb and Van Lopik, 1958), and as silty clays (Coleman and Gagliano, 1964).

Marsh deposits are identified and described as both organic and nonorganic. The organic component has been described as containing high organic content with roots and wood fragments (Fisk and McFarlan, 1955), as highly organic clays and peats (Coleman and Gagliano, 1964), and as brown to black fibrous or felty masses of partly decomposed remains of plant material and organic float material from hurricane deposits (Kolb and Van Lopik, 1958). The inorganic component of the marsh deposit has been described as largely silty clays (Fisk and McFarlan, 1955), and as clays silts and fine sands (Kolb and Van Lopik, 1958).

Mississippi River Delta Plain Barrier Island Formation

Barrier island formation within the Mississippi River delta plain initiates with distributary abandonment and subsequent reworking of the abandoned headland by marine processes. The model for barrier island formation is a three-step process; (1) the erosion of the headland and the formation of flanking barriers, (2) the development of a transgressive barrier island arc, (3) and the formation of an inner-shelf shoal (Penland et al., 1988).

In the first stage, marine processes begin to rework the abandoned deltaic headland. Main distributary deposition ceases so there is limited sediment to fill in the accommodation space created by the subsiding headland. At this stage the transgressive headland consists of several components; an erosional headland, a beach, flanking spits and barrier islands, tidal inlets and deltas, restricted interdistributary bays, and a transgressive sand sheet (Penland et al., 1988). Longshore currents and tides transport sand that augments the flanking barrier islands. Sediment on the seaward fringe of the headland is reworked and winnowed to form a beach. There is also the formation of

restricted interdistributary bays in response to the initial rapid subsidence (Penland et al., 1988). Tidal inlets and associated tidal delta deposits form as barrier breaching occurs. Increasing bay-area causes an increasing number of tidal prisms to form inlets which allow these bays to remain open (Penland et al., 1988).

The second stage of the process consists of continued transgressive reworking of the erosional headland, and mainland detachment forming a barrier island arc, tidal inlets, lagoons, and an inner-shelf sand sheet (Penland et al., 1988). The erosional headland and flanking barrier islands constructed during stage one detach and form a transgressive barrier island arc. Storm events cut through the islands forming tidal inlets. The restricted interdistributary bay area opens up with the detachment of the barrier islands and tidal exchange with the gulf becomes a dominant process. Sand eroding away from the shoreline and the barrier islands is deposited on the shoreface to form transgressive inner shelf sand sheet (Penland et al., 1988).

The third and final stage of the process consists of the development of inner shelf shoals. As a result of RSL and marine reworking the barrier island is inundated. The components comprising this stage include shoal crest, shoal front, shoal base, sand sheet, and maximum shoreline (Penland et al., 1988). The shoal crest, front, and base are all reworked remnants of the barrier island arc. Reworking and landward migration of the shoal continues after submergence (Penland et al., 1988).

Raccoon Island, Whiskey Island, and Trinity Island of the Isles Dernieres island arc (stage 2) of Penland et al., (1988) are the primary barrier islands located in the study area (Figure 1.11).

Delta Plain Subsidence

The Mississippi River delta plain is actively subsiding as a result of numerous contributing mechanisms (e.g. compaction, faulting, regional isostatic adjustment) (Figure 1.3) (Roberts et al., 1993; Kulp et al., 2002). Subsidence rates have been previously determined using age-depth relationships of radiocarbon-dated peat deposits located in the subsurface of the study area. These data yield subsidence rates that range between approximately 33.4cm/100 yr to 39.6 cm/100 yrs (Roberts et al., 1994). Roberts et al. (1994) also noted that subsidence patterns closely follow the distribution of Holocene deposit thickness; the highest subsidence rates are located above the thickest Holocene strata because of greater compaction potential in the thick, highly compactable sediments of the Holocene interval.

Compaction Studies

In this study, the compaction of sediment is considered to be the most significant component of marsh-platform subsidence in the study area (Figure 1.3).

The most widely accepted theory of one-dimensional consolidation was developed by Terzaghi (1943). Terzaghi recognized that when sediments are compressed, water is released and pore space diminishes (Clayton et al., 1995). Under natural conditions compaction occurs because of sediment dewatering that occurs as strata are buried by overlying sediment.

Compaction can be simply defined as a "change in sediment dimensions during burial (Giles et al., 1998). Initial compaction is the result of sediment loading, which leads to a vertical reduction in sediment volume (Giles et al., 1998). Thus as sediment accumulates and becomes buried, water flows out of the sediment, pore space is reduced, and the sediment compacts. Sediment size and distribution has been related to

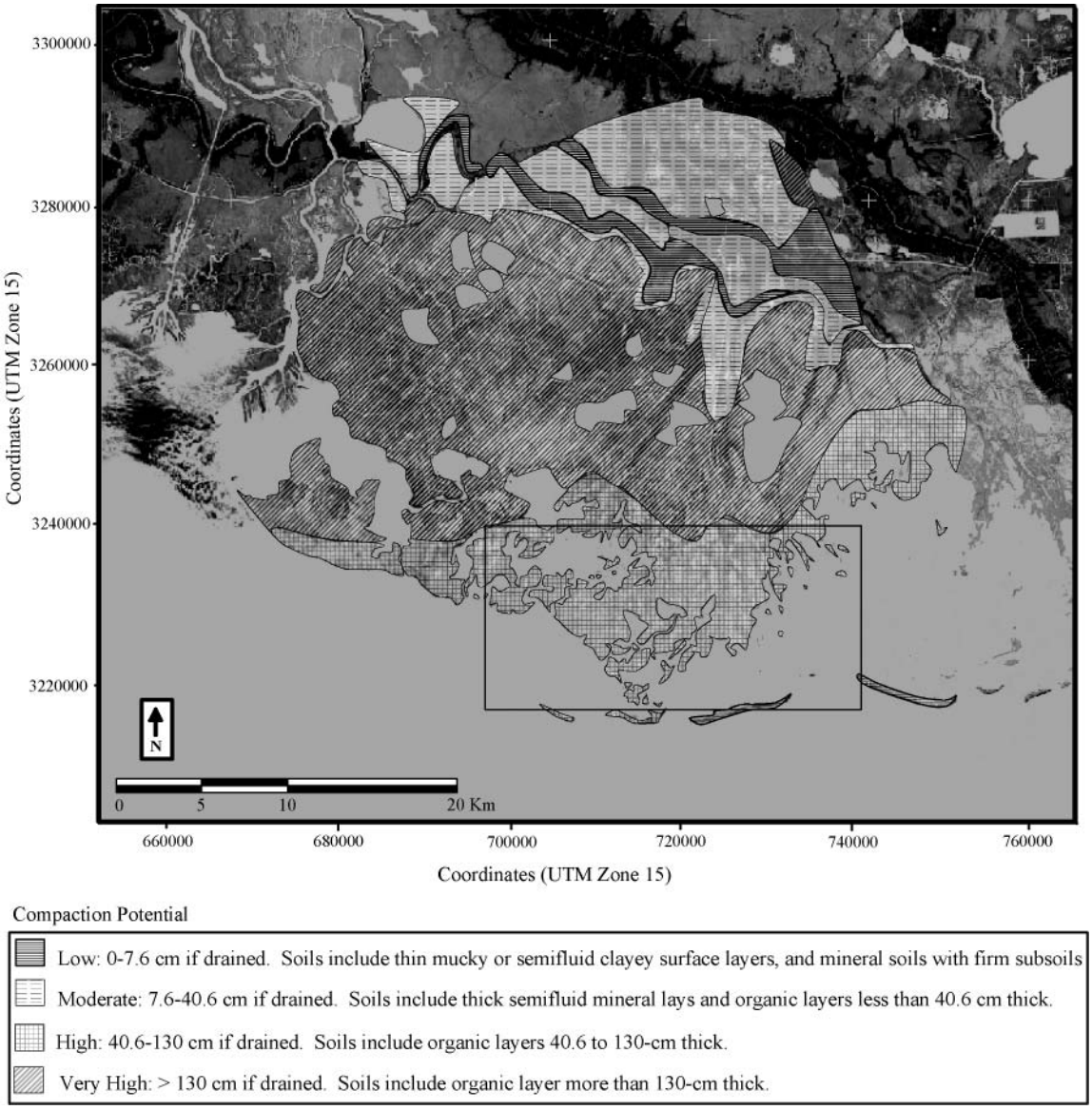

Figure 1.3 - Soil subsidence potential map showing the distribution of subsidence likelihood across a portion of the south-central coastal zone (adapted from Louisiana State Planning Office, 1976). The box outlines the study area of this project. Note: the soils of the study area are mapped as high compaction potential if drained, soils in this area consist of more than 130-cm thick organic material.

compaction. Coarser grained sediments such as sand have been observed to be more resistant to compaction than finer grained sediments such as clay (Holbrook, 2002).

The compaction rate of sediments is highly variable, so previously determined rates in the study area were used for comparison in this study. Keucher (1994)

determined compaction indices for various deltaic facies in the Terrebonne region. Keucher (1994) found that the most compactable facies were finer-grained, such as peats and clays; he found that the least compactable facies were coarse-grained such as silt.

Land Loss in the Caillou Bay Headland Area

Land Loss on the Mississippi River delta plain is a topic of particular concern to those living and working in Southeastern Louisiana. Current estimates place land loss in some areas as high as 62 km^2 per year (Barras et al., 2003). This land loss has both natural and anthropogenic origins. The natural causes include subsidence, herbivory, and storm and wave action (Kindinger et al., 2002). Anthropogenic causes include direct removal of land for the purpose of channel and pond construction, borrow pits, and altered hydrology (Kindinger et al., 2002)

A significant amount of research has evaluated land loss on the Mississippi River delta plain (Barras et al., 2003; Britsch and Dunbar, 1993; Gagliano et al., 1981). In a recent study (Barras et al., 2003) several land loss trends were noted. From 1956-1978 large areas of marsh have converted to open water, and from 1978-1990 this trend continued at a less rapid rate (Barras et al., 2003). During the last decade, however, the primary mode of land loss has been the formation of small ponds in the interior marsh and shoreline erosion. In the Terrebonne region, where this study was conducted, significant erosion continues for the 1990–2000 interval. Most of the recent loss is occurring in areas that have already undergone the most significant land loss (Barras et al., 2003). Shoreline erosion and interior marsh pond formation are the most significant impact on the area, but there is also erosion of the fringe marsh platform (Barras et al.,

2004). Observed land gain can possibly be attributed to the movement of detached, or floating marshes (Barras et al., 2003).

Chapter 3

Methods

Stratigraphic Framework

A primary objective of this investigation is to establish the fundamental stratigraphic framework of the Caillou Bay Headland. The goal is to identify and map the primary subsurface lithofacies. The UNO Coastal Research Laboratory (UNO CRL) core database and a United States Army Corp of Engineers (USACE) database were searched to determine whether any cores had been previously obtained within the study area. For each core the database contains a physical description sheet, and in many instances grain size analysis data and core photography. A total of ten cores from the UNO database and thirteen cores from the USACE database were identified as having potential value to the project. The cores were loaded into a GIS platform and plotted to visualize the distribution of the cores.

The distribution of the preexisting cores was used to develop a strategy for obtaining new cores, thereby avoiding redundancy, obtaining data where cores were missing and increasing the overall number of cores available for a stratigraphic analysis of the headland. For this purpose a team of field geologists, as part of a larger project on delta plain subsidence collected a total of 26 cores within the study area (Figure 1.4). Core locations were located by plotting target sites on a base map of the area. Slight adjustments, generally less than 25 m offset, to the locations of cores were made in the field when obstacles such as oil and gas pipelines, and private property, or other obstructions were encountered.

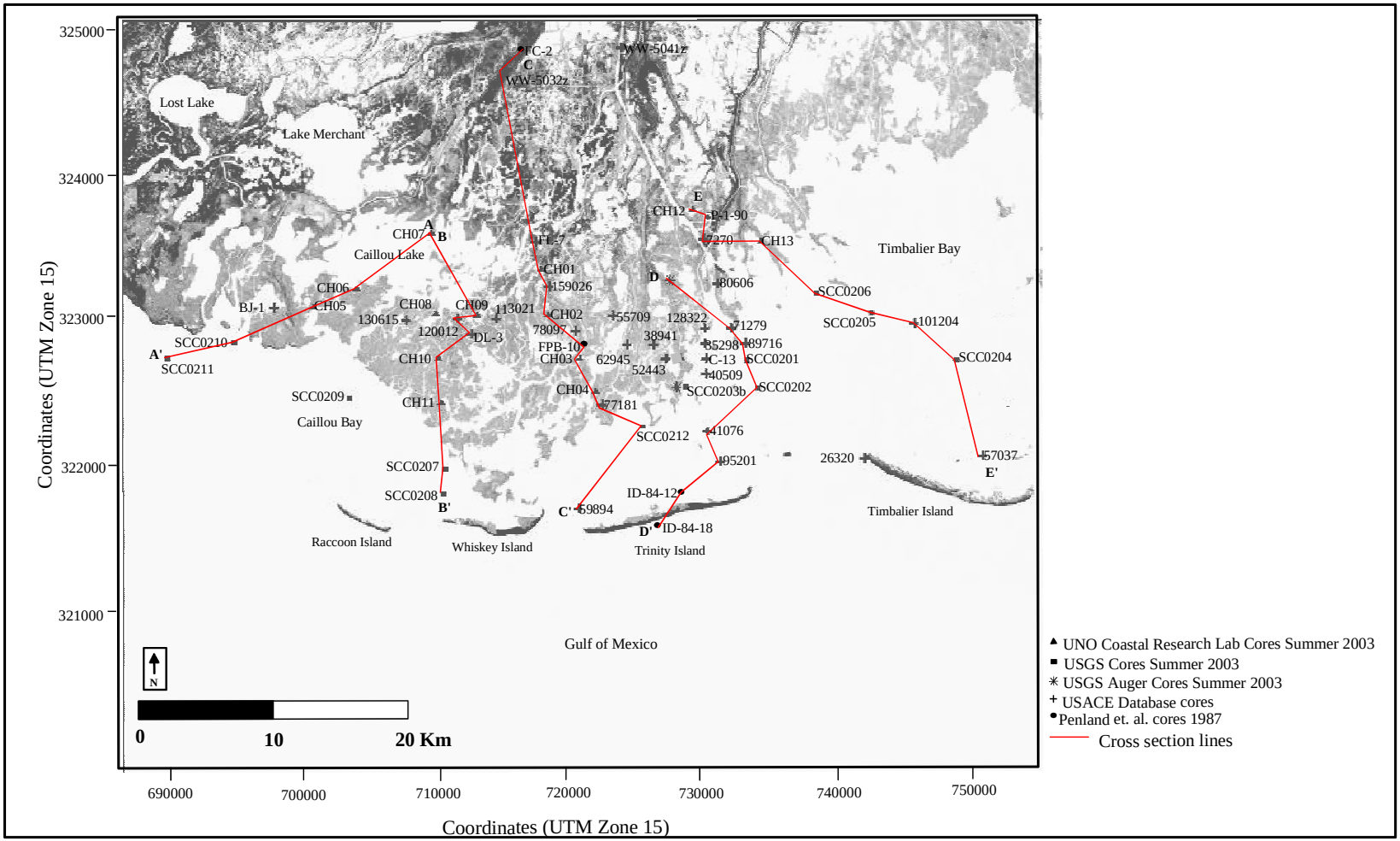

Figure 1.4 – Basemap showing the locations of cores and cross sections used in this study to characterize the framework stratigraphy of the Caillou Bay headland.

Two distinctly different vibracoring rigs were used to obtain the cores during the 2003 summer field season. A field team on the UNO *R/V Greenhead* acquired 13 cores located in areas where the water was less than 1.5 m deep. In locations where the water depth exceeded 1.5 m the USGS *R/V Gilbert* was used as a vibracoring platform, resulting in the acquisition of an additional 13 cores. Vibracore sites were reached using the geographic coordinates acquired from the core database and recorded in a logbook.

R/V Greenhead Vibracore Platform

The vibracoring system used by the UNO CRL consists of a tripod mounted to a flat bottom boat. The tripod is positioned over a moon pool in the hull of the *R/V Greenhead*, which allows for access to the water below. A 9-meter long aluminum tube with an approximately 7.5 cm diameter is inserted vertically into the center of the tripod. A weighted vibracore head is attached to the aluminum pipe and tightened in place. A cable to a gas-powered combustion engine that powers the system is connected to the head. The motor speed is adjusted until a vibration frequency is attained that liquefies the underlying sediments and allows the aluminum tubing to penetrate into the subsurface. The vibration frequency must be adjusted when the tubing encounters strata that are compositionally different or have undergone different degrees of compaction. Vibracoring continues until a depth is reached at which further penetration cannot be made, even when additional pressure is applied and when the frequency of vibration is altered by varying the engine speed. Penetration can be interrupted when coarser units such as sand or shell lag are encountered. Care was used when additional pressure was applied to avoid compaction of the sediment as a product of the vibracoring process.

A metric tape measure was used to record water depth at the site and the depth to the top of the sediment water interface inside the penetrated core. This information was used later to calculate the magnitude of sediment column compaction that occurred during the vibracoring process. This value is important when constructing cross sections to accurately determine the original thickness of sediment units. It is crucial to determine if the core extracted replicates the strata, or if excess compaction must be accounted for. After these measurements have been made any excess tubing is cut off and properly discarded. In order to extract the core intact and within the tubing, water is poured into the top of the core barrel and a plug is inserted and tightened in the top of the tubing to create a vacuum within the tube above the sediment section retained within the core barrel. A hook attached to a steel cable is fastened to the barrel and a hand winch is used to extract from the ground the aluminum tube containing the core. After the core barrel has been removed from the subsurface, the top and bottom of the core is sealed with a plastic cap and taped at both ends to hold the sediment sample in place within the core. The total core length is then measured, the core is labeled, and the top and bottom of the core is clearly marked before being transported back to a laboratory for analysis.

R/V Gilbert Vibracoring Platform

The USGS vibracoring system operates off the *R/V Gilbert* and is capable of obtaining cores in as much as 37 meters of water depth. A Global Positioning System (GPS) was used to position the rig at the preselected core sites and the core locations were recorded in a logbook. The *R/V Gilbert* vibracoring system consists of a reciprocating head that is mounted to a platform. The platform slides down a 22-ft

stationary aluminum mast attached to a 400-lb rectangular frame. Two electric compressors drive a 6-meter long aluminum tube with an approximately 7.5 cm diameter into the subsurface. A check-ball valve is located on the vibracore head and is attached to the top of the core to act as a vacuum seal. This is combined with a core catcher consisting of collapsible brass at the base of the core. This helps to retain the sediment in the core when it is extracted from the seabed. The core is extracted using an electric winch that pulls a braided wire cable attached to the vibracore head. Similar to the procedure used on the *R/V Greenhead,* the core was sealed with a plastic cap and tape at both ends. The core was then measured, labeled, and the top and bottom of the core clearly marked before being transported back to a UNO laboratory for analysis.

Core Preparation

Cores acquired in the field were then brought back to the UNO-Chevron Earth Science laboratory and prepared for visual description, sampling, and photography. In the laboratory the cores were marked in two-meter increments along the length and cut into more manageable sections at these marks. The exposed ends where then resealed with a plastic cap and tape. A circular saw was used to make two opposing cuts vertically along the length of the cores. A thin wire was then run down the center of the cores along these length-wise cuts and the cores were split into two even halves. The half with the least amount of wire marks was designated the archival half of the core, whereas the other half was designated the work half. The work half was set aside for grain size sampling and the collection of material, such as peat and shells that could be radiocarbon dated. To obtain a fresh and even surface on the archival half an osmotic knife was used

to remove the top layer of sediment that may have been smeared by the wire. Core halves that had been smoothed were then visually described.

Core Description Technique

A visual description was completed on each core (individual description sheets are included in Appendix A). Standard templates designed by Coastal Research Laboratory (CRL) researchers were used to record the data. The cores were described from top to bottom. The approach employed in this study was to first make note of major sedimentary units by looking for changes in lithology, erosional surfaces, significant change in sediment color, or changes in sedimentary structures. These individual units were then described in detail to provide an in depth description of the core.

The approach was to first determine the textural classification of the sediments. For this the Udden-Wentworth scale was relied upon. The classifications used for the cores described were clay (<1/256 mm), silt (1/256 to 1/16 mm), fine sand (1/8 to 1/4 mm), medium sand (1/4 to 1/2 mm), and coarse sand (1 to 2 mm) (Wentworth, 1922). Percent sand was then identified, from zero to one hundred percent. Additional physical characteristics that were described for each previously determined sedimentary interval were color, style of bedding, bed thickness, percent shell material, percent organic material, and percent bioturbation. Stratification types that were noted included wavy, flaser, lenticular, massive bed, inclined, and horizontally laminated. A detailed physical description sheet was completed and the information entered into the CRL core database.

Photography

Upon completion of the core description, photographs were taken of each core. These pictures are archived at UNO within the CRL core database. For the first set of photographs, the two-meter increments of each core were photographed in 40-cm increments. A cardboard template with a scale and project title was created and placed over each increment. These detailed photographs are helpful when cross checking the core description sheets after the original cores have aged and desiccated. The two-meter core sections were then cut into one-meter sections and placed on a rack with a scale in order to obtain a whole-core photograph.

Radiocarbon Dating

Four peat samples and two whole *Rangia cuneata* shell specimens were sent to the University of Arizona (UA) Isotope Geochemistry Laboratory for radiocarbon dating to aid with stratigraphic analysis. Before the samples were sent to UA they were prepared by drying them in an oven at 30° C for 36 hours as requested by the UA laboratory. The peats and whole shells were then weighed and this information was recorded on a data sheet that was additionally submitted with each sample that was sent to UA.

Peat samples were chosen from cores with thick continuous peat deposits that contained negligible amounts of clastic material so enough organic material would be present in the sample to accurately date. Whole articulated shells were chosen because

they are not likely to be reworked and thus are assumed *in situ*. The samples were wrapped in aluminum foil as specified by the UA laboratory, labeled, and each placed in individual sealed bags with their corresponding data sheet. They were then shipped to UA for analysis.

Each sample was dated using the liquid scintillation counting technique. This process included stable carbon isotopic analysis and calibration. The calibration process corrects for fluctuations in the amount of radiocarbon present in the atmosphere throughout time (Stuiver et al., 1998). UA's calibration curve is based on the known age of tree rings, corals (independently dated by U-Th) and annually laminated sediments (Stuiver et al., 1998).

Results

Stratigraphic Framework

A total of 26 new vibracores (Appendix A) were described and incorporated into the UNO core database. From these cores a total of five stratigraphic cross-sections were constructed across the Caillou Bay headland to aid in depicting the subsurface geology (Figure 1.1). The cross sections are constrained by sea level at the top and the Teche Ravinement surface at the base of the section as defined by Penland et al., (1987).

The sedimentary units identified in the cores were peat, clay, silty clay, sandy clay, clayey sand, and sand. Peat units were defined when the organic content of the unit was greater than 50% organic material, and clays and silty clays were sometimes interbedded with the organic material. Clay units were defined when the unit was composed of clay.

Stratigraphic cross section A-A'

Stratigraphic cross section A-A' trends from the North East to the South West from Moncleuse Bay to South of Oyster Bayou (Figure 1.5). A peat unit tapers from 1.0 meter in thickness at Moncleuse Bay to 0.50 m thick at the southern portion of Caillou Lake and pinches out over Bayou Grand Caillou. The peat unit contains numerous roots throughout and has shell fragments near Moncleuse Bay. The peat overlies a clay unit 2.0 m thick that tapers to 1.25 m at the southern portion of Caillou Lake and pinches out. The clay unit shows horizontal lamination and some organic fragments where it pinches out. The clay overlies a sandy clay unit that is a 1.0 m thick at Moncleuse Bay and thickens to 3.0 m where it ends at the southern portion of Caillou Lake. A 4.0-m thick silty clay unit begins where the clay and sandy clay units end laterally. The silty clay unit thins to 1.0 m at Caillou Bay and is overlain by a 0.25 m thick silt unit. The silty clay then thickens to 2.0 m south of Oyster Bayou. The silty clay unit has shell fragments throughout, and burrow tubes where it is overlain by the silt unit. The silty clay overlies a clay unit that is 25 cm thick at Bayou Grand Caillou and thickens to 2.0 m south of Oyster Bayou. The clay unit has shell and organic fragments throughout. Three samples were obtained from the cores in the cross section for radiocarbon dating, two peat samples and one articulated shell.

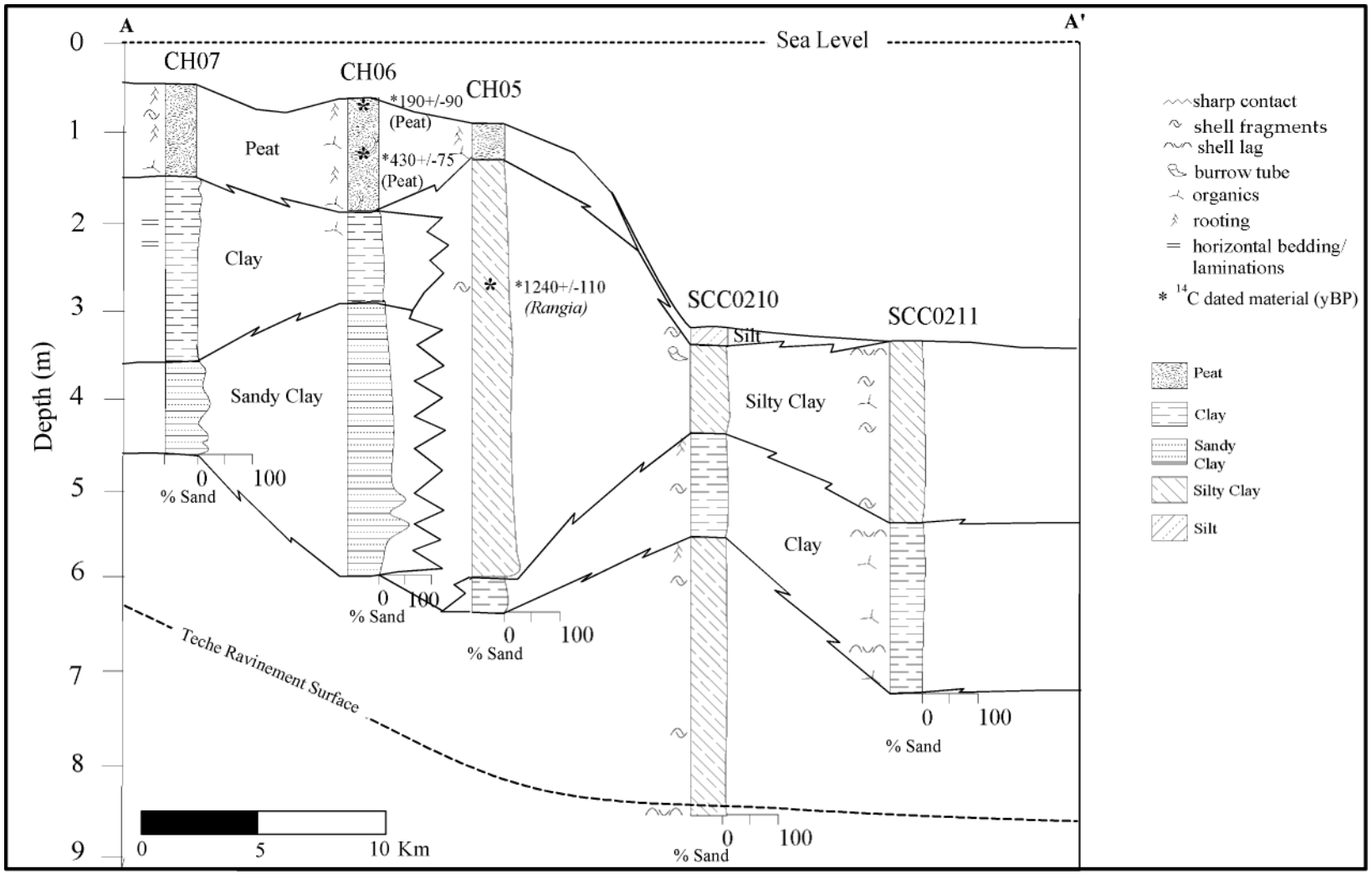

Figure 1.5 – Stratigraphic cross section through the study area to show the lateral and vertical relationships of primary lithosomes discussed in the text.

Stratigraphic cross section B-B'

Stratigraphic cross section B-B' trends from the North to the South from Moncleuse Bay to South West of Bay Wilson (Figure 1.6). A 1.0 m thick peat unit stretches from Moncleuse Bay to Grand Pass Ilettes. The peat thickens to 2.0 m at Hackberry Lake then thins again until it pinches out at the seaward extent of the headland. The peat overlies a clay unit approximately 2.0-m thick that extends across the entire section. The peat has rooting throughout and some shell fragments at the northern end of the section. The clay thickens to 4.5 m west of Bay Wilson and is overlain by a 50 cm thick silt deposit. It then thins to 2.0 m and is overlain by a clayey sand lens. The clay is horizontally laminated and there are numerous shell fragments and burrow tubes west and southwest of Bay Wilson. The clay overlies a sandy clay unit that thickens from 1.0 m to 2.0 m at Hackberry Lake and thickens again to 3.0 m southwest of Bay Wilson. The sandy clay is horizontally laminated throughout and there are numerous shell fragments west and southwest of Bay Wilson.

Stratigraphic cross section C-C'

Stratigraphic cross section C-C' trends from the north to south from Dulac, LA to Whiskey Pass (Figure 1.7). A 1.0 m thick peat unit extends the entire length of the section. The peat unit has abundant rooting. The peat overlies a 2.0-meter thick clay unit that extends to Charleys Lake where it ends. The there are infrequent organic fragments and some rooting. The clay overlies a 1.0 m thick sandy clay unit that gradually increases to 2.0 m then tapers to 1.0 m where it ends at Charleys Lake. There are few shell and organic fragments present. A 1.0 m thick silty clay unit underlies the sandy

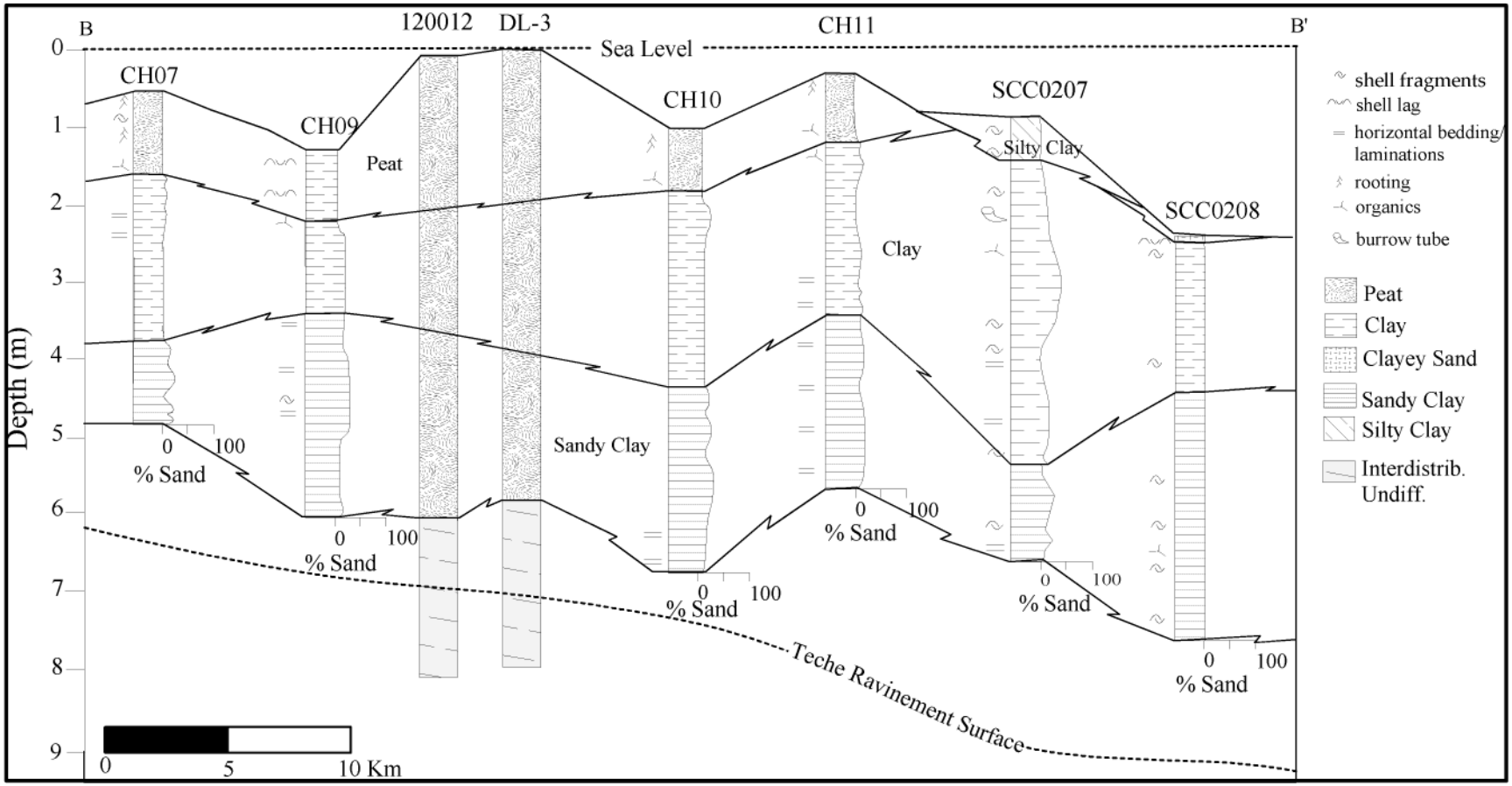

Figure 1.6 – Stratigraphic cross section consisting of cores from the USACE and summer 2003 fieldwork conducted for this study. The Teche Ravinement surface was projected onto cross section from Penland et al., 1987.

clay at core sites FC-2 and ww-5032z. The sandy and silty clay overlies a clay unit that is 4.0 m thick and gradually tapers to approximately 3.0 m southwest of Charleys Lake and abruptly ends. The clay is horizontally laminated and a few shell fragments are present in the unit. There are three 25 cm sand lenses in the clay unit, one at core site FC-2, one at FPB-10, and one at CH03. South of Charleys Lake a silty clay unit underlies the peat unit. The silty clay unit starts at 3.0 m thick and gradually increases to 6.0 m at Whiskey Pass. The unit is horizontally laminated and has sparse shell fragments. Three samples were obtained from the cores in the cross section for radiocarbon dating, two peat samples and one articulated shell (Table 1.2).

Stratigraphic cross section D-D'

Stratigraphic cross section D-D' trends from the north to south from Bay Sale to Trinity Island (Figure 1.8). A 1.0 meter thick peat unit extends from Bay Sale to Trinity Island and gradually thickens to 2.0 m. The peat overlies a 1.5 m thick silty clay unit that ends at Pass la Poule. The unit has sparse organic and shell fragments. The silty clay overlies a 4.5 m thick clay unit that extends from Bay Sale to Trinity Island and gradually thins to 3.0 m. The clay unit is horizontally laminated. A 3.0 m thick sand unit overlies the clay unit at Trinity Island.

Stratigraphic cross section E-E'

Stratigraphic cross section E-E' trends from the northwest to the southeast from Cocodrie, LA to Timbalier Island (Figure 1.9). An approximately 2.0 m thick peat unit extends from Cocodrie to Timbalier Bay, except where it is absent under Bay Chaland. The peat shows sporadic rooting in the northwest portion of the section. The clay overlies a 1.0 m thick sand unit at core number 7270. The peat and sand overlie a 5.0 m

clay at core sites FC-2 and ww-5032z. The sandy and silty clay overlies a clay unit that is 4.0 m thick and gradually tapers to approximately 3.0 m southwest of Charleys Lake and abruptly ends. The clay is horizontally laminated and a few shell fragments are present in the unit. There are three 25 cm sand lenses in the clay unit, one at core site FC-2, one at FPB-10, and one at CH03. South of Charleys Lake a silty clay unit underlies the peat unit. The silty clay unit starts at 3.0 m thick and gradually increases to 6.0 m at Whiskey Pass. The unit is horizontally laminated and has sparse shell fragments. Three samples were obtained from the cores in the cross section for radiocarbon dating, two peat samples and one articulated shell (Table 1.2).

Stratigraphic cross section D-D'

Stratigraphic cross section D-D' trends from the north to south from Bay Sale to Trinity Island (Figure 1.8). A 1.0 meter thick peat unit extends from Bay Sale to Trinity Island and gradually thickens to 2.0 m. The peat overlies a 1.5 m thick silty clay unit that ends at Pass la Poule. The unit has sparse organic and shell fragments. The silty clay overlies a 4.5 m thick clay unit that extends from Bay Sale to Trinity Island and gradually thins to 3.0 m. The clay unit is horizontally laminated. A 3.0 m thick sand unit overlies the clay unit at Trinity Island.

Stratigraphic cross section E-E'

Stratigraphic cross section E-E' trends from the northwest to the southeast from Cocodrie, LA to Timbalier Island (Figure 1.9). An approximately 2.0 m thick peat unit extends from Cocodrie to Timbalier Bay, except where it is absent under Bay Chaland. The peat shows sporadic rooting in the northwest portion of the section. The clay overlies a 1.0 m thick sand unit at core number 7270. The peat and sand overlie a 5.0 m

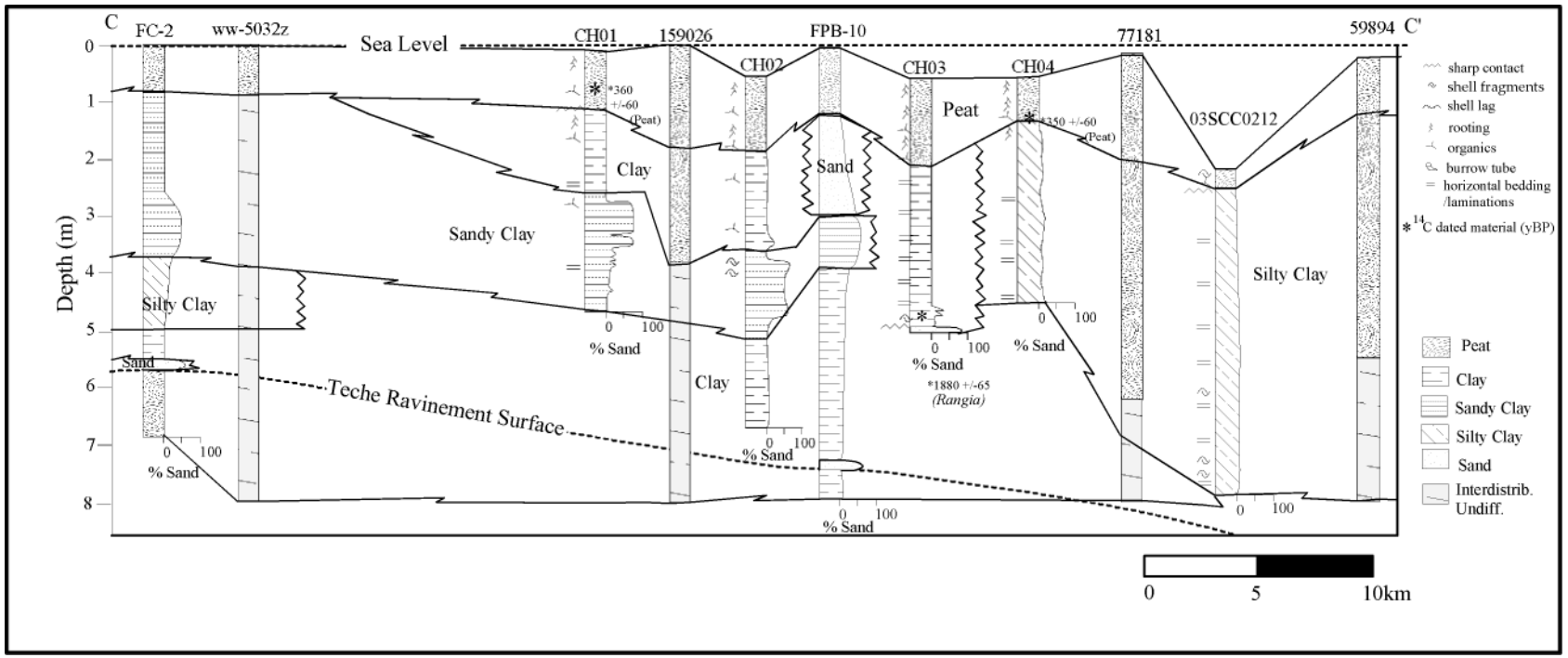

Figure 1.7 – Stratigraphic cross section consisting of cores from the USACE database, summer fieldwork 2003, and Penland et.al. 1987. The cross section shows the lateral and vertical relationship of primary lithosomes discussed in the text.

thick clay unit that thickens gradually to 7.0 m at Bay Chaland. The clay abruptly thins back to 5.0 m, and then tapers to 1.5 m at Timbalier Island. The clay is horizontally laminated and contains numerous shell fragments south of Bay Chaland. A 2.0 m thick silty clay unit begins at Bay Chaland and gradually thickens to 3.5 m. The silty clay unit is horizontally laminated and numerous shell fragments and shell lags are present north of Timbalier Island. Two clayey sand lenses containing organic and shell fragments are present in the silty clay unit at core numbers SCC0206 and SCC0204.

Lithosome Contour Maps

Four contour maps were constructed using the sedimentological data for each lithosome. Sedimentary units described from the cores were grouped into four lithosome categories; peat, clay, silty clay, and sandy clay. The contour maps were constructed in order to evaluate the extent of subsurface lithosomes identified from the cross sections. The *interpolate to raster* function within *ArcGis* 8.3 was used to construct contour maps with interval values based on lithosome thickness. *ArcGis* 8.3 provides a variety of contouring algorithms and each one has a particular use depending upon the character of the data being contoured. In this case inverse distance weighted (IDW) was chosen. *Arc GIS* 8.3 provides three contouring operations, and the IDW best fit the data set assembled. The Z value chosen was unit thickness, the power selected was four, the search radius was variable, and the output cell size was designated as three pixels to match the land loss map cell size.

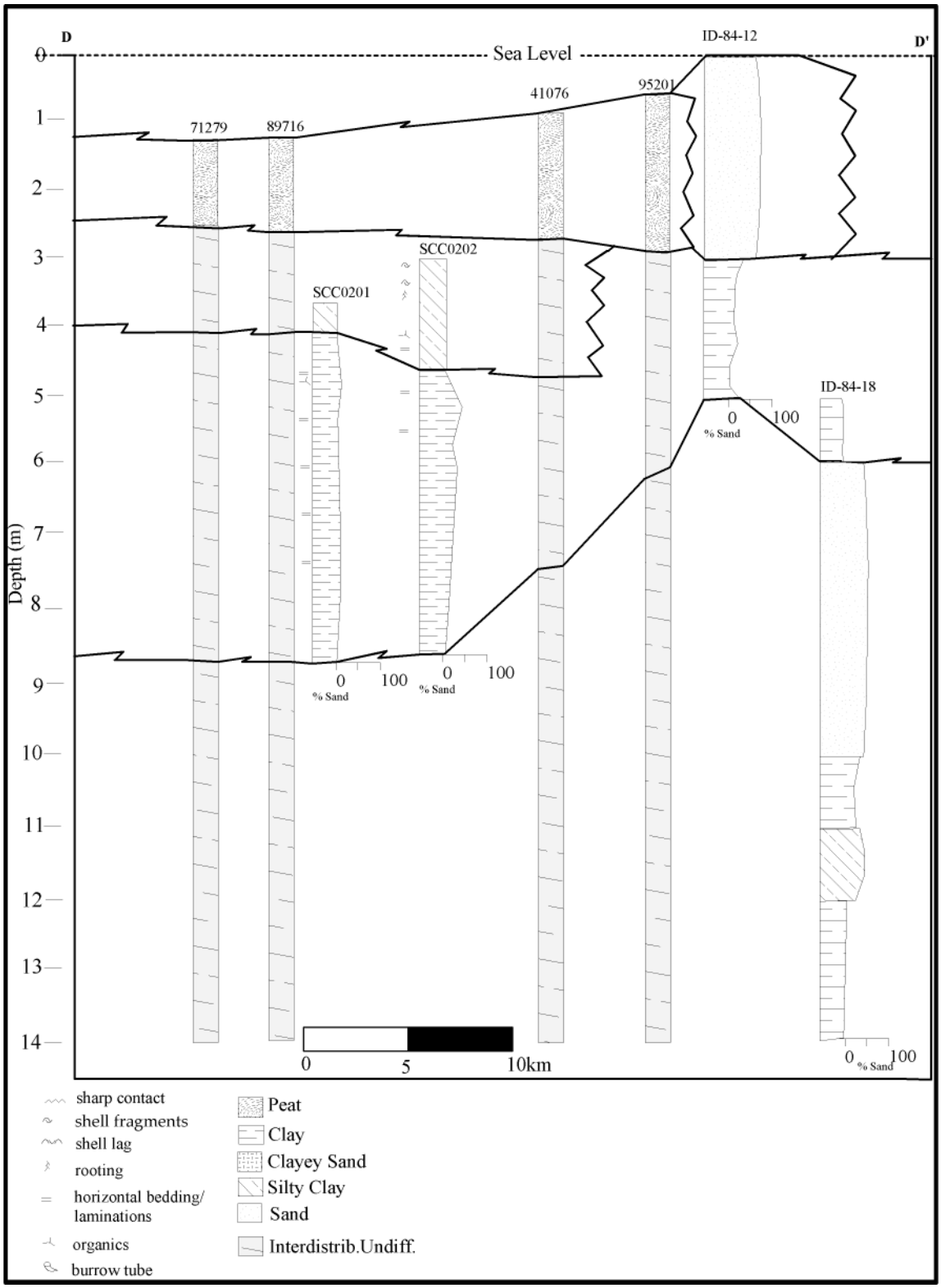

Figure 1.8 – Cross section includes cores from the USACE database, summer fieldwork 2003, and Penland et.al. 1987.

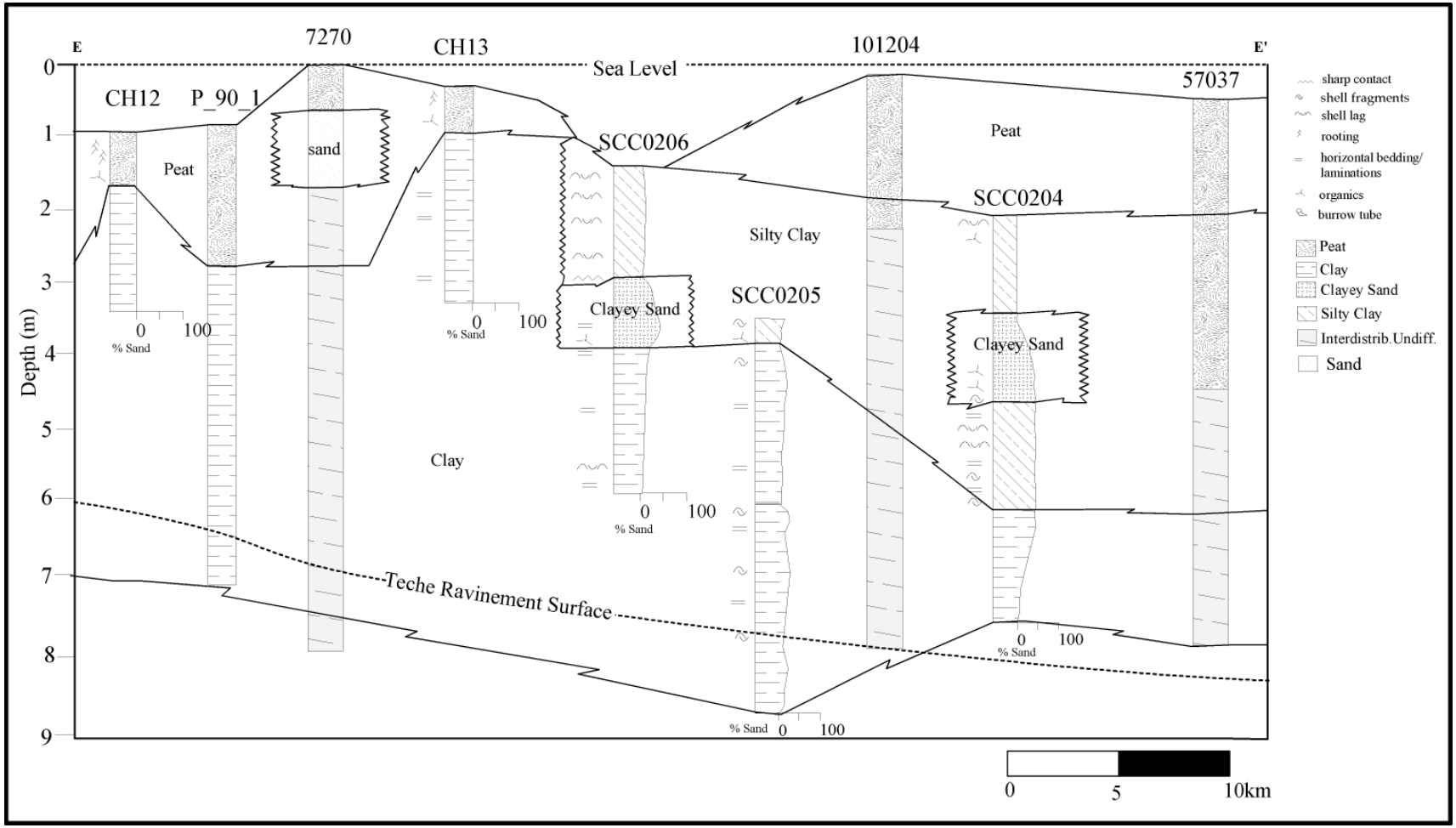

Figure 1.9 – The Stratigraphic cross section consists of cores from USACE database, summer 2003 fieldwork, and a Louisiana Geologic Society initiative. The cross section shows the lateral and vertical relationship of primary lithosomes discussed in the text. The Teche Ravinement surface was projected onto the cross section from Penland et al., 1987.

Discussion

Five transects were constructed across the headland in order to capture the stratigraphic framework. Identifying the major lithosomes was necessary in order to determine were the units of varying compatibility are located.

Stratigraphic cross section A-A'

This section transects Caillou Lake and the seaward marginal marshes southwest of the lake (Figure 1.10). Underlying Caillou Lake the stratigraphic architecture is simple, marsh deposit overlying clay that overlies sandy clay. This has been interpreted to be an interdistributary fill deposit. Towards the seaward marshes however this deposit abuts a deposit that is interpreted as reworked interdistributary bay clays and silty clays, due to the presences of several shell lags and organic fragments at depth.

Stratigraphic cross section B-B'

This section is comprised of a simple stratigraphic arrangement of sedimentary units (Figure 1.11). It lies between Bayou Grand Caillou and Pass de Ilettes. The marsh deposit extends to the seaward extent of the headland where it pinches out. The marsh unit overlies a thick clay unit and a thick sandy clay unit. The clay and silty clay units are interpreted as interdistributary bay fill deposits.

Stratigraphic cross section C-C'

This section transects the center of the headland and ends just north of the Isles Dernieres (Figure 1.12). In this section two distinct thick clay strata were observed. They possibly represent two overlapping delta lobes, as they are separated by

interdistributary bay fill. This interval is overlain by marsh platform and appears to abut the same sedimentary package as cross section A-A'. The silty sand here has preserved horizontal laminations and only shows reworking near the marsh platform contact, and is interpreted to be prodelta silty clays.

Stratigraphic cross section D-D'

This section transects the eastern edge of the headland and the western edge of Terrebonne Bay (Figure 1.13). The base is massively bedded clay and is interpreted as a prodelta deposit. It is overlain by a silty clay package that is interpreted as interdistributary bay fill. The section is overlain by subsided marsh platform until it bisects the Isle Derniers, where a thick barrier island sand interval is observed.

Stratigraphic cross section E-E'

This section transects Terrebonne Bay to the eastern edge of Timbalier Island (Figure 1.14). The entire section overlies massively bedded clays with few shell fragments. This is interpreted as a shelf clay deposit. It is overlain by the marsh platform and laterally abuts a silty clay deposit similar to the one seen in transect C-C'. This silty clay deposit is again identified as prodelta silty clays.

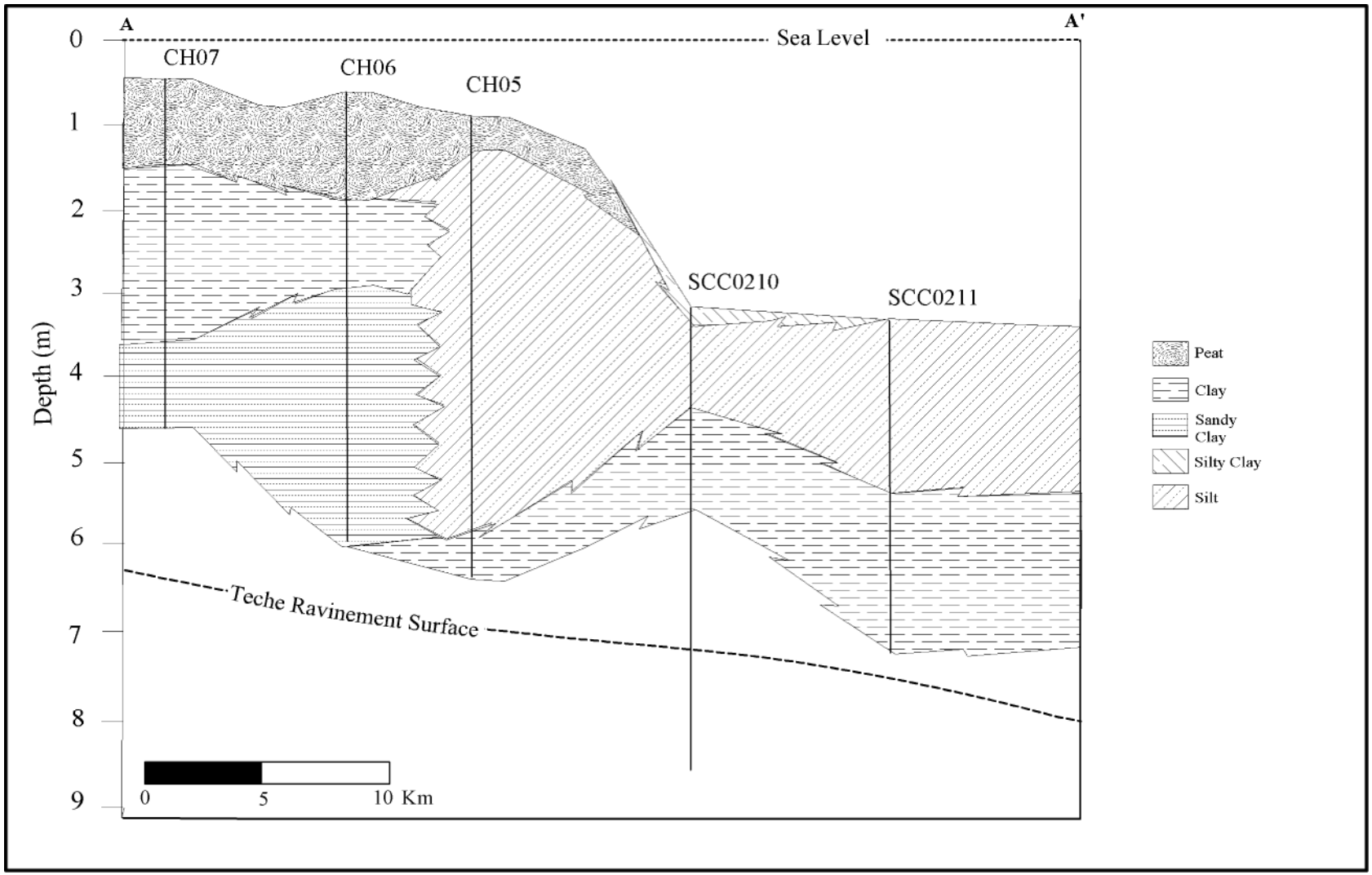

Figure 1.10 – Stylized cross section including cores from the summer 2003 fieldwork.

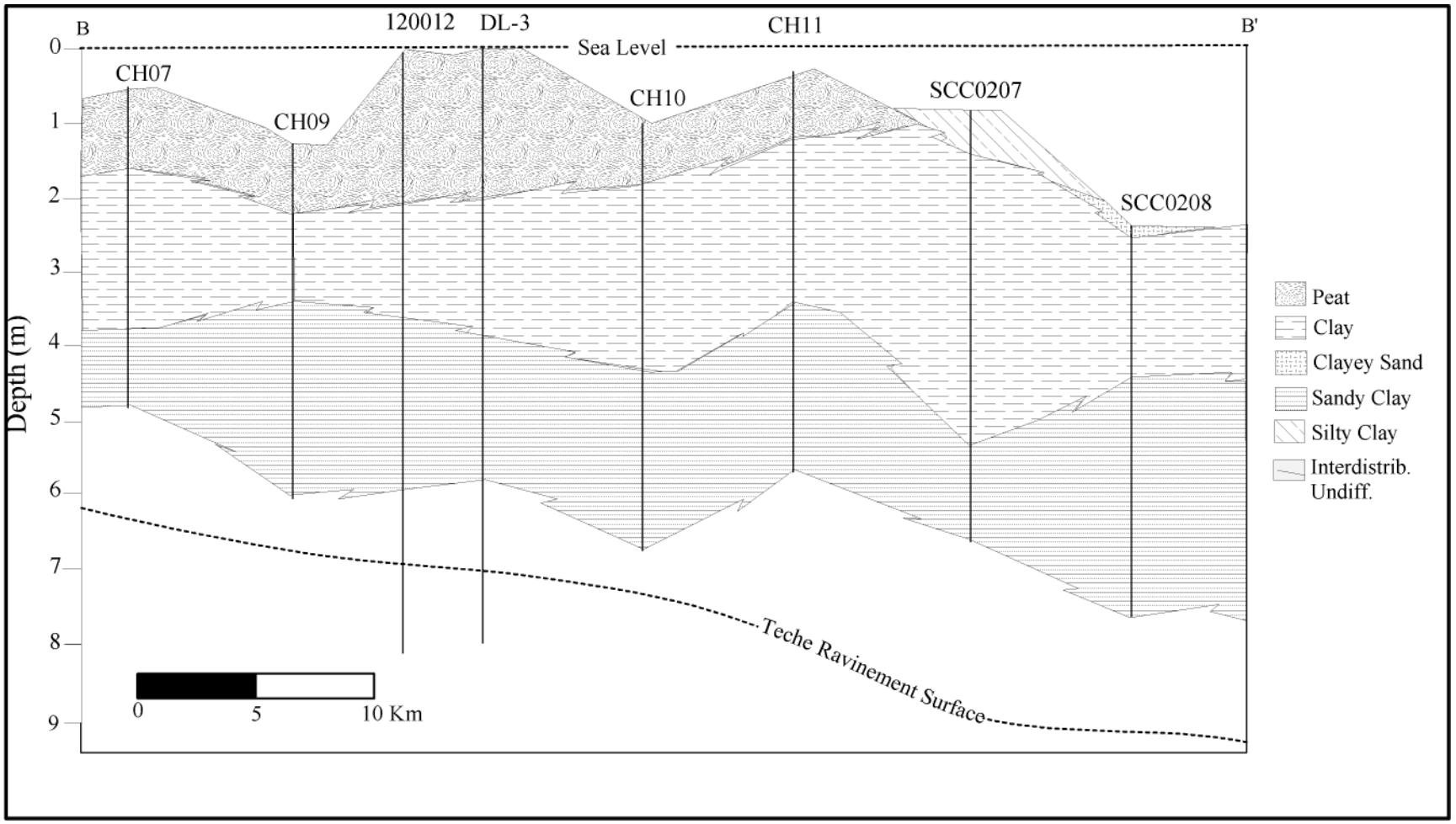

Figure 1.11 Stylized cross section includes cores from the USACE database and the summer 2003 fieldwork.

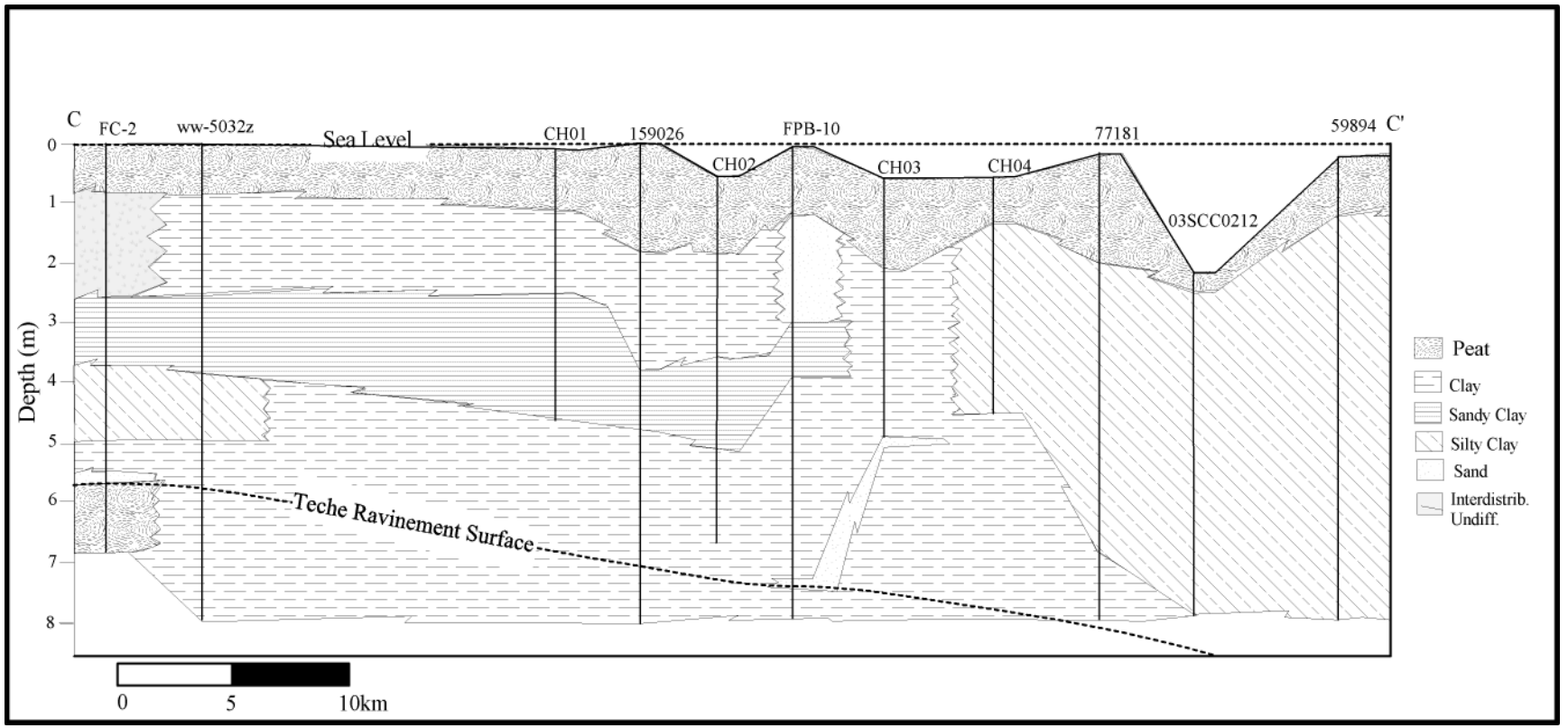

Figure 1.12 – Stylized cross section includes cores from the USACE database, summer fieldwork 2003, and Penland et.al. 1987.

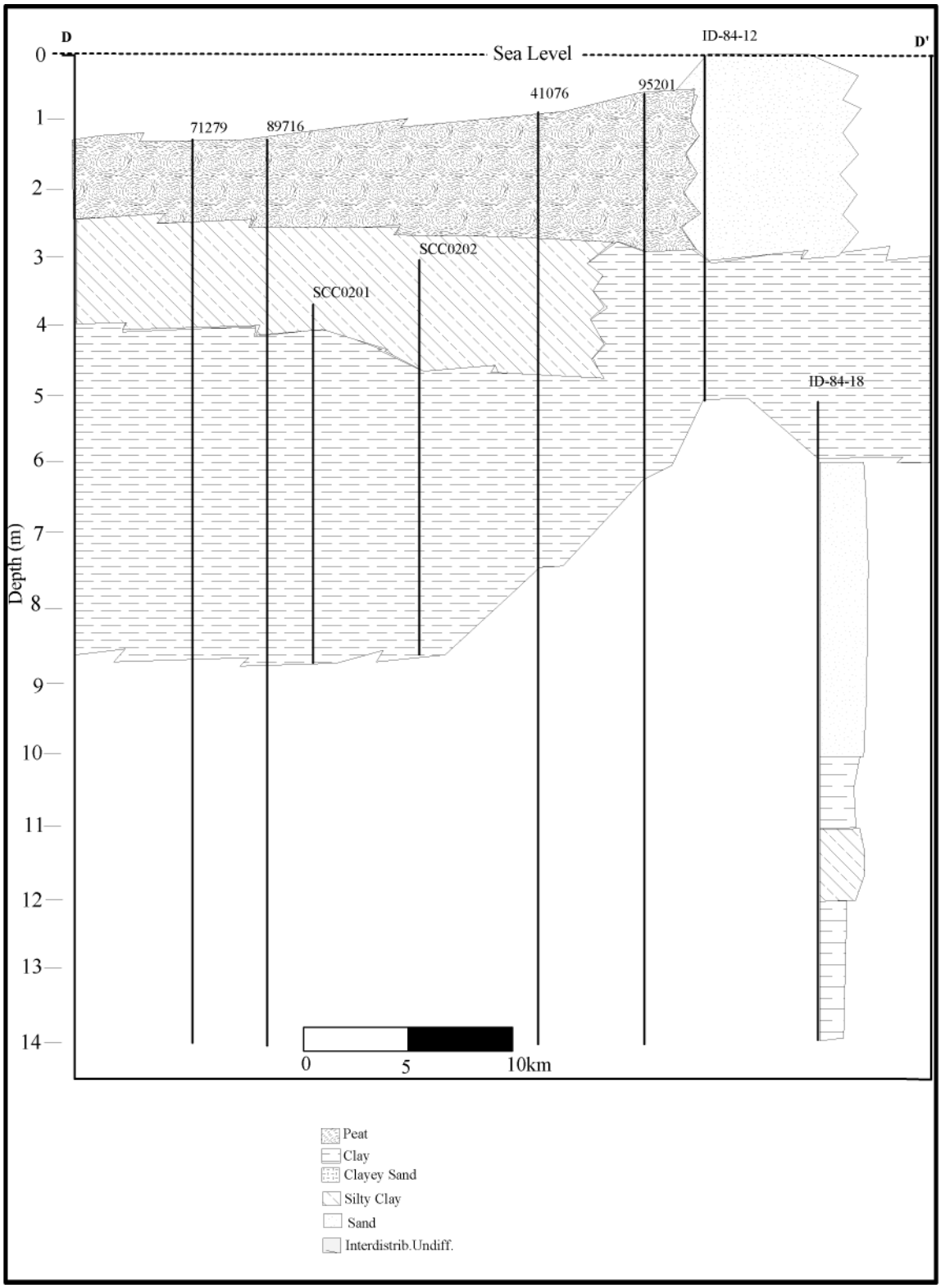

Figure 1.13 Stylized cross section includes cores from the USACE database, a Louisiana Geologic Society Initiative and the summer 2003 fieldwork.

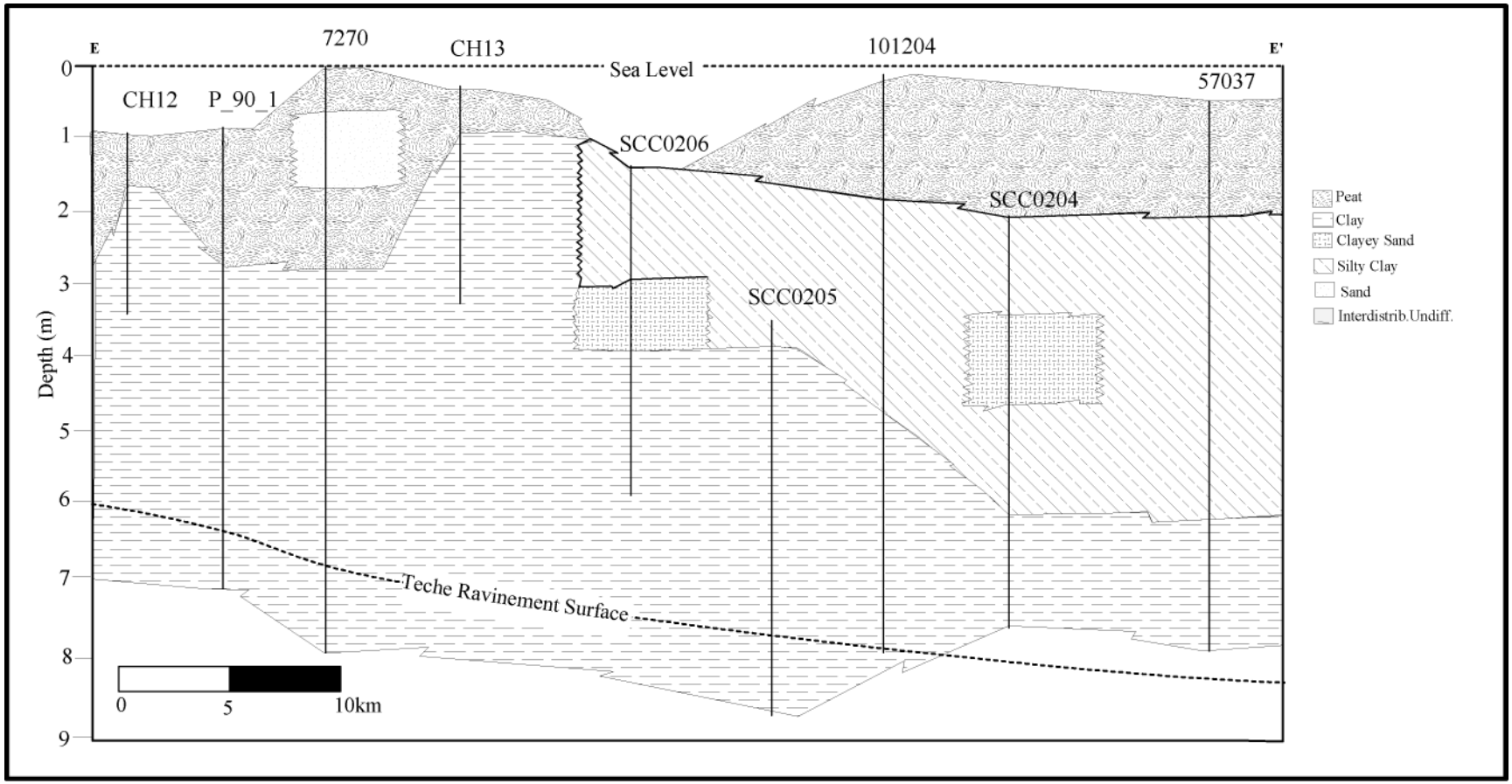

Figure 1.14 – Cross section contains cores from USACE database, summer 2003 fieldwork, and a Louisiana Geologic Society initiative.

Chapter 4

Methods

The second component of this research project consisted of analyzing a collection of historic maps in order to reconstruct the geomorphic evolution of the Caillou Bay headland. A detailed record of wetland loss and shoreline change was sought in order to determine whether; 1) the loss was uniform across the study, 2) patterns of land loss were evident and, 3) there appeared to be any relative increase or decrease in the rates of change. A detailed determination of where land has converted to water is necessary for comparison to the subsurface geologic framework dataset.

Map Preparation

In order to determine historical shoreline change and interior wetland loss, a collection of historical maps was assembled. In order to document land surface change a series of maps were chosen in approximately 40-year increments spanning from 1863 to 2002. This increment of time was chosen because shorter intervals of time represented by the maps would not likely show significant changes in geomorphology and therefore historical headland evolution would be difficult to determine. The intent was to analyze areas where land has converted to open water. This is significant because conversion indicates where subsidence has occurred.

In order to compare modern and historic maps, the historic maps were georeferenced to a modern coordinate system. The georeferencing process assigns a map projection system to image data (Erdas, 2001). This is done by either assigning

coordinates to specific points on the image, or by linking image data to a previously georeferenced map. The coordinate system North American Datum 1983 (NAD83) was chosen for this project. It is the geocentric datum and coordinate system most commonly used by geologists in North America (Kennedy and Kopp, 2002). In order to achieve the most accurate results 20 to 30 reference points are preferred in order keep the route mean square (RMS) error below 0.1%. The program automatically calculates the RMS error thereby decreasing the overall validity of any comparisons that are to be performed. When the error exceeds 0.1% RMS, distortions of the map can occur when the map is reprojected in the NAD83 coordinate system. After the maps undergo the georeferencing process, they can then be easily imported into all of the software packages used in this study.

The collected maps each presented unique challenges with regard to georeferencing. Permanent features such as lighthouses, military forts, and railroads were necessary for assigning a coordinate system to a map. These are numerous on the modern maps, and less frequent on the historic maps. When the georeferencing of the maps was completed, they were integrated into a GIS database within which calculations of land loss could be performed and total changes in area of land and water could be quantified.

Final map preparations consisted of producing an image with each pixel of the map coded as either water or land. In this way changes in total land were assessed by calculating the number of pixels that had changed from water to land for a given time period represented by the maps under comparison. The preparation for each map differs up until this point; and the specific methods of preparation are presented for each map in

the following sections. In order to reach this point however, each paper map was scanned, georeferenced, land and water were demarcated, and each was coded as a separate value to provide a control for later calculations. *Erdas Imagine* 8.6 software was used for this part of the map preparation. The 2002 map was previously georeferenced, and was used as the control map for the project.

1863 Map

This map was located in the National Archives in Washington, D.C. The Bureau of Topographic Engineers completed it in 1863 as part of reconnaissance work conducted by the Union army during the Civil War (Figure 1.15). It was located in a section of the archives not available to the public and consequently could only be retrieved by an approved graphics company. The one company able to scan the 24 x 22 map was *Do-You-Graphics* in Frederick, Maryland. They obtained and scanned the map at 300 dots per square inch (dpi), producing a digital image. The image was saved to a compact disc and mailed to UNO.

In order to georeference the 1863 map, a previously georeferenced map was required. There were few permanent features on this map, and no latitude or longitude grid to assign coordinates too. The map chosen to georeference the 1863 map was a 2002 map (see below) was used as the source of coordinate points. One lighthouse, six train stations, two forts, and eight natural features including intersecting waterways were used to reference this map. This is less than optimal, but these were the only well known locations with a history of existence and known coordinates that enabled the comparison. For this process, 15 to 30 reference points would have been preferential. The RMS value calculated was .21%. The map was then reprojected using the reference points to assign

coordinate values to all points on the map. This map was then clipped to the dimensions of the predefined study area. The 1863 map and the 2002 map were overlain to determine the relative accuracy of the referencing process. A visual examination of the maps revealed a misalignment of historic locations and significant distortion of the land area in the 1863 map. The lack of permanent features hindered accurate georeferencing for this map.

This map did not show significant detail in the marsh, so polygons of land and water were selected with a drawing tool. Within the software these polygons were filled with a uniform color and pixels representing water were coded as zero, whereas pixels representing land were coded as one. Each feature was assigned a numerical value in order to analyze land loss when the 1863 map was compared to the other maps in the collection.

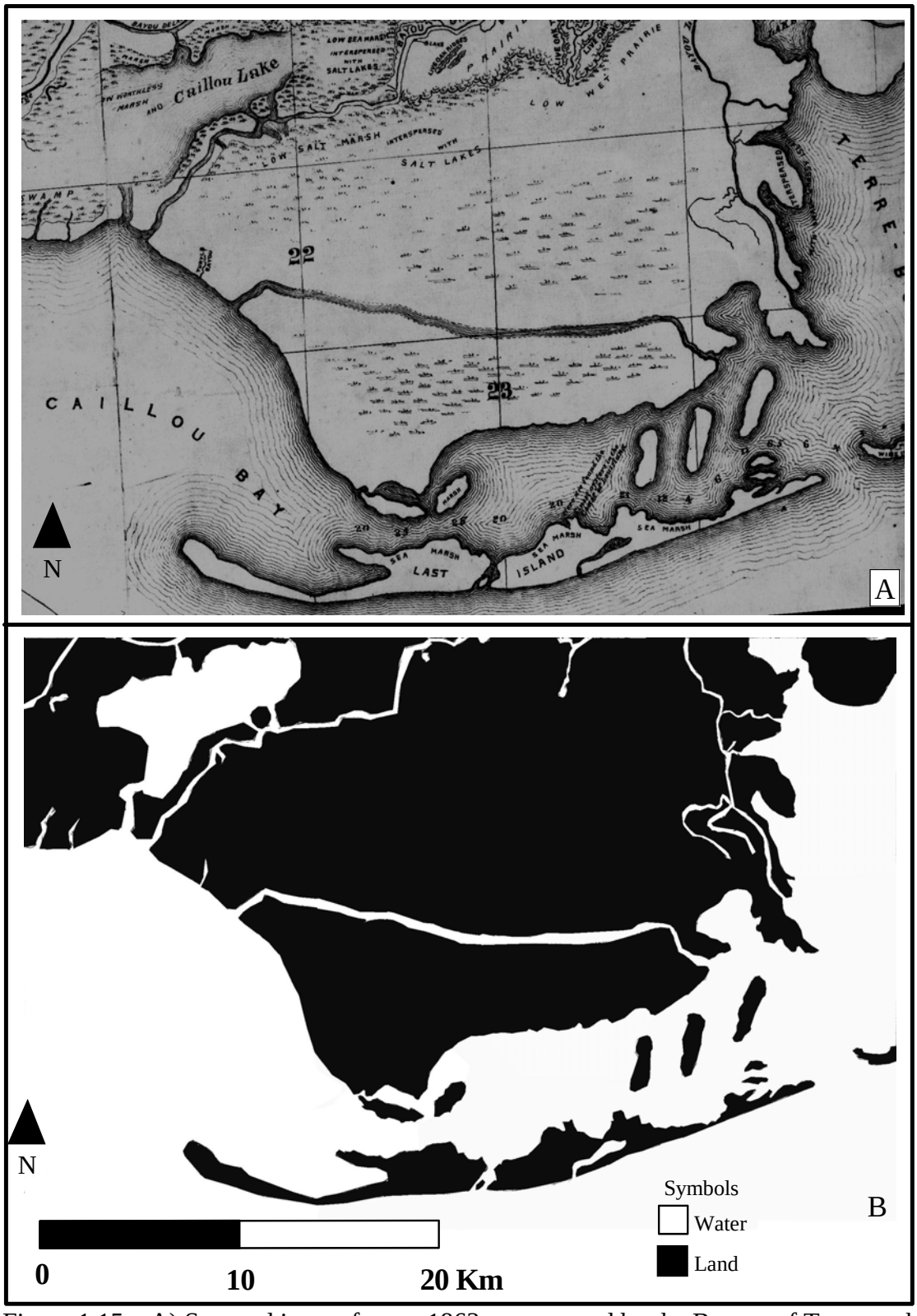

Figure 1.15 – A) Scanned image from a 1863 map created by the Bureau of Topographic Engineers. B) Final image created using Imagine software. The map in B was used as the input into the land change modeler.

1895 Map

The 1895 map was completed by the Hardee's map company and a copy is archived in the library in the Pontchatrain Institute for Environmental Studies (PIES), at the Center for Energy Resource Management on the UNO campus. It was prepared in a similar fashion to the 1863 map except that canals were utilized in the georeferencing process instead of natural waterway features. After completing the georeferencing process the RMS value was .09%. The map was then clipped to the study area, and overlain with the 1863 and 2002 map to determine the relative accuracy of the georeferencing. Since the 1863 and 1895 maps did not show the same amount of detail that the later maps did, the only available feature that could be checked for positional accuracy were the major bayous on the headland, including Bayou Grand Caillou, Bayou du Large, Bayou Sale, and Bayou Petite Caillou.

The 1895 map did not show fine details, such as minor breaks and small open water bodies in the marsh area, so polygons were drawn where the land and water was identified within the map. The water pixels were coded as zero and the land pixels were coded as two. Since the land pixels in the 1863 map were assigned a value of one, the land pixels on the 1895 map were assigned a value of two. This was done to differentiate between land on the 1863 and the 1895 maps. This was required to perform land loss calculations with the *Imagine 8* software. All following maps were assigned a new number accordingly. The image was then ready to be used to calculate land change when compared to the other maps (Figure 1.16).

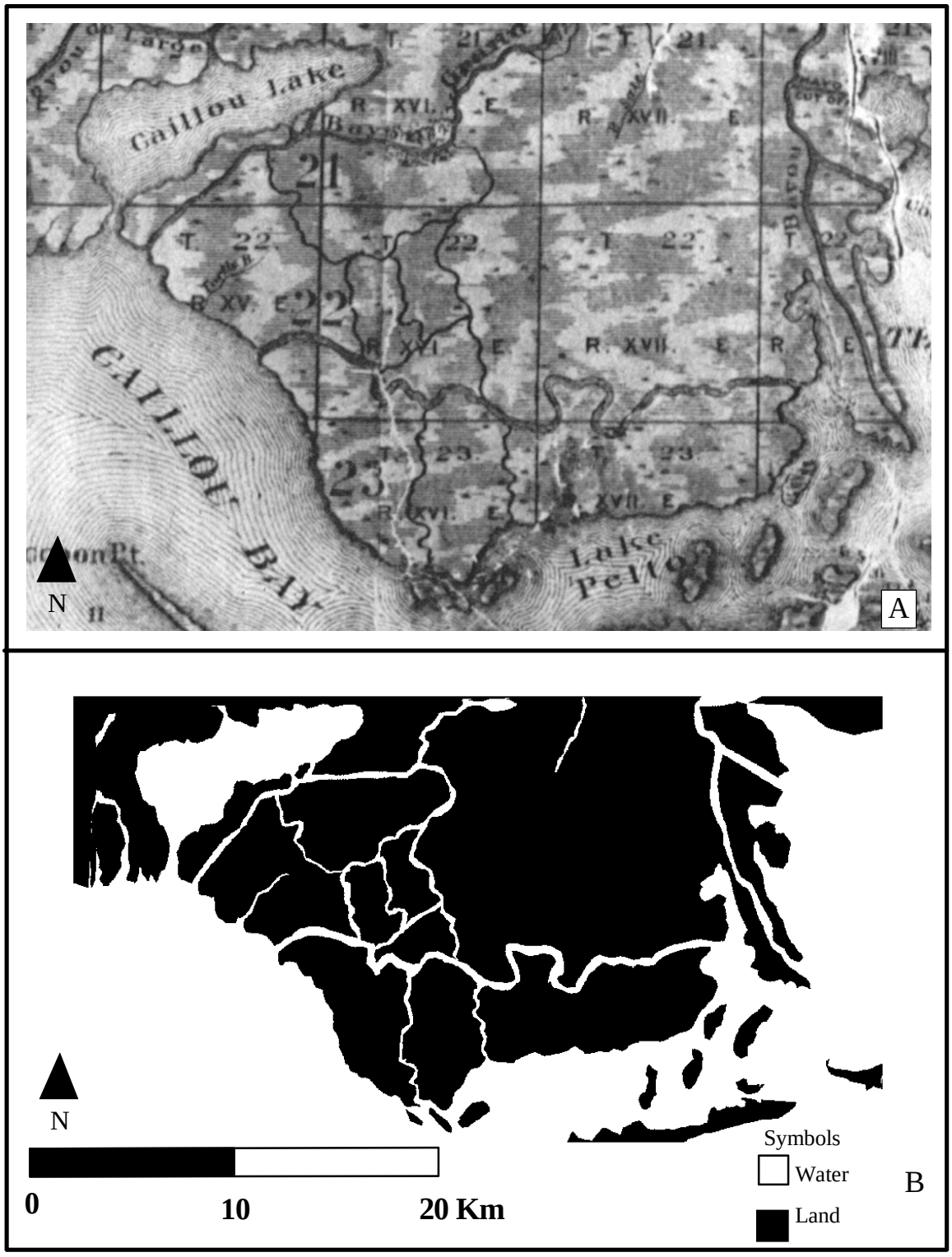

Figure 1.16 – A) Image from a scanned Hardees 1895 map. B) Final image created using Imagine software. This georeferenced and rasterized map was input into the land change modeler.

1956 Map

The 1956 map used in this study was a U.S. Geodetic and Coastal Survey map archived in the PIES library on the UNO campus. It was constructed using aerial photography and contained more detail than the previous maps. Universal Transverse Mercator (UTM) tic marks were present on the map, so a grid was drawn across the map using these points as anchors. Coordinate points were then entered at grid nodes where the grid lines intersected. As with the map-to-map method, RMS error was automatically calculated; a total of 30 reference points were used and resulted in a RMS value of 0.12%. Similar to the other maps, the 1956 the map was clipped to the study area dimensions to visually test the compatibility to the 2002 map. The 1956 map and the 2002 map, however, did not fit perfectly. Though the land area matched, a slight offset could be observed in the bayou and canal intersections. A rubber sheeting method was then applied to correct for the small discrepancies observed between the two maps. Rubber sheeting is a term that refers to a process that is conceptually similar to the map-to-map georeferencing process, but the points are used to refine the projection, not to reproject the map entirely. For example, a point with the incorrect coordinates is chosen on the 1956 map, and the correct location on the 2002 map is then chosen. The software program created a file that listed the incorrect 1956 coordinates linked to the new correct 2002 coordinates. 40 points were collected in order to realign the map. The map was reprojected using the corrected points in the file, and the 1956 map corresponded on the basis of visual inspection with the 2002 map.

There were significant color differences and breaks in the land polygons on the map so the image was meticulously hand digitized using the drawing tool. As in the previous maps, the fill for the water pixels was zero. The pixel value for the land in the 1895 map was two, so the land pixels in the 1956 map were designated three. The image was then ready to be used for land change calculations (Figure 1.17).

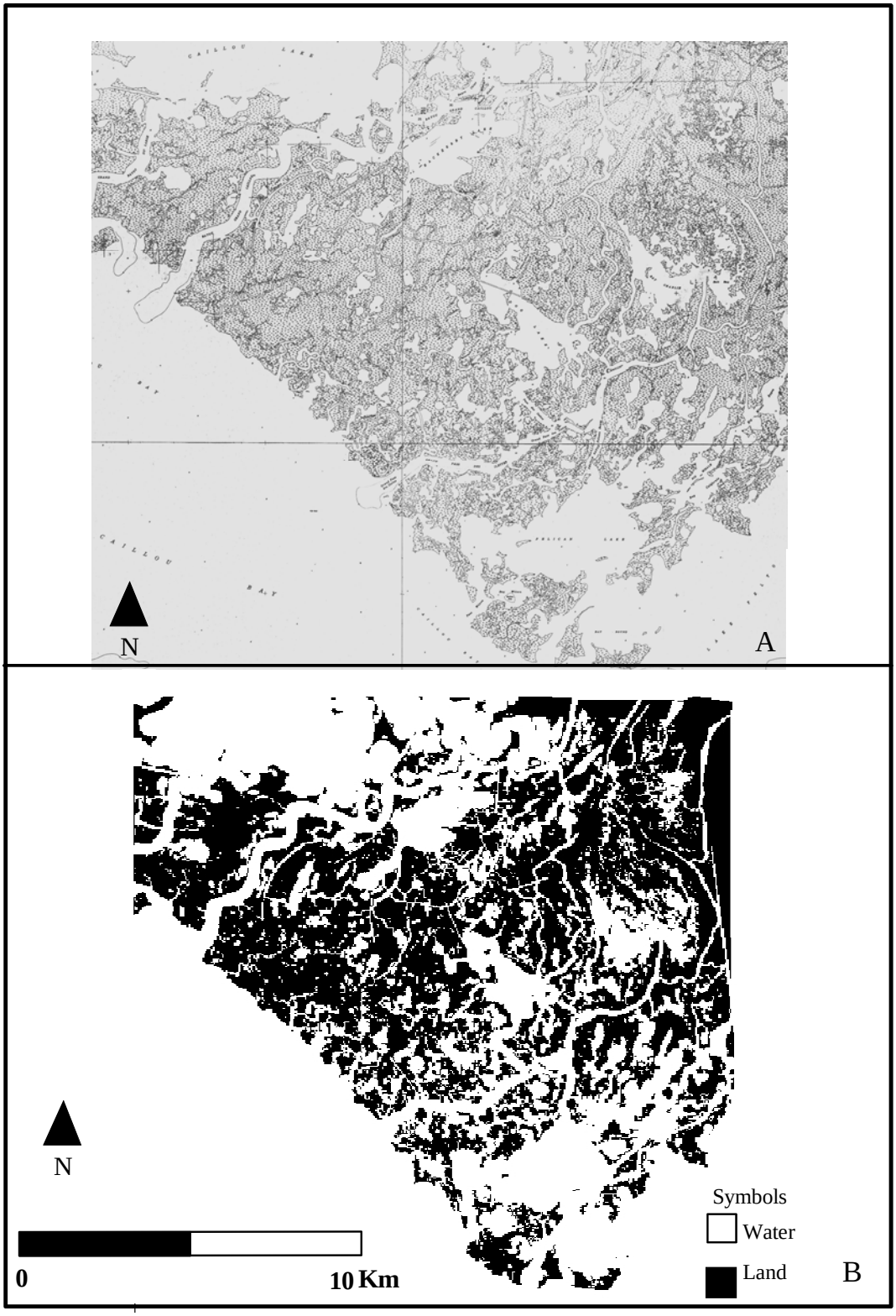

Figure 1.17 – A) Image from a scanned a 1956 map (U.S. Coast and Geodetic survey). B) Final image created using Imagine software. This georeferenced and rasterized map was input into the land change modeler.

1983 Map

The 1983 map was scanned and available for download from the NOAA Office of Coast Survey. This online map source has since been taken offline, and is now only available directly from the NOAA main office. UTM tic marks were present on the map, so a grid was drawn using these points as anchors and coordinate points were entered at the grid nodes. Twenty-five points were referenced using this method, and a RMS method of 0.13% was calculated. The map was then clipped to the study area and overlain with the 2002 map. The rubber sheeting method used on the 1956 map was also used to refine the projection of the 1983 map as well. When the map was reprojected the 1983 and the 2002 images matched. The land area, bayous, canals, and permanent features were in alignment.

The image contained highly fragmented marsh that would have made manually defining the land and water polygons an extremely time consuming process. Instead, the map was processed by a model developed by Louis Martinez at UNO's PIES. The modeler separates land from water in a raster image. The process scans the map, one row of pixels at a time. The color range for water and land pixels was determined, and the model was able to identify land and water by the color value that each pixel had. The pixel value range associated with water was reassigned a value of zero, and the pixel value range associated with land was reassigned a value of four. Areas such as text that are improperly classified as land are reassigned manually by drawing polygons around the text that are subsequently assigned the value denoting water (Figure 1.18).

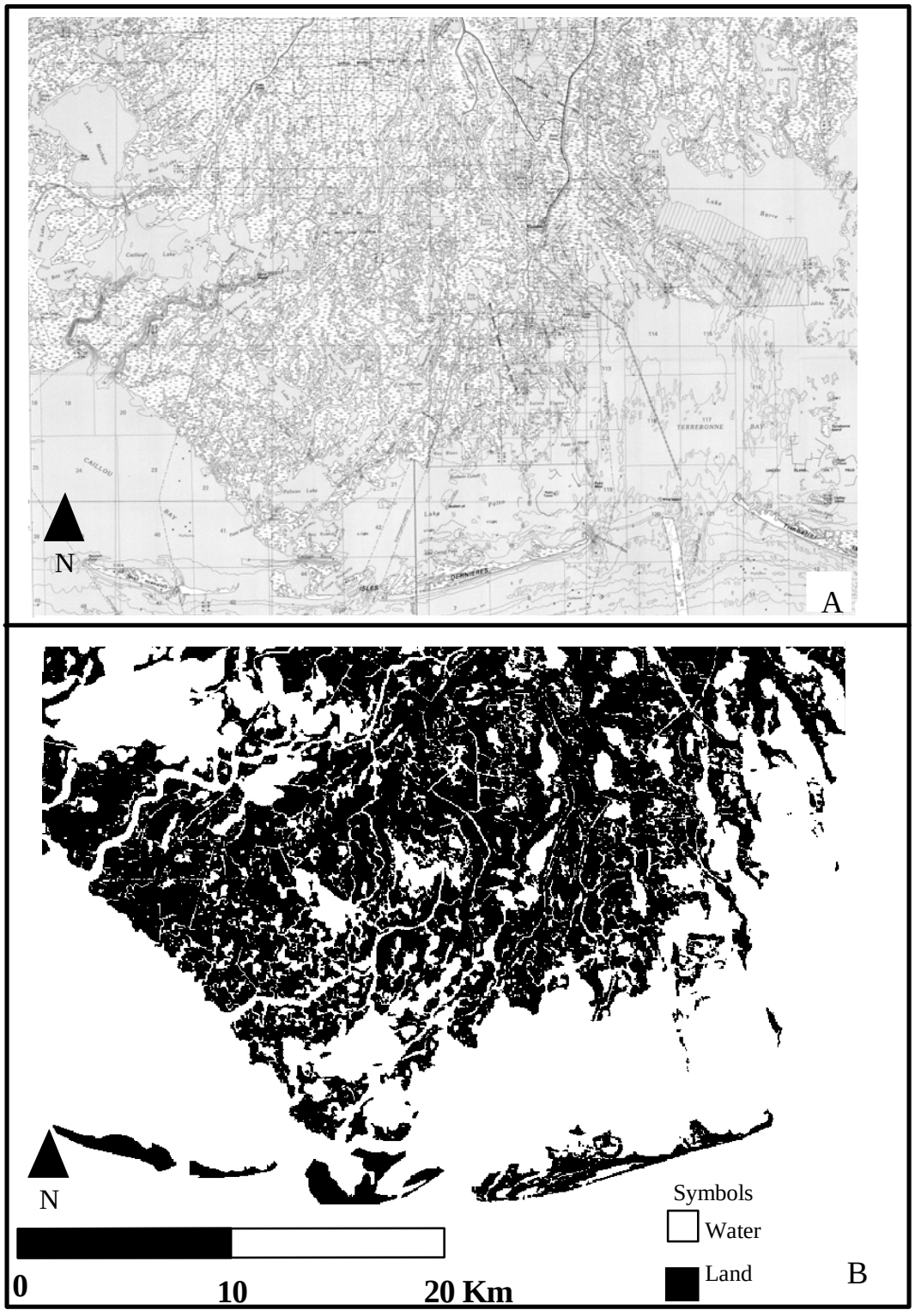

Figure 1.18 – A) Image from a scanned 1983 map (U.S. Geodetic Survey). B) Final image created using Imagine software. This georeferenced and rasterized map was input into the land change modeler.

2002 Map

This map was acquired as a georeferenced image and, as previously mentioned, served as the control map for this project. The study area was clipped from the map and processed using the Martinez model. Areas on the map that were misclassified because of map features such as text or coordinate lines were corrected by assigning appropriate values to manually designated polygons. As before, pixels associated with water were classified as zero, and pixels associated with land classified as five (Figure 1.19).

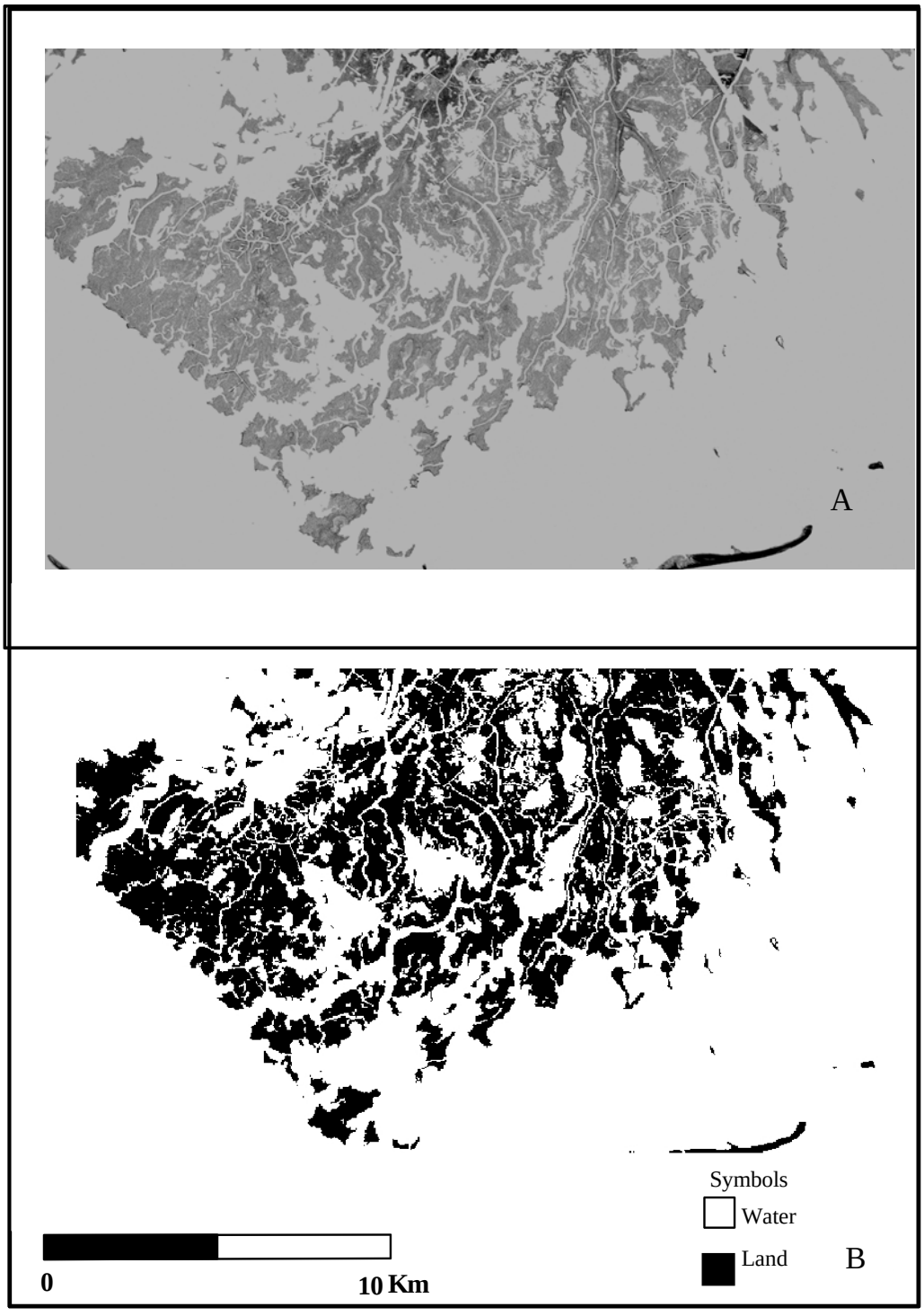

Figure 1.19 – A) Image from a 2002 satellite imagery. B) Final image created using Imagine software. This georeferenced and rasterized map was input into the land change modeler.

Land Loss Map Production

The final step of the map preparation process was to produce maps that depict land loss during intervals of time represented by the temporal spread between the specific maps. In order to conduct the analysis of sequential land changes the georectified and processed map images were loaded as pairs of two into a quantitative model designed using the *Imagine 8* modeler to calculate land change. As indicated in the previous discussion of each map, land for each image was classified as a different value for this process.

For images between 1863 and 1895, land was classified as a numerical value of one and two respectively. They were imported into the model built in *Imagine 8*. The model subtracted the 1863 map from the 1895. The model searched for pixels classified as number one that were not overlain by number two pixels. This absence of pixel overlap represented land loss. This produced a map illustrating the total land loss amount. This process was carried out with map couplets representing the time intervals 1895 to 1956, 1956 to 1983, and 1983 to 2002. This procedure allowed for the construction of four land loss maps. Each one of these land change comparisons was constructed for the purpose of comparing the lithosome contour maps developed from the data collected for the framework geology portion of the study.

Results

This component of the project resulted in land-loss calculations that included interior wetland loss (e.g. conversion to open water) and shoreline erosion. These calculations and the resulting images provided an assessment of the geomorphic evolution that the Caillou Bay Headland has undergone within the time period

represented by the maps (1895-2002). Land change was calculated for each of the three time intervals in order to develop and estimate rates and patterns of total land surface change within the study area.

Land Loss Totals

Land versus water coverage maps were produced from the maps acquired for the project (Figures 5 figures). These maps were used to produce land loss maps for three time intervals. For time interval A (1895-1956) 62.6km^2 was lost (Figure 1.20); for time interval B (1956-1983) 56.6km^2 was lost (Figure 1.21); and for time interval B (1983-2002) 57.1km^2 was lost (Figure 1.22).

Land Loss Determination

The percent land loss over each contour interval was calculated with the following formula:

[(T1 – T2)/(T1)] x 100 = Percent Land Loss

where

T1 = Total land for initial time period of each contour interval

T2 = Total land for preceding time period of each contour interval

The headland overlies contours of varying widths. In order to account for this, the formula uses total land for a specific contour interval instead of total land loss. In this way the percent land loss figures do not represent the surficial extent of a contour, but the actual percentage of land lost over a time interval.

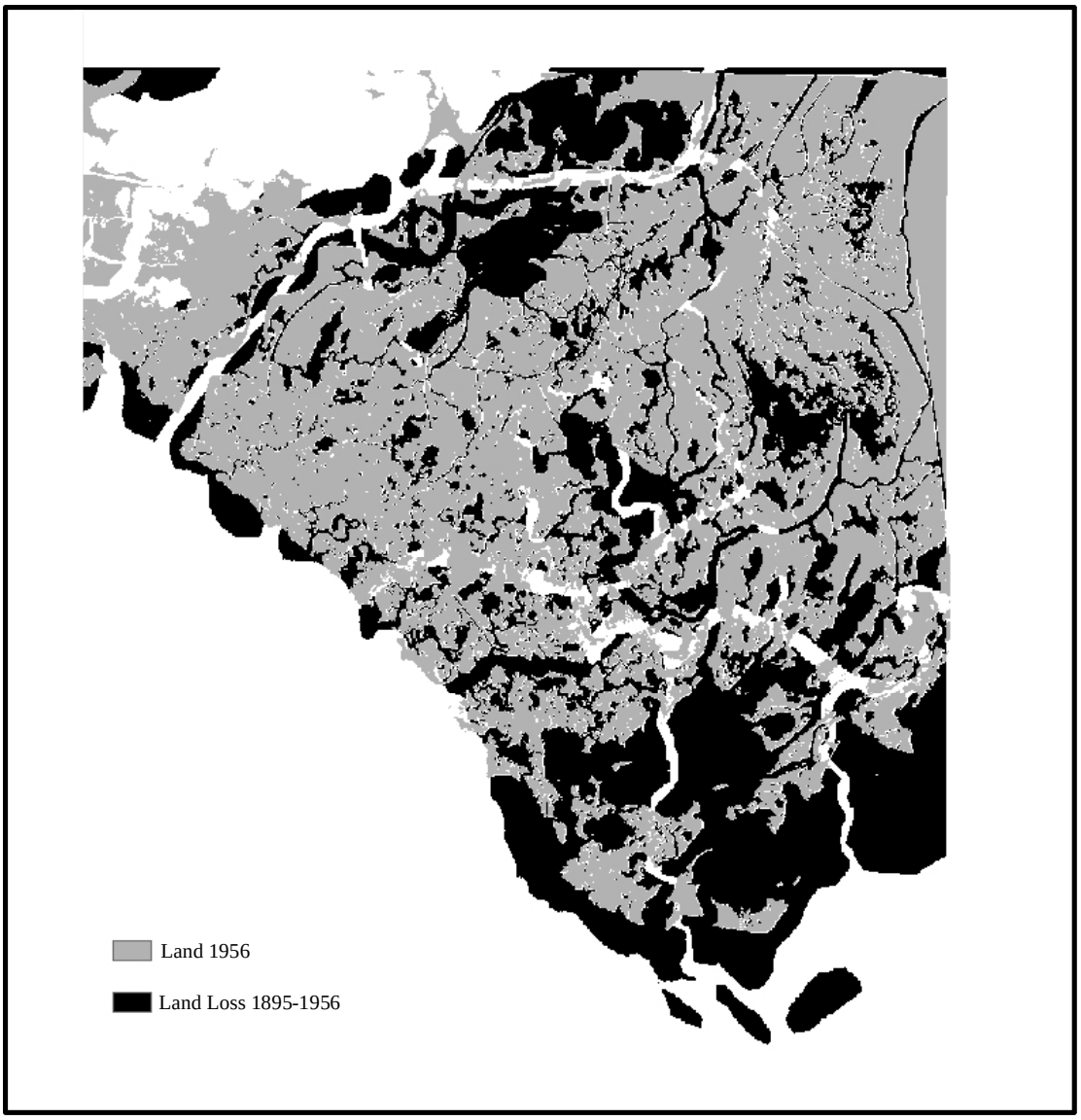

Figure 1.20-Land loss from 1895 to 1956. Land lost from 1895-1956 is shown in black, while extant land in 1956 is shown in gray.

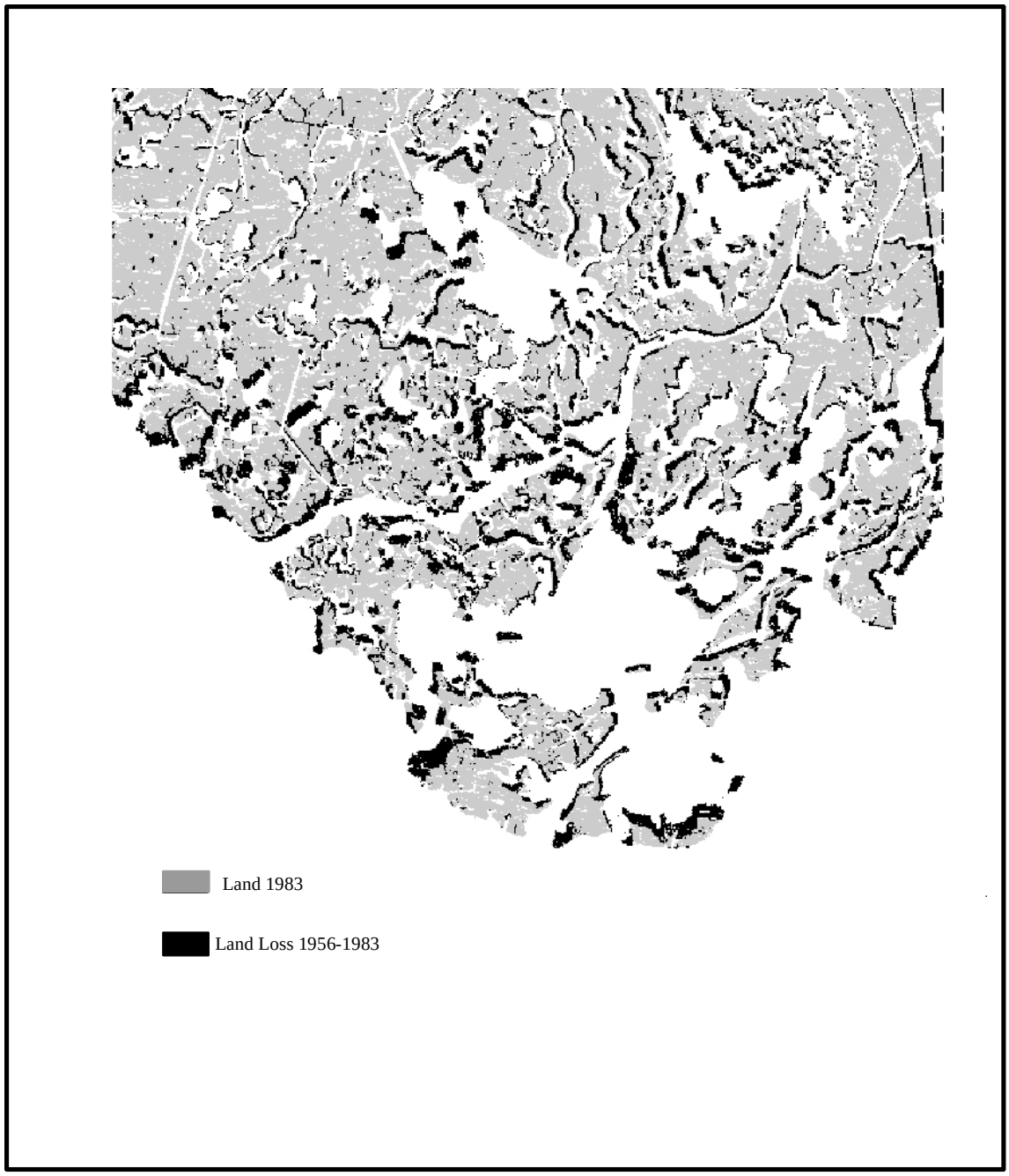

Figure 1.21 – Land loss from 1956 to 1983. Land lost from 1956-1983 is shown in black, while extant land in 1983 is shown in gray.

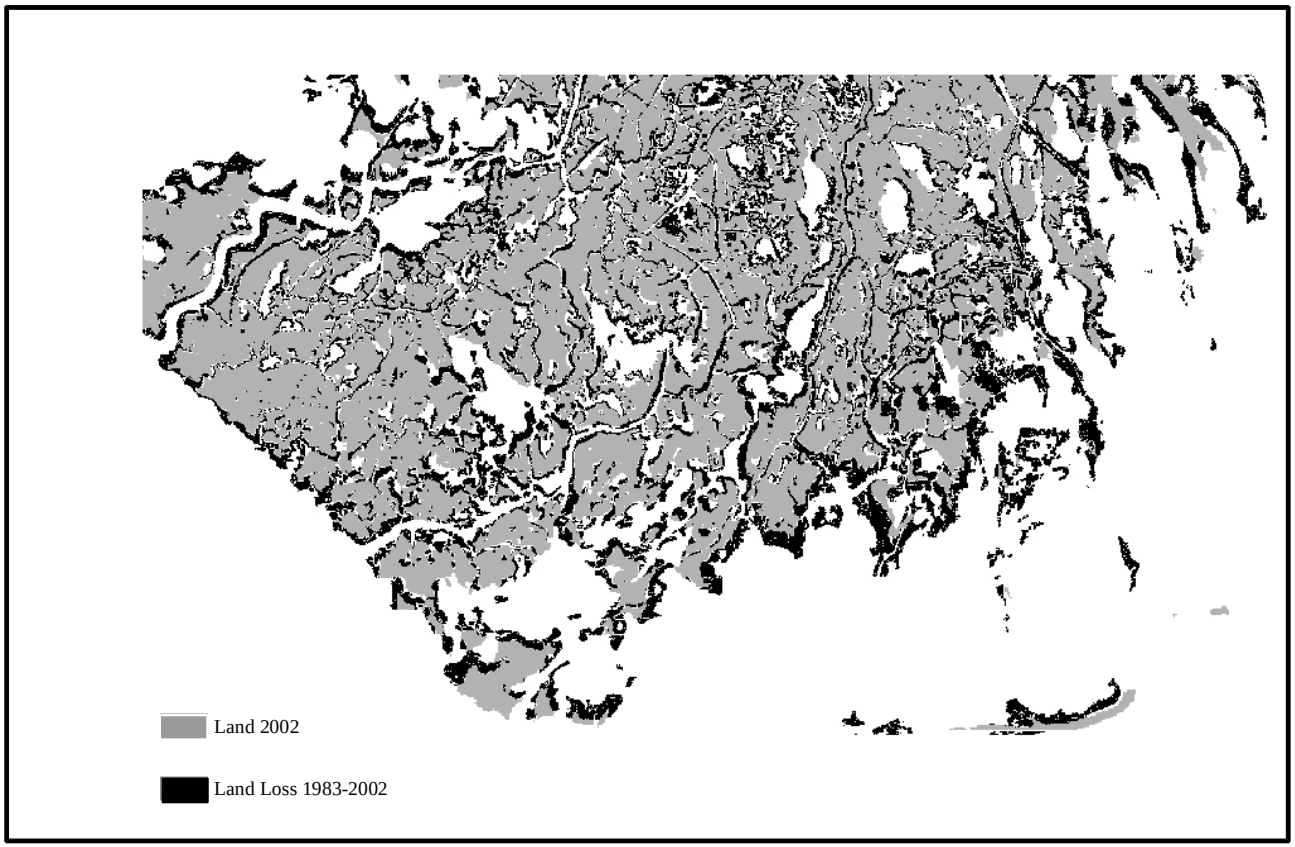

Figure 1.22 – Land loss from 1983-2002. Land lost from 1983-2002 is shown in black, while extant land in 2002 is shown in gray.

Discussion

Map Evaluation

The map database was used to develop a history of headland evolution for the Caillou Bay Headland throughout the last 150 years. In the course of this study however, a variety of considerations emerged regarding the validity of results obtained from the analysis. The intent was to determine rates and patterns of erosion of the interior wetlands and the coastal area. One of the first factors that required consideration was the overall accuracy of the maps created before the 1900's. The 1863 map and the 1895 map both have coastlines, bayous, and major lakes that are reasonably mapped when compared to modern maps (Figures 1.15 and 1.16). The problem arises in the lack of detail in the interior marshes. Examination of the map from 1863 compared to 1956, for example, clearly indicates that a level of detail is absent in the early historic maps. This reflects the status of the technology available at the time the map was constructed. A key component to the study is to understand and quantify not just how much land was lost but specifically where the land changes took place. Consequently, an examination of the potential problems associated with the successive change analysis is warranted.

Comparison of change: 1863-1895

Comparison of the 1863 map to the 1895 map was conducted by overlaying them. The resulting was a land loss map and land change calculations that did not seem reasonable or realistic. Across much of the area covered by the maps the shorelines and bayous matched in a geomorphic sense, but because there was little detail of land versus water indicated for the interior marsh on both maps, change data was insignificant. These

maps provide and interesting opportunity to visually gauge the headland configurations as interpreted by the early map makers, but because of the limited detail have an extremely limited application for accurate quantification of geomorphic change.

Comparison of change: 1895 –1956

As mentioned above, the 1895 map had reasonable shorelines and bayous but the details of the interior marsh geomorphology (e.g. tidal channels, small embayments) was not well constrained or depicted (Figure 1.20). Comparison of this map to the 1956 map is difficult. The 1956 map was created with modern mapping techniques including aerial photography. The data results that were acquired when the two maps were overlain is more reliable than the 1863-1895 interval, but still has inaccuracies as a result of the earlier map making techniques used in 1863 relative to those of 1895.

Comparison of change: 1956-1983

The 1956 and 1983 maps are both the product of good and substantially more advanced map-making techniques (e.g. aerial photography, satellite imagery, and geographical positioning systems) (Figure 1.21). The geographical coverage of the 1956 map is not as extensive as the 1983 map (Figure 1.18), so data could only be acquired for the area covered by the 1956 map.

Comparison of Change: 1983-2002

The 1983 map was produced with the aid of aerial photography, and the 2002 map is the product of satellite imagery (Figure 1.22). The land loss map created when these maps were overlain was the most accurate and covered the largest amount of area. The time frame within which these maps were acquired is also an interval of time when

the delta plain was most heavily impacted by anthropogenic activities such as the construction of access canals, the excavation of dredge holes, and placement of dredge spoil that artificially creates land.

Chapter 5

Discussion and Conclusions

This section examines the results of the comparison of the subsurface stratigraphic framework to the surficial geomorphic evolution of the headland. The results of the comparison are evaluated in order to determine if patterns of land loss can be correlated to subsurface facies distribution.

Percent Land Loss versus Lithosome Thickness

The patterns of land loss indicated by the analysis of sequential map pairs appears to chronologically reflect transition from natural to anthropogenic influenced geomorphic change. The natural land loss progression is difficult to gauge because of the limitations imposed by earlier maps; primarily the incompleteness of coverage and details in the marsh interior. The progression of anthropogenic land loss is affected by hydrologic alterations from canal dredging, levee augmentation, and dredge and fill operations. These types of modifications create two distinct problems. The first is the mechanical removal of land that can skew results, as this removal is not a reflection of natural processes such as compaction and the underlying mechanisms of change that are being tested. There is also the altered hydrology that can result from this process and contribute to marsh degradation. There is no way to absolutely determine the area of marsh platform eliminated by the effects of salt-water intrusion versus the area reduced to open water from subsidence; both are recorded as land loss in the change analysis performed for this study.

Comparison 1: Percent Land Loss versus Lithosome Thickness – Time Interval A (1895-1956)

Four land-loss versus thickness maps were constructed to evaluate patterns of land loss (Figure 1.23, 1.26, 1.23, and 1.32). During time interval A, a distinct increase in land loss was identified in locations where the clay lithosome was 150 to 250-cm thick (Figure 1.36 box a). This area of clay thickness is overlain by the seaward margin of the headland, at the current location of Lake Pelto. Distally deposited distributary sediments support the marsh platform here. This area serves to buffer the interior marsh from the erosive effects of wave and storm surge that impact the coast. Despite the problems associated with interior marsh coverage on the early maps, significant land loss has been documented for the edge of the headland.

Comparison 2: Percent Land Loss versus Lithosome Thickness – Time Interval B (1956-1983)

Four land-loss versus thickness maps were constructed to evaluate patterns of land loss for time interval B (1956-1983) (Figure 1.24, 1.27, 1.30, and 1.33). During this time interval, two distinct areas of substantial land loss were documented. Both areas overlie the silty clay lithosome from 500 to 550 cm (Figure 1.36, box b) and the sandy clay lithosome from 200 to 250 cm (Figure 1.36, box c). The silty clay interval 500 to 550 cm thick underlies the eastern margin of the headland. There has been significant erosion to the marsh platform edge, resulting in the loss of protection to the marginal marshes with time. Land lost on the sandy clay interval, ranging between 200 and 250 cm thick, is located on the western central portion of the headland. Land loss here is of a

more interior nature, but some loss is observed from the seaward margin. As the seaward margin continues to lose marsh platform, the interior marsh becomes more susceptible.

Comparison 3. Percent Land Loss versus Lithosome Thickness – Time Interval C (1983-2002)

Four land-loss versus thickness maps were constructed to evaluate patterns of land loss (Figure 1.25 1.28, 1.31, and 1.34). During this time interval, two distinct areas show significant land loss and overlie the clay lithosome where it is 150 to 250 cm thick (Figure 1.34 box d) and the silty clay lithosome where it is 500 to 650 cm thick (Figure 1.36, box e). The land lost over the clay interval is located on the western interior of the headland. Much of the marsh overlying the seaward margin was lost during time interval A and B leaving the interior marshes more vulnerable to coastal processes. Also at this point anthropogenic influences appear to become a significant factor. Alterations of hydrologic processes on the entire coast appear to impact the headland evenly, as canals have been excavated over the entire headland. This increases the amount of interior land loss by direct removal. The placement of canals is not a function of subsurface lithology, so land loss would be seen over every lithosome contour interval.

The land lost the silty clay interval is located at the southern extent of the headland. The map record shows that this area has undergone the highest rates of land loss. Presently stage there is little marsh platform left to protect the remaining marsh from coastal processes such as wave action, tides, and large storms.

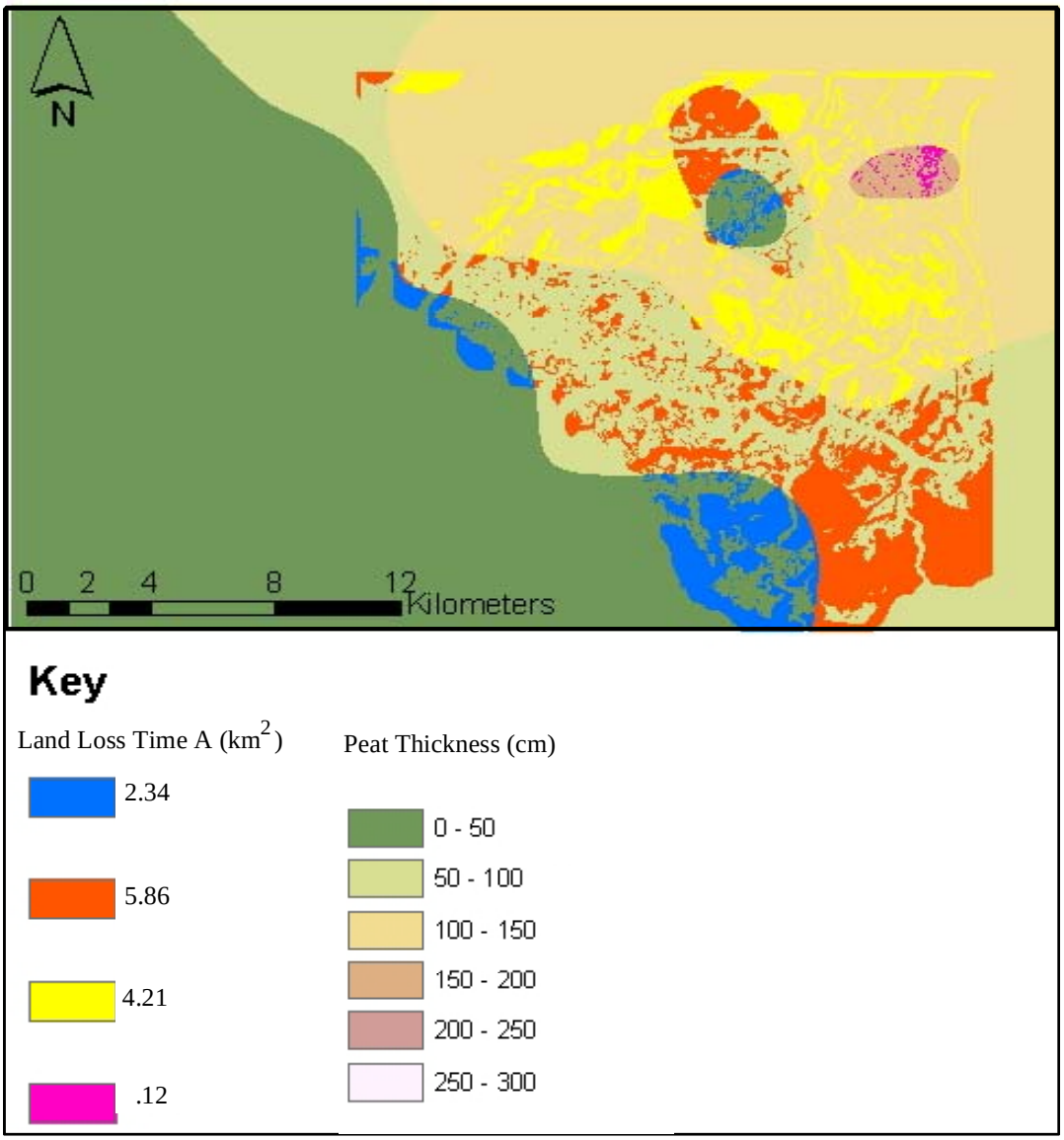

Figure 1.23. Contour map illustrating peat thickness in the study area overlain by land loss from time interval A.

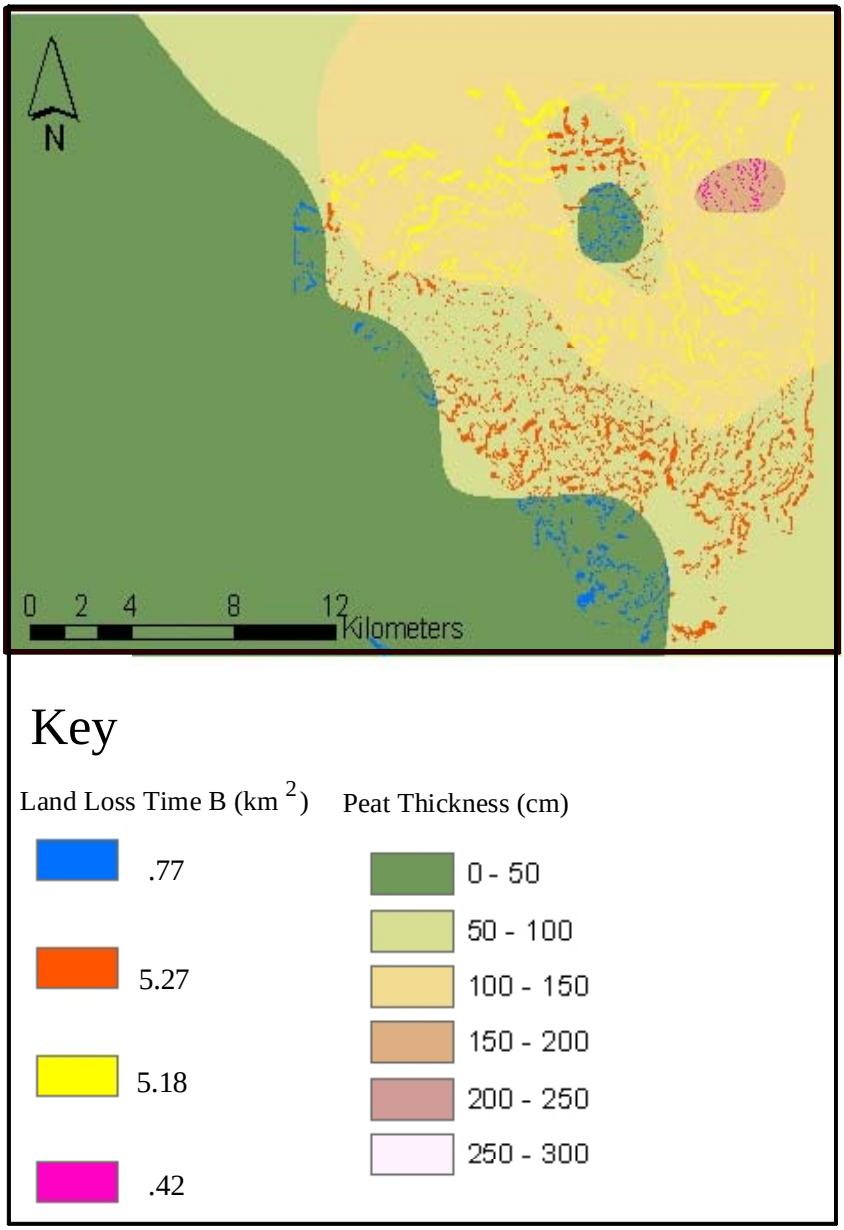

Figure 1.24. Contour map illustrating peat thickness in the study area overlain by land loss from time interval B.

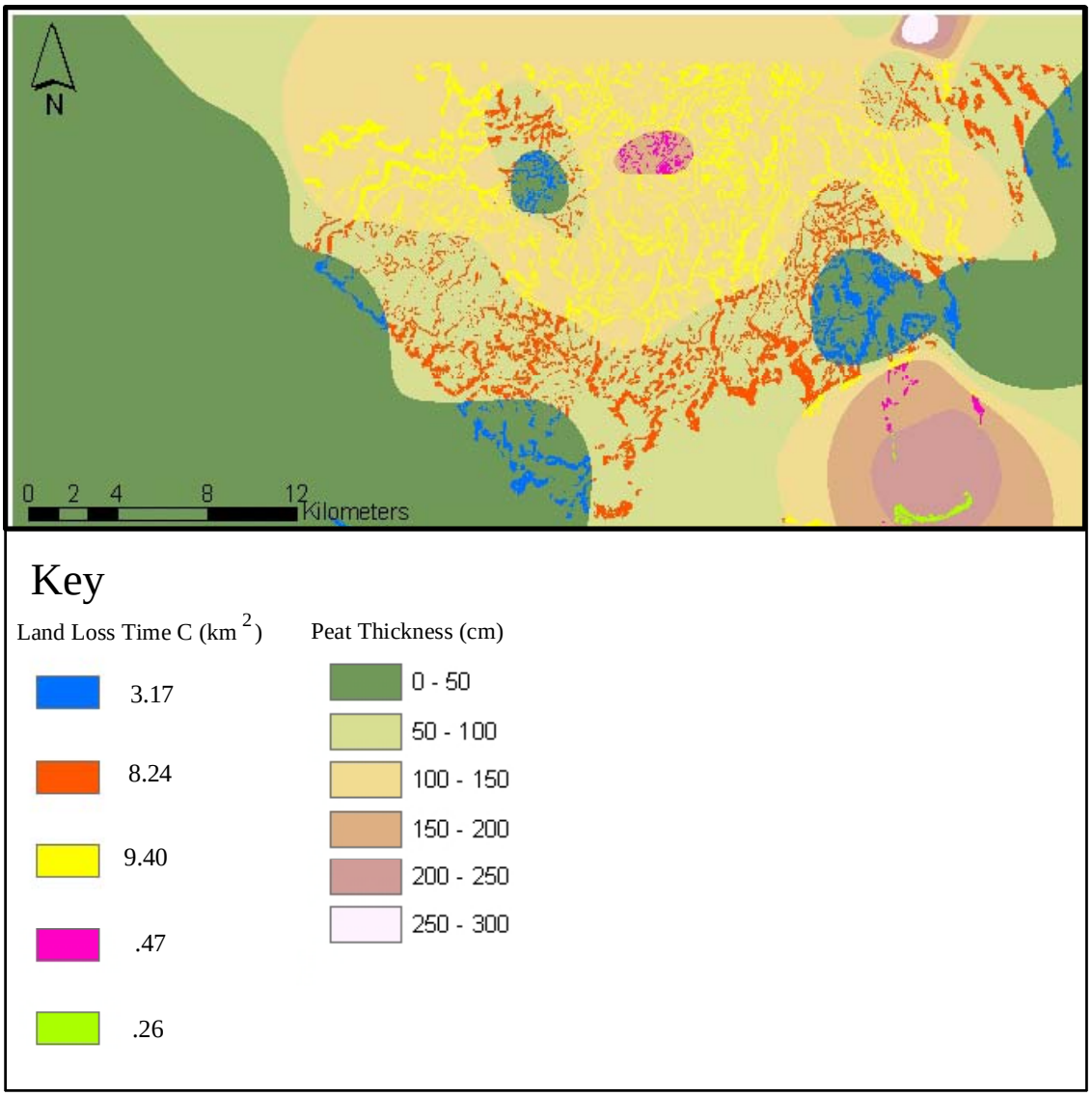

Figure 1.25. Contour map illustrating peat thickness in the study area overlain by land loss from time interval C.

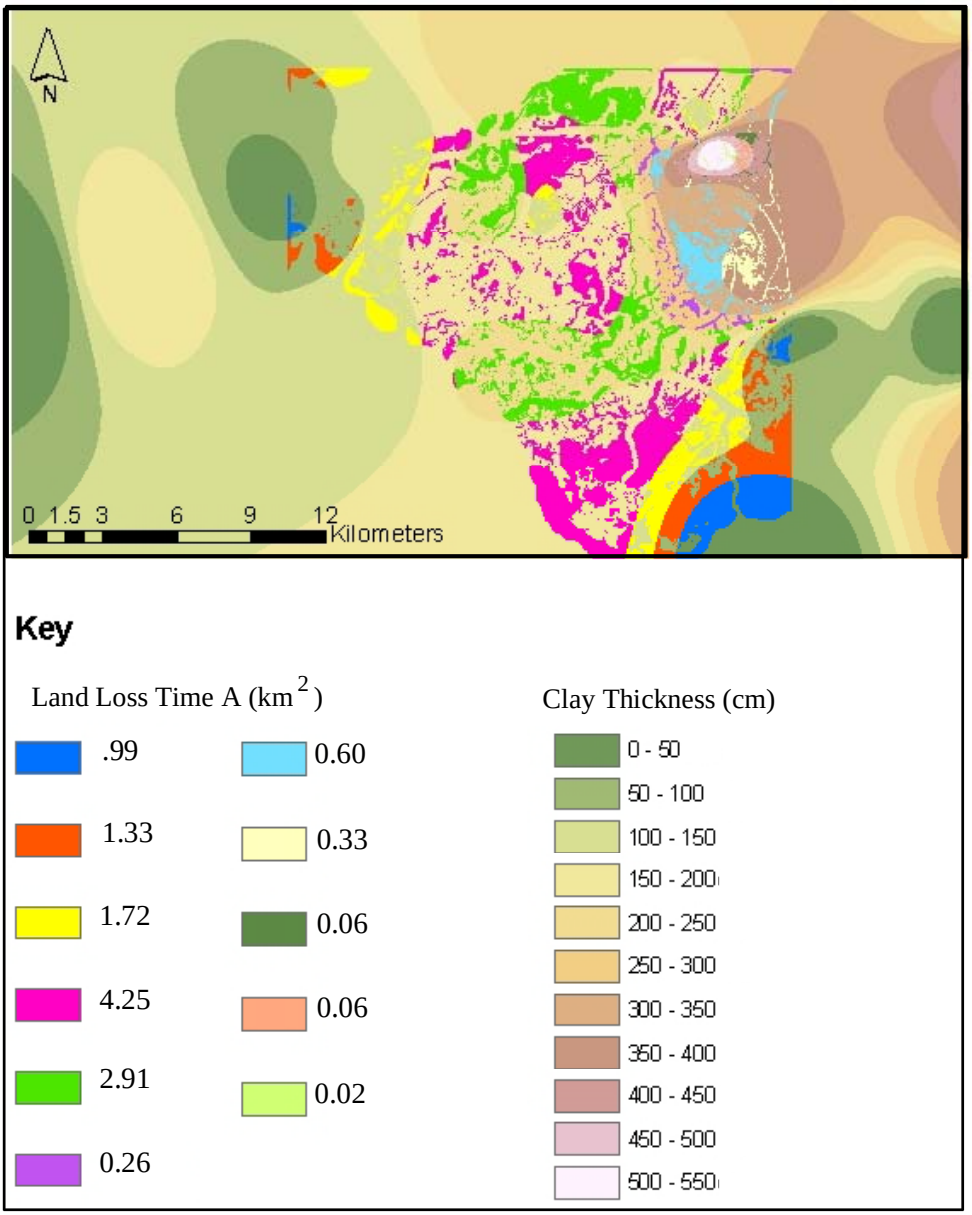

Figure 1.26. Contour map illustrating clay thickness in the study area by land loss from time interval A.

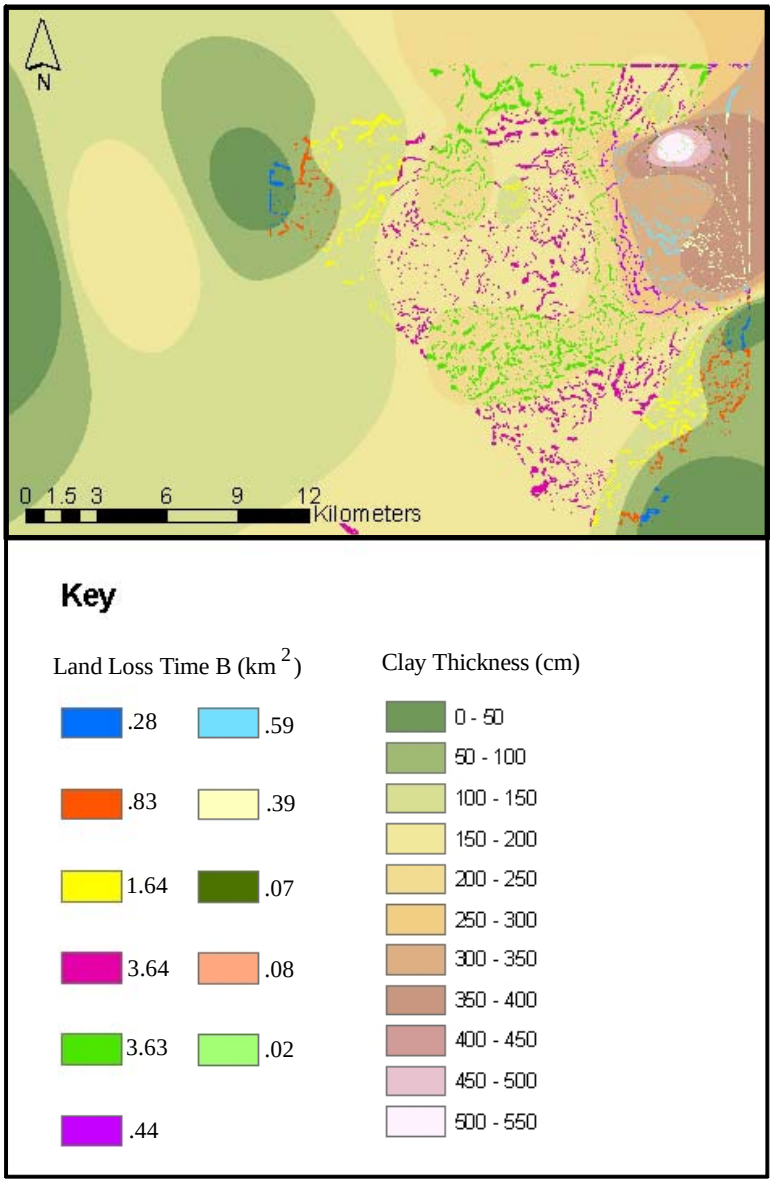

Figure 1.27. Contour map illustrating clay thickness in the study area overlain by land loss from time interval B.

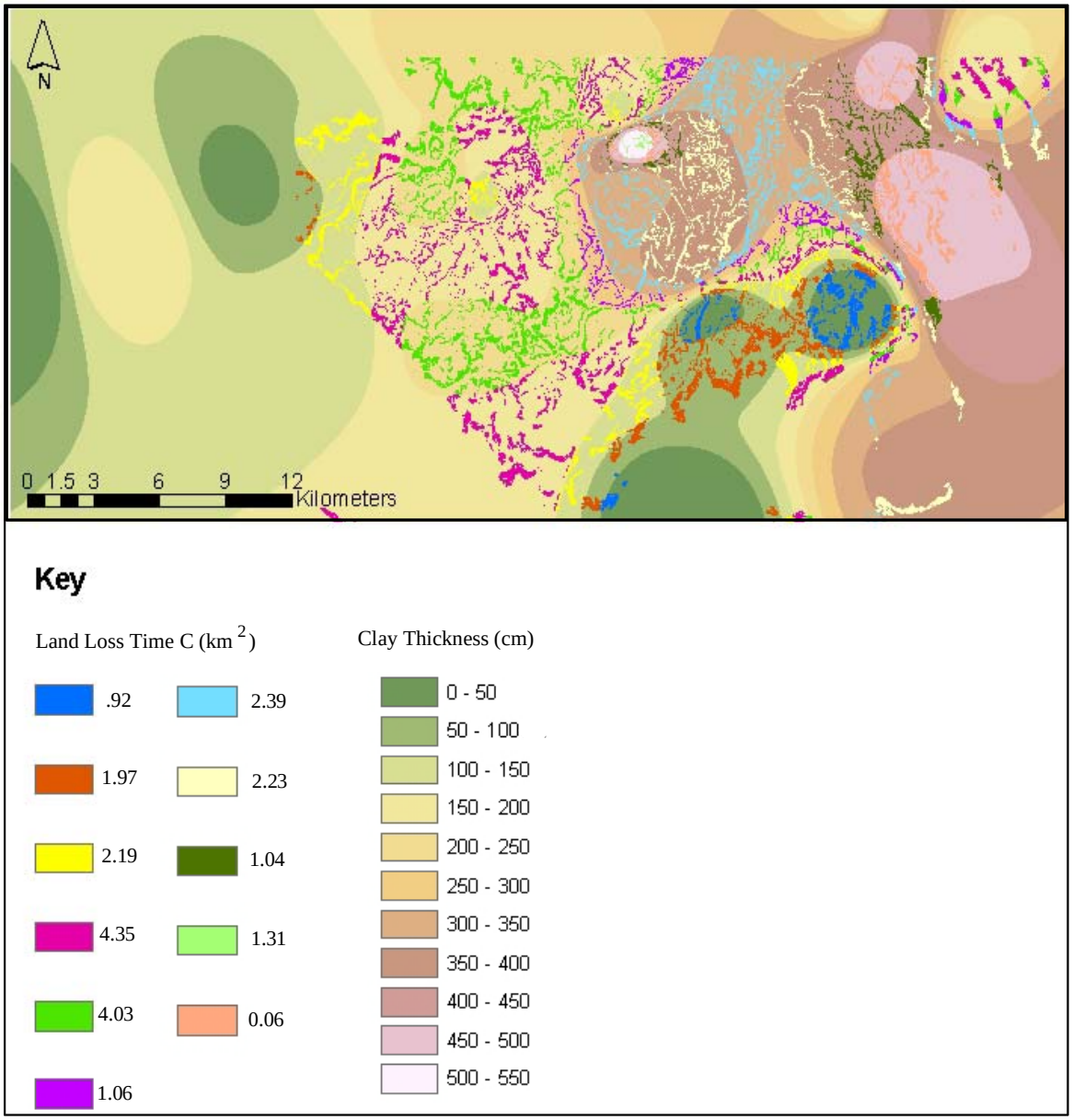

Figure 1.28. Contour map illustrating clay thickness in the study area overlain by land loss from time interval C.

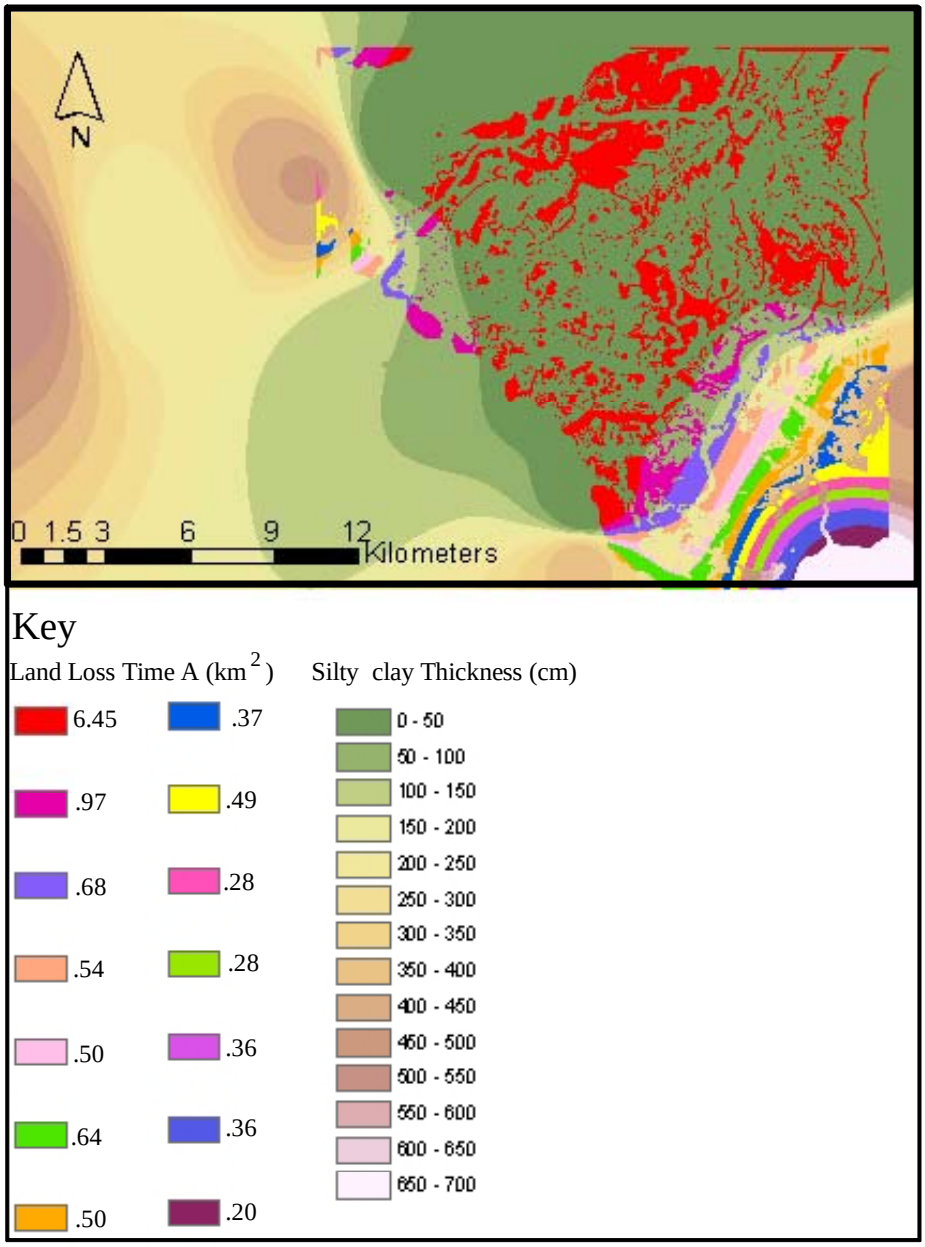

Figure 1.29. Contour map illustrating silty clay thickness in the study area overlain by land loss from time interval A.

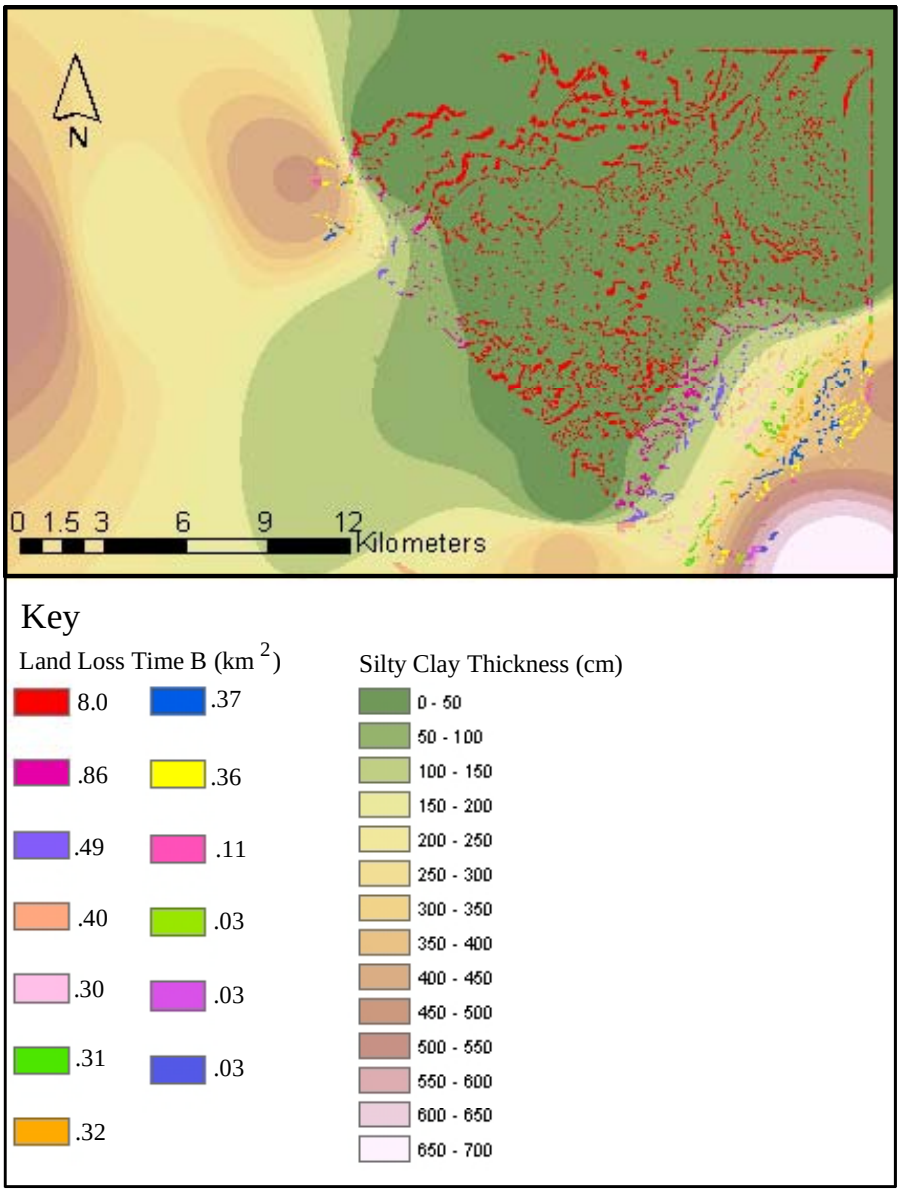

Figure 1.30. Contour map illustrating silty clay thickness in the study area overlain by land loss from time interval B.

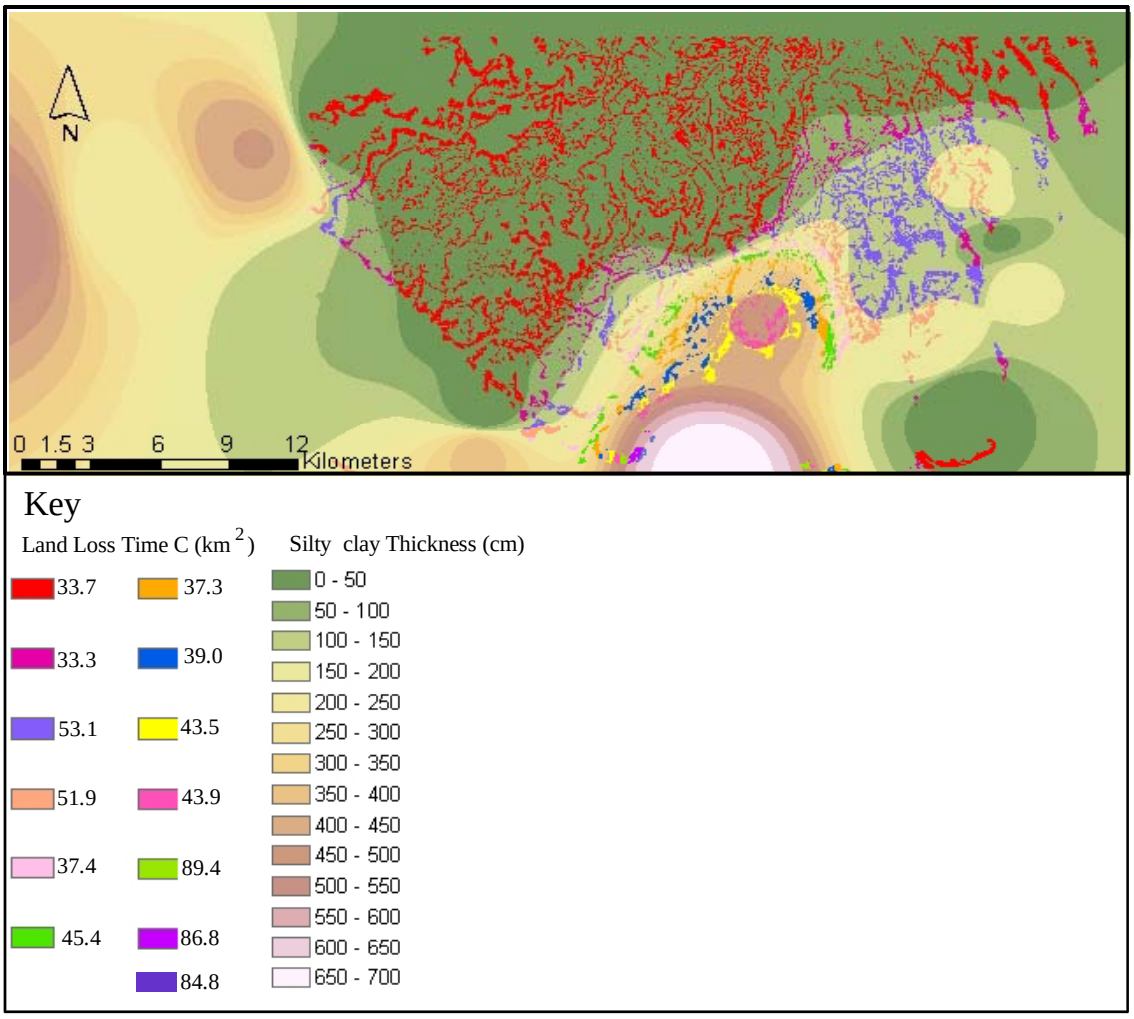

Figure 1.31. Contour map illustrating silty clay thickness in the study area overlain by land loss from time interval C.

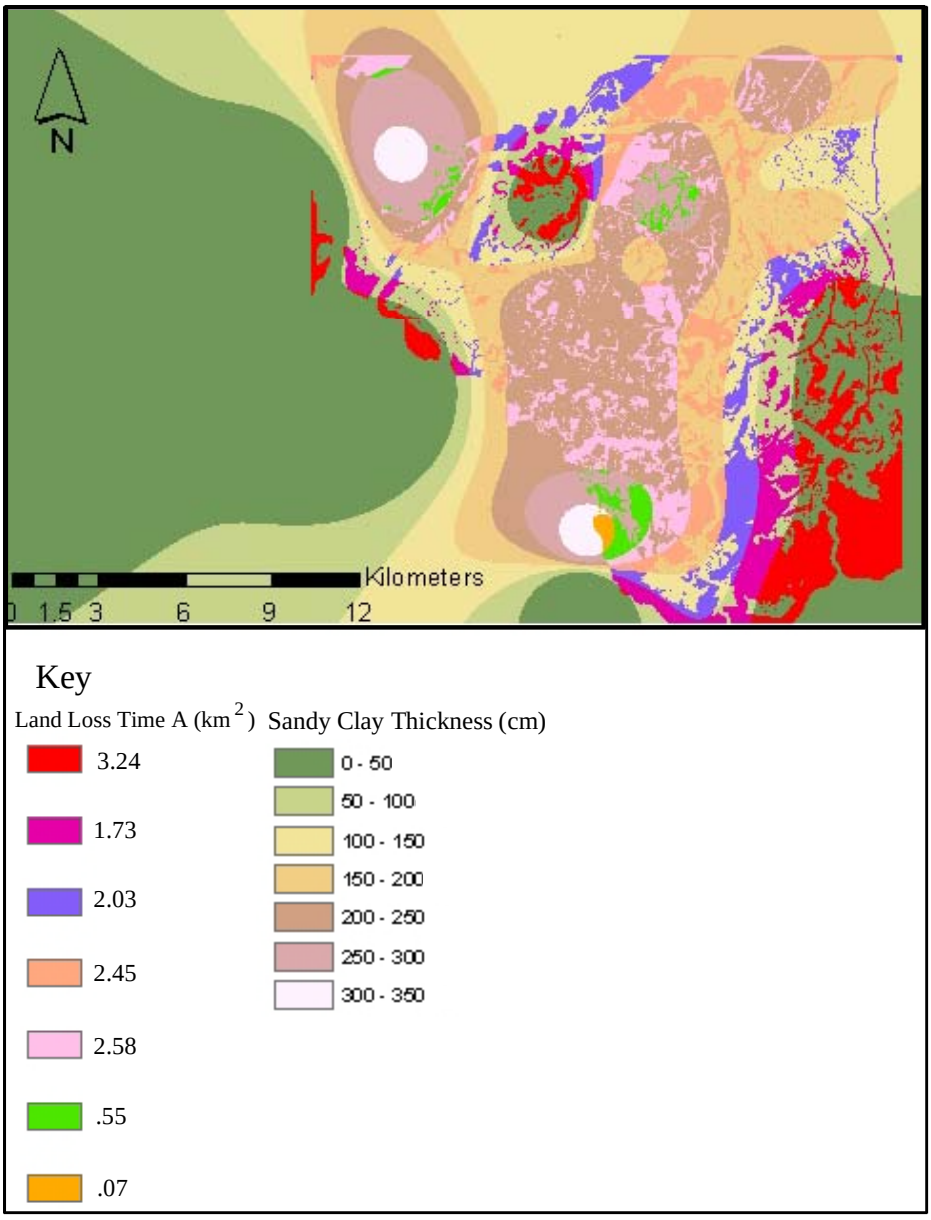

Figure 1.32. Contour map illustrating sandy clay thickness in the study area overlain by land loss from time interval A.

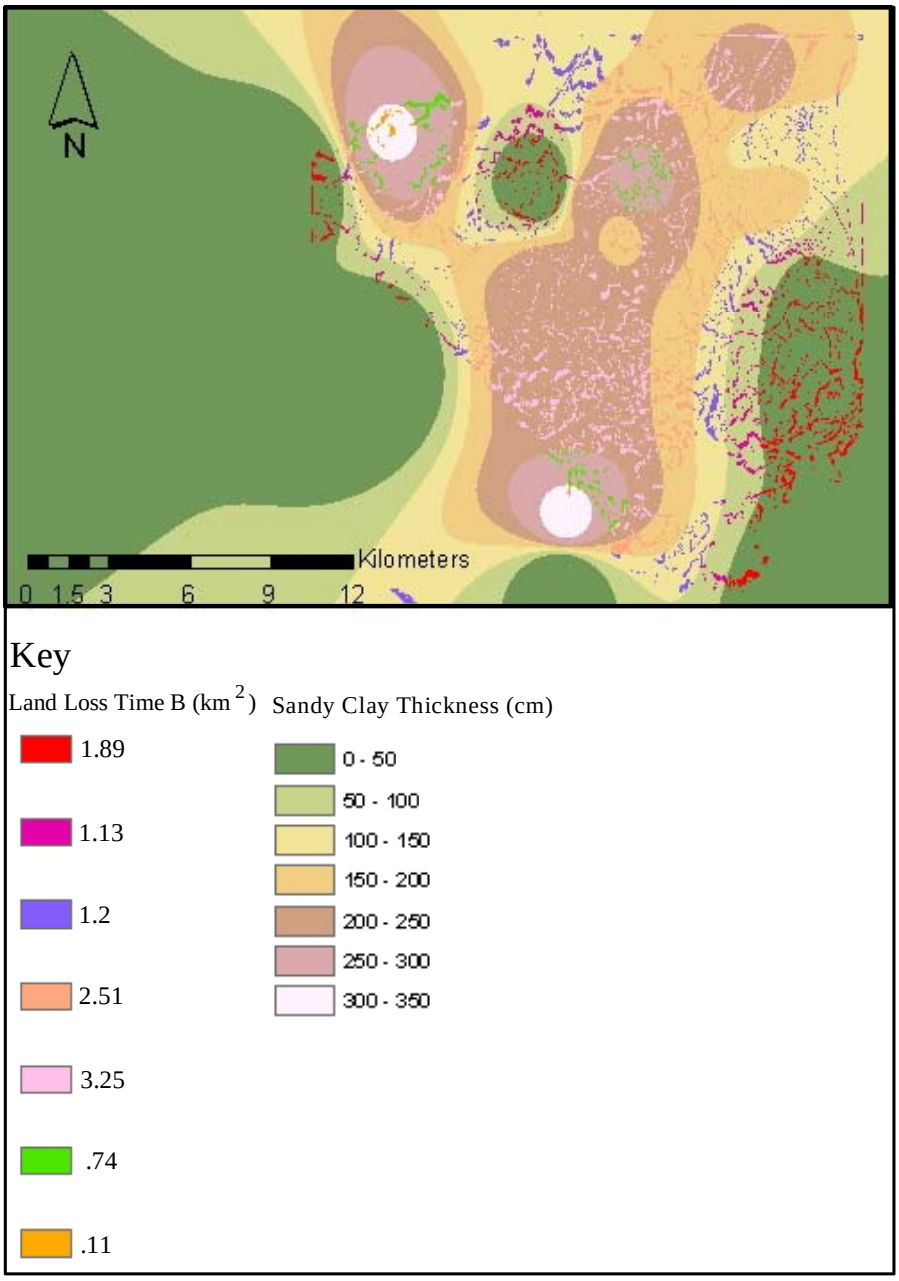

Figure 1.33. Contour map illustrating sandy clay thickness in the study area overlain by land loss from time interval B.

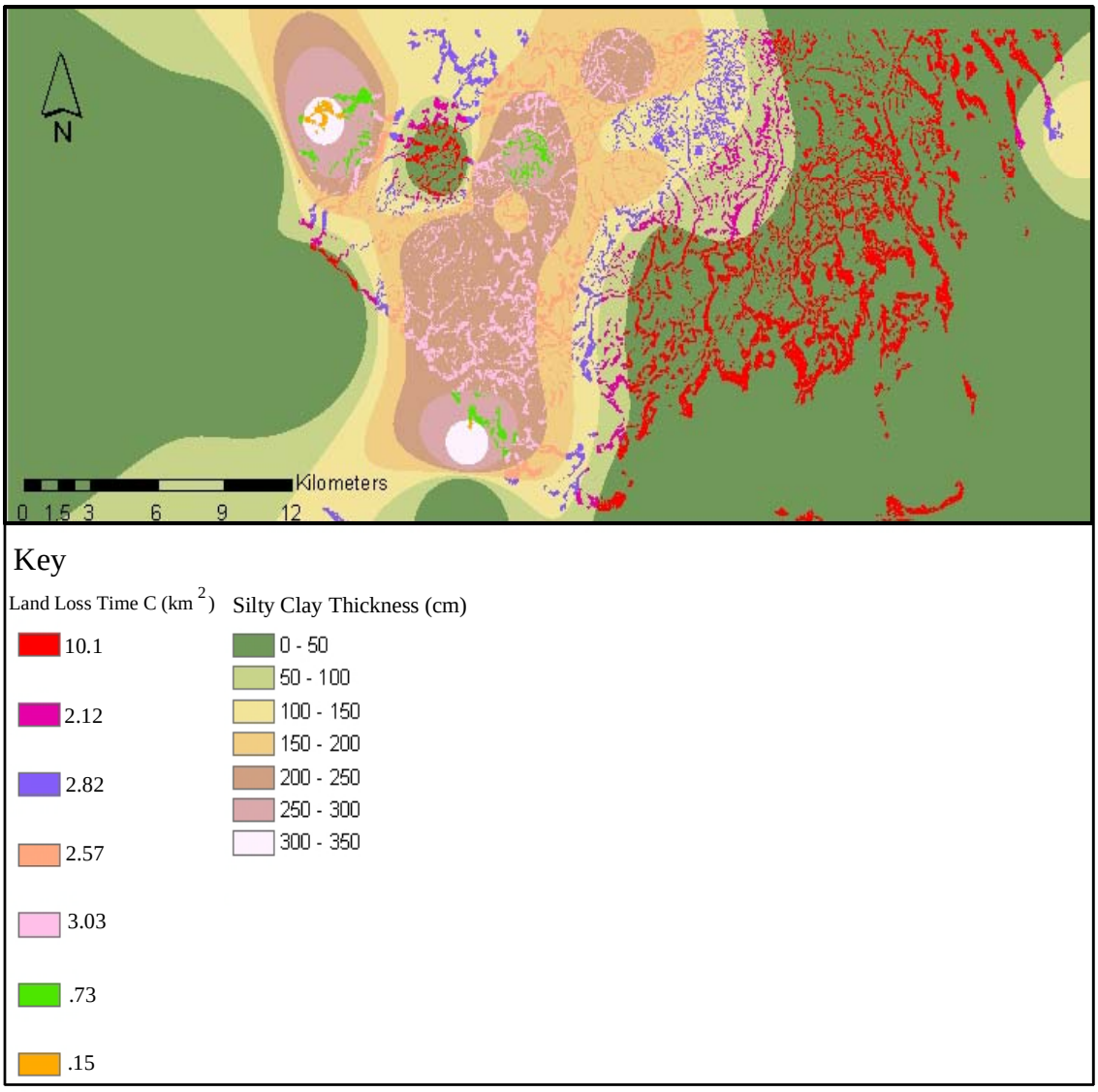

Figure 1.34. Contour map illustrating sandy clay thickness in the study area overlain by land loss from time interval C.

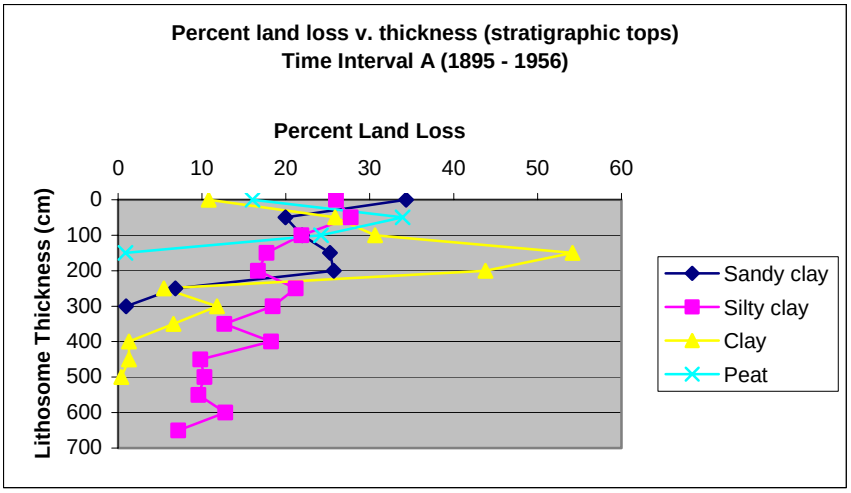

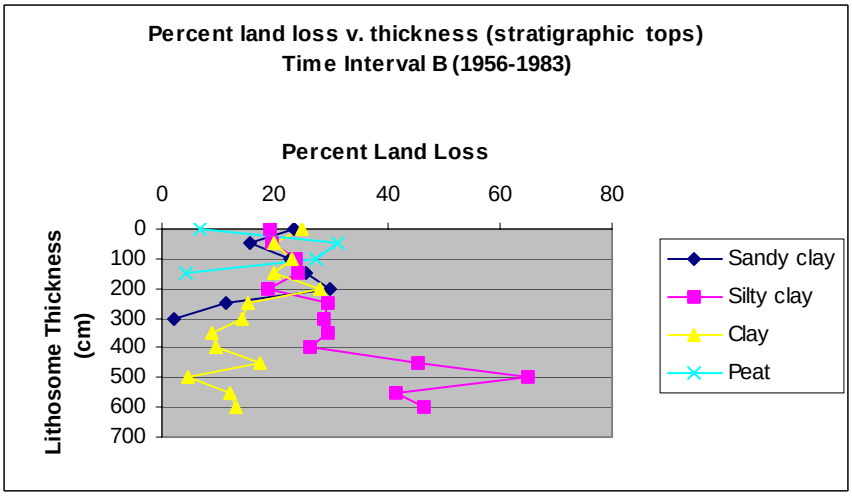

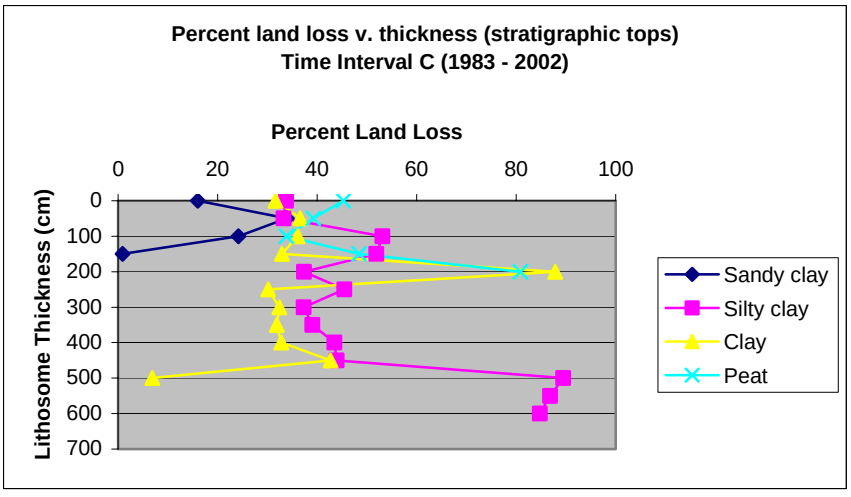

Figure 1.35. The graphs plot percent land loss versus the thickness of the lithosomes present in the study area.

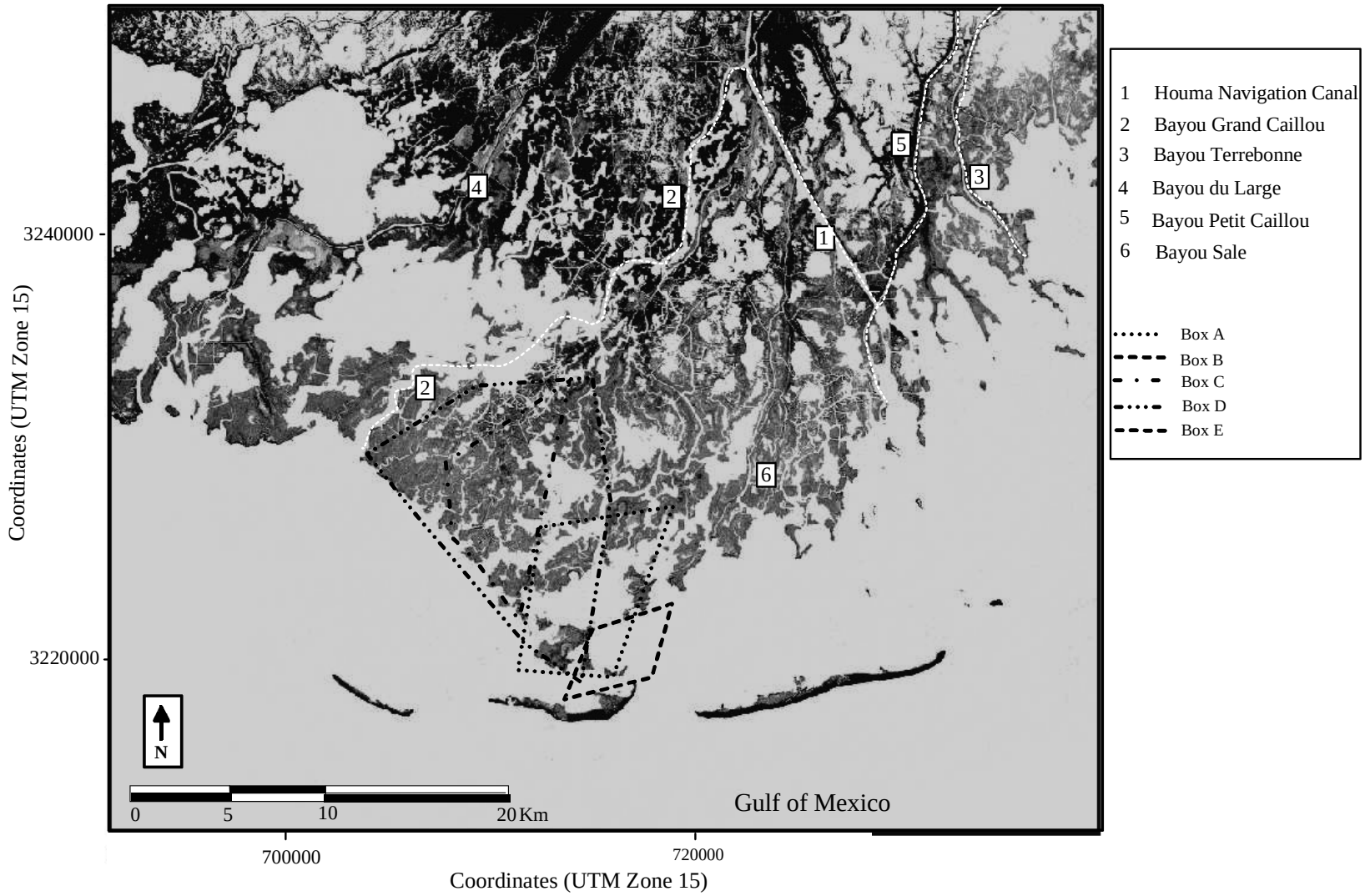

Figure 1.36 – Map highlighting the areas of significant land loss.

Summary

Data acquired in this study was analyzed to determine whether a spatial correlation exists between surficial land-loss patterns and the distribution of subsurface lithosomes within a deltaic headland. Though no direct correlation was observed, several areas of significant land loss for each time interval investigated were identified.

Overall a progression of marginal to interior headland land loss was documented with the historical map datasets. The central portion of the headland underwent minimal land loss through time, and this may reflect the presence of natural levees. Compared to most of the delta plain these geomorphic features consist of relatively coarse-grained sediment and are less susceptible to erosion.

Several problems were encountered in the development of a historical map database. The historic maps (pre-1950) had well defined shorelines and bayous, but the interior marsh coverage did not contain much detail. A major component of this project was to determine where land loss had taken place so that the geographic distribution of loss could be compared to the subsurface stratigraphic framework. In the case of the pre-1950 maps it was not possible to derive highly accurate land-loss patterns because of the limited accuracy of the early maps. For the intervals of comparison that included pre-1950 maps it was impossible to fully assess the role of subsurface stratigraphy on surficial headland evolution.

A second major problem encountered involved the modern maps (post-1950). These maps were of a much greater accuracy pre-1950 maps, but contained a much more substantial anthropogenic influence. On these maps the existence of canals and “borrow pits” increased substantially as human occupation and utilization of the coastal zone

progressed. Consequently, it was difficult to differentiate between natural and anthropogenic land loss within these.

A final factor that likely influenced the results of this study was that the subsurface sediment distribution of the Caillou headland consisted of more homogenous sediment than was expected. Background research and core data indicated a heterogeneous distribution of sediments yet, the strata logged in cores for this study was overall very fine-grained in nature. In this sense the limited variability limited the spectrum of possible surficial responses to subsurface compaction of stratigraphic units.

Future Work

There are several ways that a study similar to this project could be enhanced and refined as a means of further investigating the linkage between subsurface units and surface evolution. The first consideration would be to repeat this study in an area with few anthropogenic influences. These effects were difficult to account for in the map analysis, so studying an area less developed may help to better determine patterns of natural change. Another possibility is to constrain the geomorphic evolution with a more robust map database, so that some of the anthropogenic effects can be more easily identified. Finally, the study could be repeated on a headland with a more heterogeneous lithosome distribution to more effectively test the role of differential compaction on headland evoluion.

Works Cited

Barras, J.A., Beville, S., Britsch, D., Hartley, S., Hawes, S., Johnston, J., Kemp, P., Kilner, Q., Martucci, A., Porthouse, J., Reed, D., Roy, K., Sapkota, S., and Suhayda, J., 2003, Historical and projected coastal Louisiana land changes: 1978-2050: USGS Open File Report 03-334.

Britsch, L.D., and Dunbar, J.B., 1993, Land loss rates: Louisiana Coastal Plain: Journal of Coastal Research, v.9, no.2, p. 324-338.

Clayton, C.R.I., Muller, S. H., Powrie, W.,1995, Terzaghi's theory of consolidation, and the discovery of effective stress: Proceedings - ICE: Geotechnical Engineering, v. 113, no.4, p. 191-205

Coleman, J.M., and Gagliano, S.M., 1964, Cyclic sedimentation in the Mississippi River delta plain: Gulf Coast Association of Geological Societies Transactions, v. 14, p. 67-80.

Erdas, 2001, Erdas Imagine Tour Guides: Atlanta, Erdas, 662 p.

Fisk, H.N., 1944, geological investigations of the alluvial valley of the lower Mississippi River: U.S. Army Corp of Engineers Report, Mississippi River Commission, 78 p.

Fisk, H.N., 1955, Sand facies of the recent Mississippi delta deposits: Proceedings of the 4th World Petroleum Congress, Rome, Sect. 1-C, p. 377-398.

Fisk H.N., and McFarlan, E., 1955, Late Quaternary deltaic deposits of the Mississippi River: in: The Crust of the Earth. Geological Society of America, Special Paper 62, p. 279-302.

Frazier, D.E., 1967, Recent deltaic deposits of the Mississippi River: their development and chronology: Gulf Coast Association of Geological Societies Transactions, v. 17, p. 287-311.

Gagliano, S.M., Myer-Arendt, K.J., Wicker, K.M., 1981, Land loss in the Mississippi River deltaic plain: Gulf Coast Association of Geological Societies Transaction, v. 31, p. 295-306.

Giles, M.R., Indrelid, S.L., James, D.M.D., 1998, Compaction the great unknown in basin modeling: In: Dueppenbecker, S.J. and Iliffe, J.E. (eds) Basin Modelling: Practice and Progress. Geological Society, London, Special Publications, v. 141, p. 15-43.

Kennedy, M., and Kopp, S., 2002, Understanding map projections: New York, Environmental Systems Research Institute, 110 p.

Kindinger, J. L., Flocks, J.G., Penland, S., Kulp, M., and Britsch, L. D., 2002, Environmental Atlas of the Lake Pontchartrain Basin, http://pubs.usgs.gov/of/2002/of02-206, Open File Report 02-206 CD-ROM, and HTML, U.S. Geological Survey, Center for Coastal and Regional Marine Geology, St. Petersburg, Florida.

Kolb, C.R., and van Lopik, J. 1958, Geology of the Mississippi River deltaic plain, southeastern Louisiana: U.S. Army Corps of Engineers, Waterways Experiment Station, Technical Report 2, 482 p.

Kucher, G.J., 1994, Geologic framework and consolidation settlement potential of the Lafourche delta, topstratum valley fill sequences: implication for wetland loss in Terrebonne and Lafourche Parishes, Louisiana [Ph.D. Thesis]: Louisiana State University, 346 p.

Kulp, M.A., Howell, P., Adiau, S., Penland, S., Kindinger, J.L., and Williams, S.J.,. Latest Quaternary stratigraphic framework of the Mississippi River delta region: Transactions - Gulf Coast Association of Geological Societies, *in* Gulf Coast Association of Geological Societies and Gulf Coast Section SEPM; technical papers and abstracts. (S. P. Dutton, editor and others), v. 52, p. 573-582.

Penland S., Suter J.R., McBride, R.A., 1987, Delta plain development and sea level history in the Terrebonne coastal region, Louisiana: In: Kraus, N. (ed),Coastal Sediment Conference 1987, American Society of Civil Engineers, p. 1689-1705.

Penland, S., Boyd, R., and Suter J.R., 1988, Transgressive depositional systems of the Mississippi delta plain: a model for barrier shoreline and shelf sand development: Journal of Sedimentary Petrology, v. 58, no. 6, p. 932-949.

Roberts, H.R., Bailey, A., Keucher, J.K., 1994, Subsidence in the Mississippi River Delta – important influences of valley filling by cyclic deposition, primary consolidation phenomena, and early diagenesis: Transactions of the Gulf Coast Association of geological societies, v. 64, p. 619-629.

Stuiver M., Reimer P.J., Braziunas T.F., 1998, High-precision radiocarbon age calibration for terrestrial and marine samples: Radiocarbon, v. 40, no. 3, p. 1127-1151.

Terzaghi, K., 1943, Soil mechanics in engineering practice: New York, J. Wiley, 566 p.

Wentworth, C. K., 1922, A scale of grade and class terms for clastic sediments: Journal Geology, v.30, p. 377-392.

Appendix A

Core Description Log

UNIVERSITY OF NEW ORLEANS

DEPARTMENT OF GEOLOGY AND GEOPHYSICS

VIBRACORE DESCRIPTION SHEET

CORE ID: 03-CH-01 DATE: Aug 3, 2003 DESCRIBED BY: Liz

ELEVATION: LOCATION: Caillou Bay Headland

CORE LENGTH: 4.68 LAT/LONG: 714 279, 3234623

TOTAL DEPTH: 5.30 COMPACTION: 1.32cm

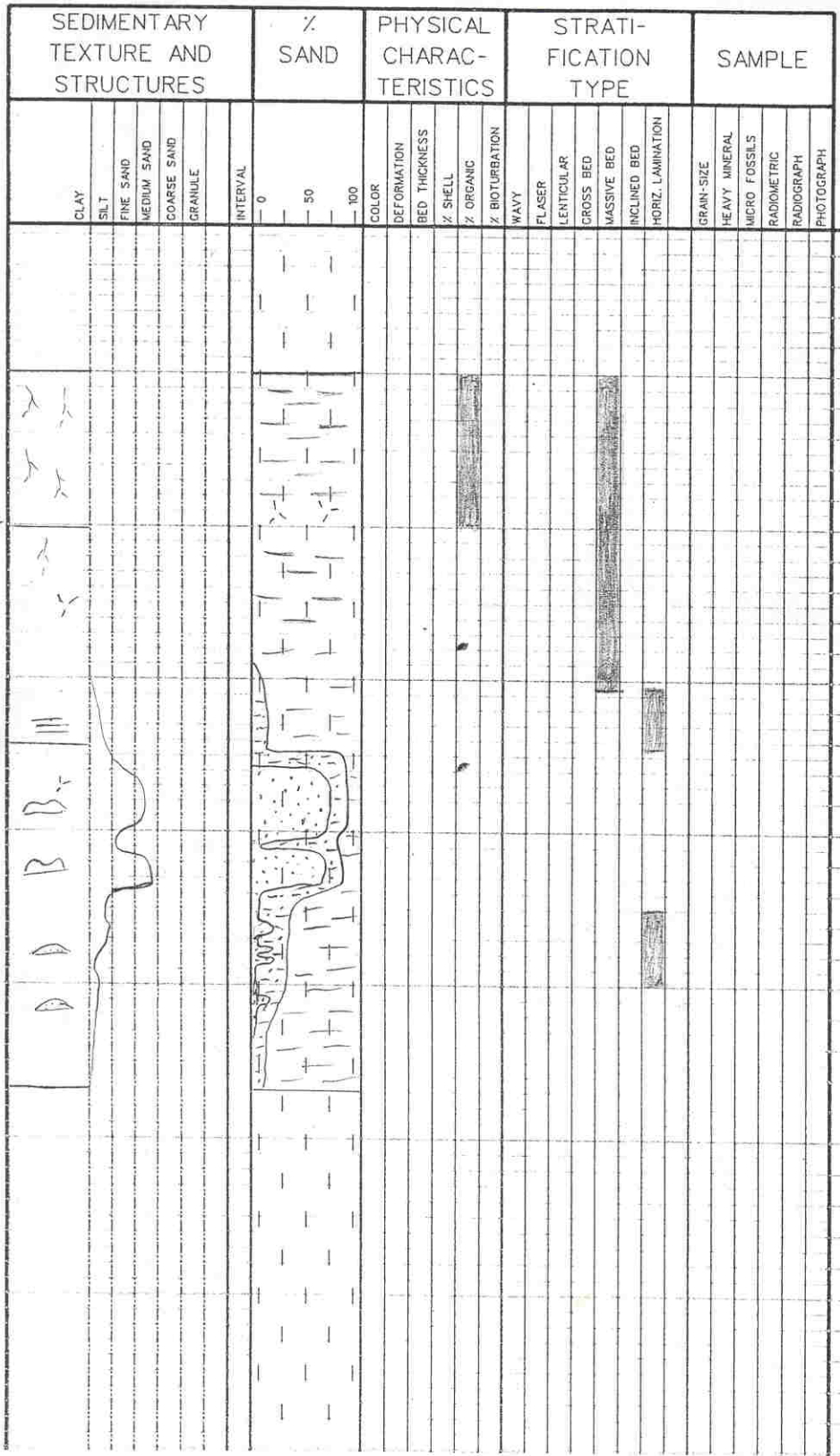

PHYSICAL DESCRIPTION

0 - 102 cm

0-74cm, near Marsh surface with thick in situ rooting that grades to clay with organics and sparse rooting, olive black (5Y 2/1), sharp contact;

74-102 cm, unconsolidated organic material, greenish black (5GY 2/1), sharp bottom contact.

102 - 243 cm

102-193, massive clay, brownish gray (5YR 4/2), some organic fragments present (170, 173, 179 cm);

193-243, sandy clay, olive gray (5Y 4/1), horizontal laminations, yellow fragments, gradational contact.

243 - Bottom

Sandy clay, olive gray (5YR 4/2), horizontal lamination and sand stringers (320-324, 353-361, 365-367, 382-384, 412-421, 422-423, 435-437, 447-449 cm), interbedded yellow clay lamina (300, 330, 340, 369, 380, 405, 440, 452 cm) root fragments at 255cm.

UNIVERSITY OF NEW ORLEANS

DEPARTMENT OF GEOLOGY AND GEOPHYSICS

VIBRACORE DESCRIPTION SHEET

CORE ID: 03SCC02-02 DATE: 11-15-03 DESCRIBED BY: liz

ELEVATION: _____ LOCATION: Caillou Bay Headland

CORE LENGTH: 5.20 LAT/LONG: 230485, 3225712

TOTAL DEPTH: 8.40 COMPACTION: _____

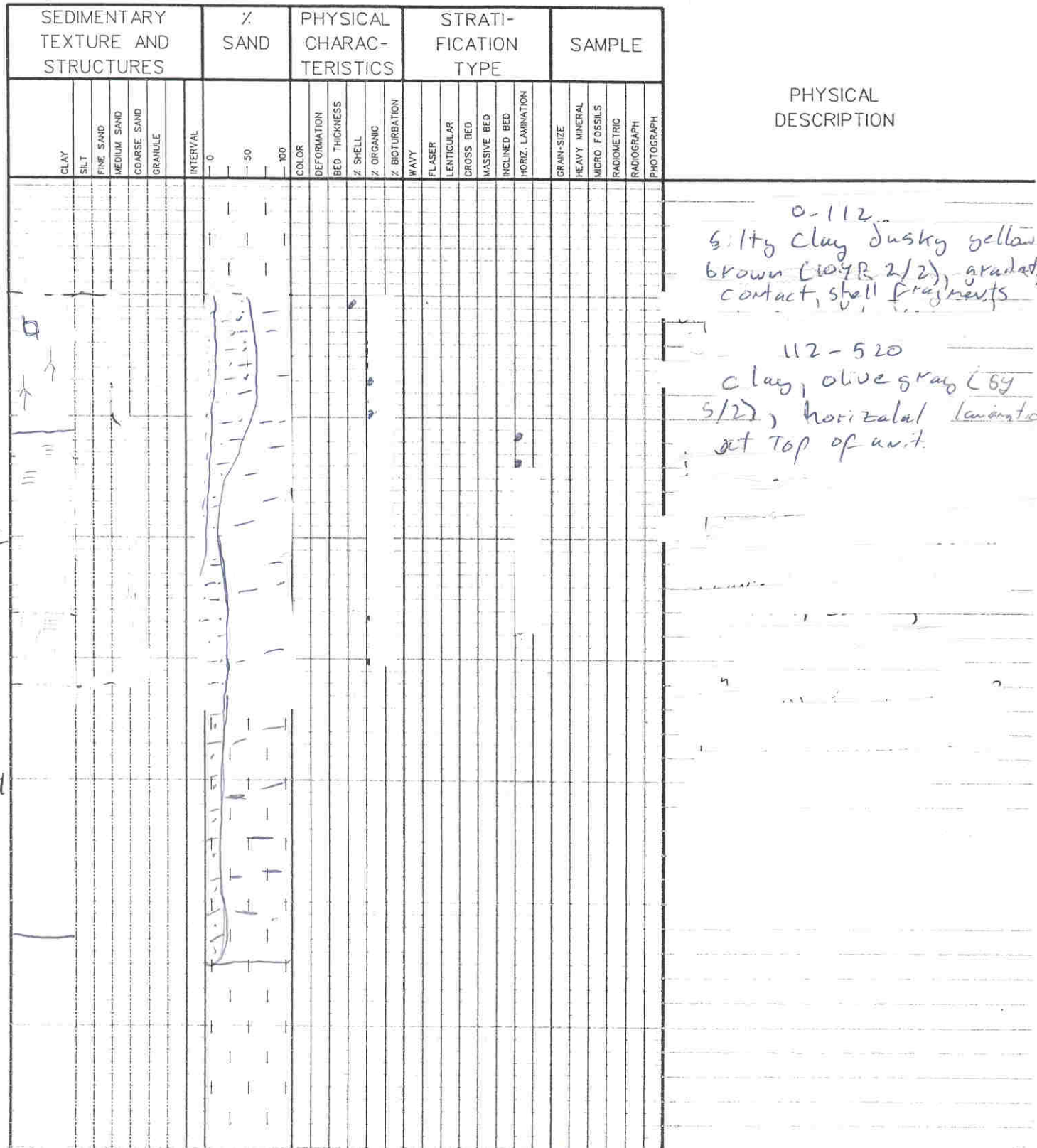

0-112

silty clay dusky yellow brown (10YR 2/2), gradational contact, shell fragments

112-520

clay, olive gray (5Y 5/2), horizalal lamination at top of unit

UNIVERSITY OF NEW ORLEANS

DEPARTMENT OF GEOLOGY AND GEOPHYSICS

VIBRACORE DESCRIPTION SHEET

CORE ID: 03-CH-03 DATE: Sep 15, 2003 DESCRIBED BY: Liz

ELEVATION: LOCATION: Caillou Bay Headland

CORE LENGTH: 5.35m LAT/LONG: 717197, 3228021

TOTAL DEPTH: 5.95m COMPACTION: 1.50m

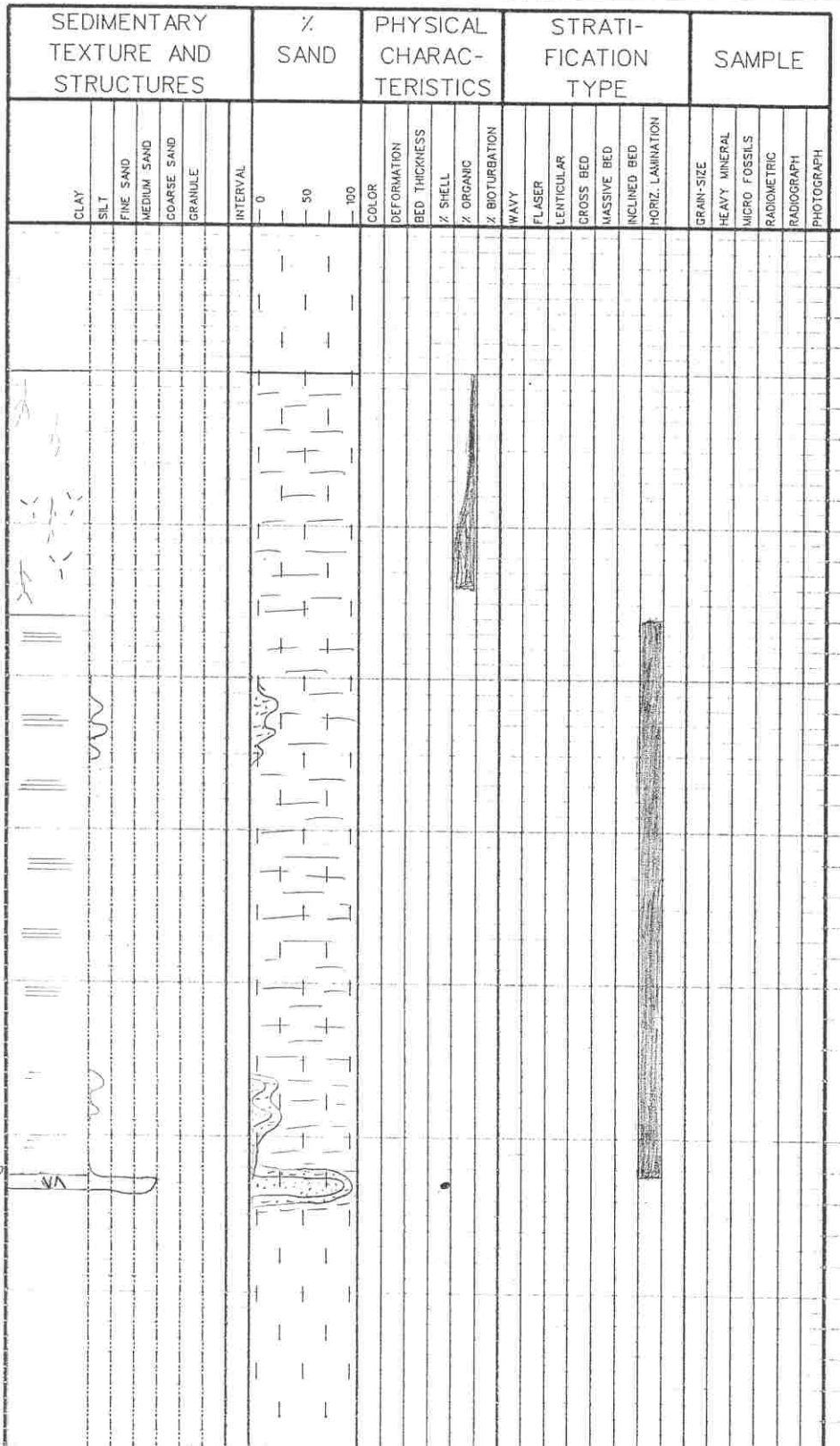

PHYSICAL DESCRIPTION

0 - 159 cm

0-73cm, clay near marsh edge, unconsolidated organic matter and in situ rooting, dusky yellow brown (10YR 2/2), gradational contact; 73-159cm, unconsolidated organic matter with thick in situ rooting grading to clay, olive black (5Y 2/1) grading to brownish gray (5Y 4/1), gradational contact.

159 - 525 cm

Clay, olive gray (5Y 4/1) horizontal laminations, sharp contact.

525 - bottom

Sand, light olive gray (5Y 6/1), interbedded clay (530 - 535), organic fragments (525, 527), large rangia clam shell (531 cm).

UNIVERSITY OF NEW ORLEANS

DEPARTMENT OF GEOLOGY AND GEOPHYSICS

VIBRACORE DESCRIPTION SHEET

CORE ID: 03-CH-04 DATE: Aug 3 2003 DESCRIBED BY: Liz

ELEVATION: LOCATION: Caillou Bay Headland

CORE LENGTH: 3.96m LAT/LONG: 718421, 3225509

TOTAL DEPTH: 4.46m COMPACTION: 1.10m

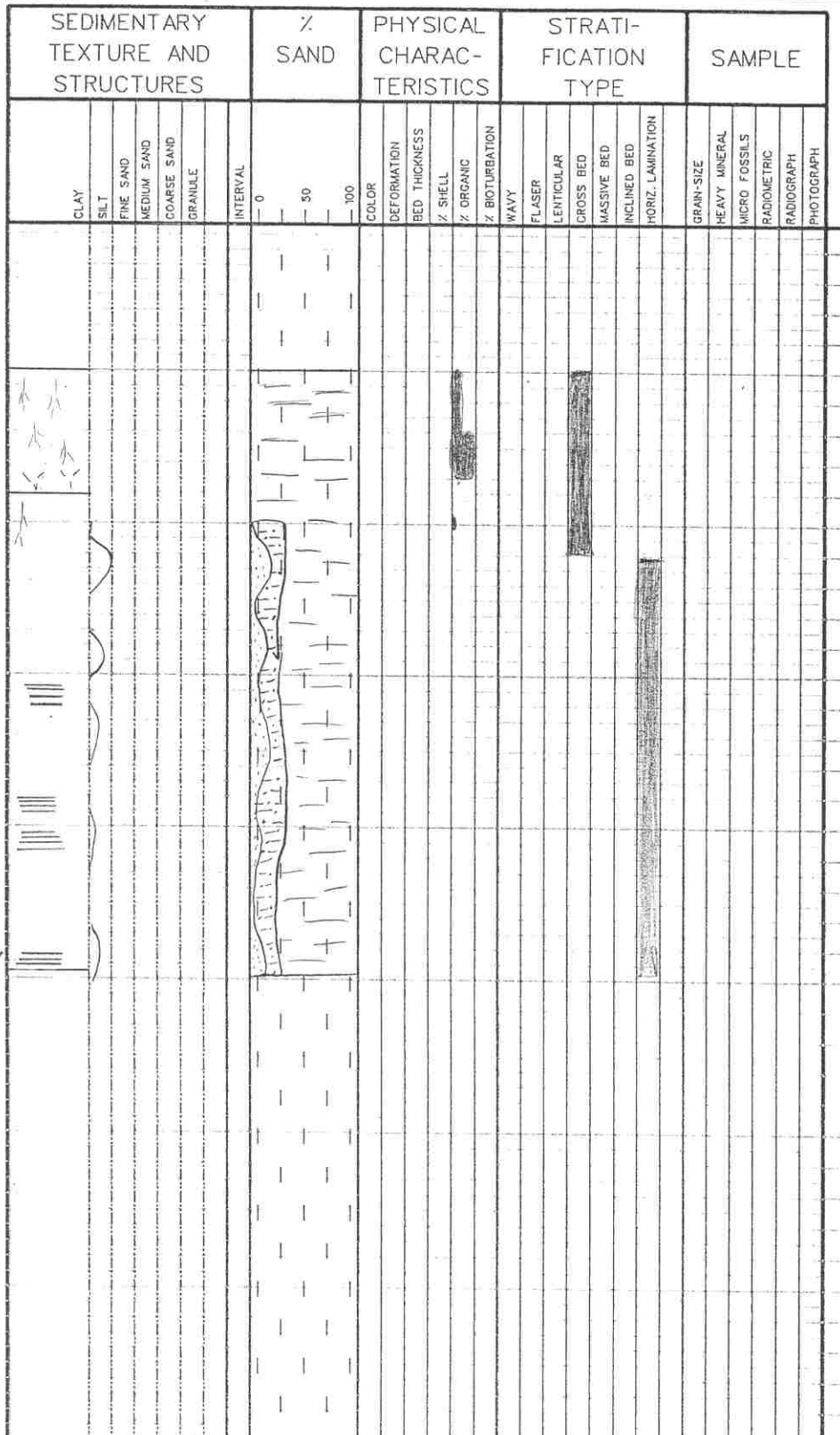

PHYSICAL DESCRIPTION

0-81 cm

0-45 cm, near Marsh surface, clay with sparse in situ rooting, dusky yellowish brown (10YR 2/2);

45-81 cm, Thick unconsolidated organics, sparse in situ rooting, greenish black (5G 2/1), sharp bottom contact

81 - Bottom

81 - 173 cm, silty clay, pale yellowish brown (10YR 6/2), sand layers (115-119, 120-173 cm), interbedded yellow clay lamina (122, 132, 156, 163 cm), sharp bottom contact;

173 - Bottom, silty to sandy clay, dark yellowish brown (10YR 4/2), reddish clay lamina 180 cm, Yellow clay lamina (300, 311, 343, 356 cm), Interbedded Sand (173-178, 192-207, 230-232, 240-242, 260-268, 287-291, 304-309), horizontal bedding.

UNIVERSITY OF NEW ORLEANS

DEPARTMENT OF GEOLOGY AND GEOPHYSICS

VIBRACORE DESCRIPTION SHEET

CORE ID: 03-CH-05 DATE: 11-03-03 DESCRIBED BY: Liz

ELEVATION: LOCATION: Caillou Bay Headland

CORE LENGTH: 5.42 m LAT/LONG: 6972908, 3231854

TOTAL DEPTH: 6.34 m COMPACTION: .81 m

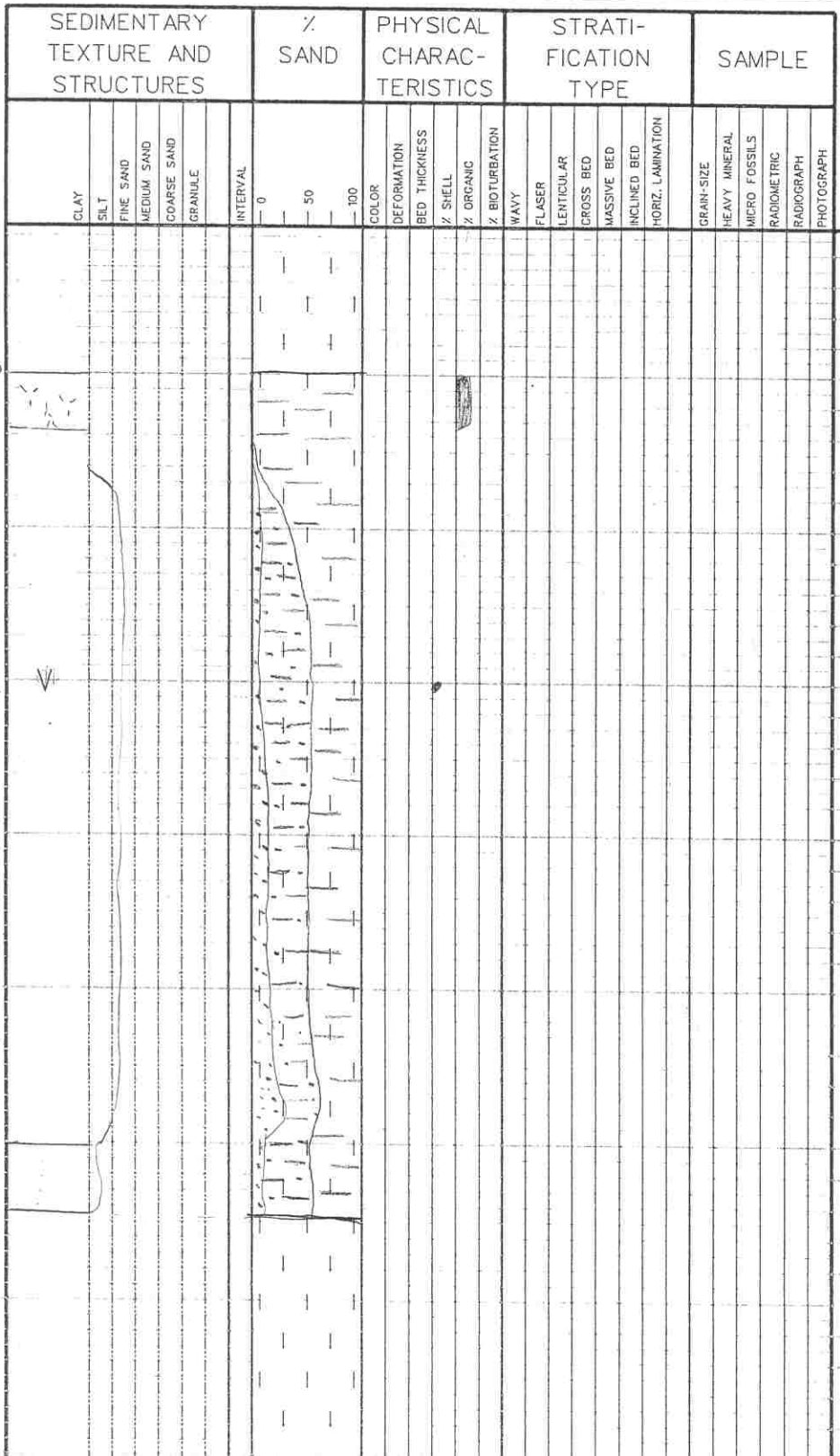

PHYSICAL DESCRIPTION

0-33cm
Near marsh surface, clay with unconsolidated organic matter, dark yellowish (10YR 2/2), sparse in situ rooting, sharp contact,

33-501 cm
silty clay, dusky brown (5YR 2/2) silty stringers (161-163, 179, 201, 207-210, 216, 221, 223, 240, 243, 367, 401, 425-430, 450-454, 461) sandy lamina 497-501, articulated ranella clam shell 200 cm, sharp contact

501-542 cm
clay, dusky yellow brown (10YR 2/2), silt stringers (510, 520),

UNIVERSITY OF NEW ORLEANS

DEPARTMENT OF GEOLOGY AND GEOPHYSICS

VIBRACORE DESCRIPTION SHEET

CORE ID: 03-CH-06 DATE: 10-30-03 DESCRIBED BY: Liz

ELEVATION: LOCATION: Caillou Bay Headland

CORE LENGTH: 5.22m LAT/LONG: 700528, 3233166

TOTAL DEPTH: 6.09m COMPACTION: .24m

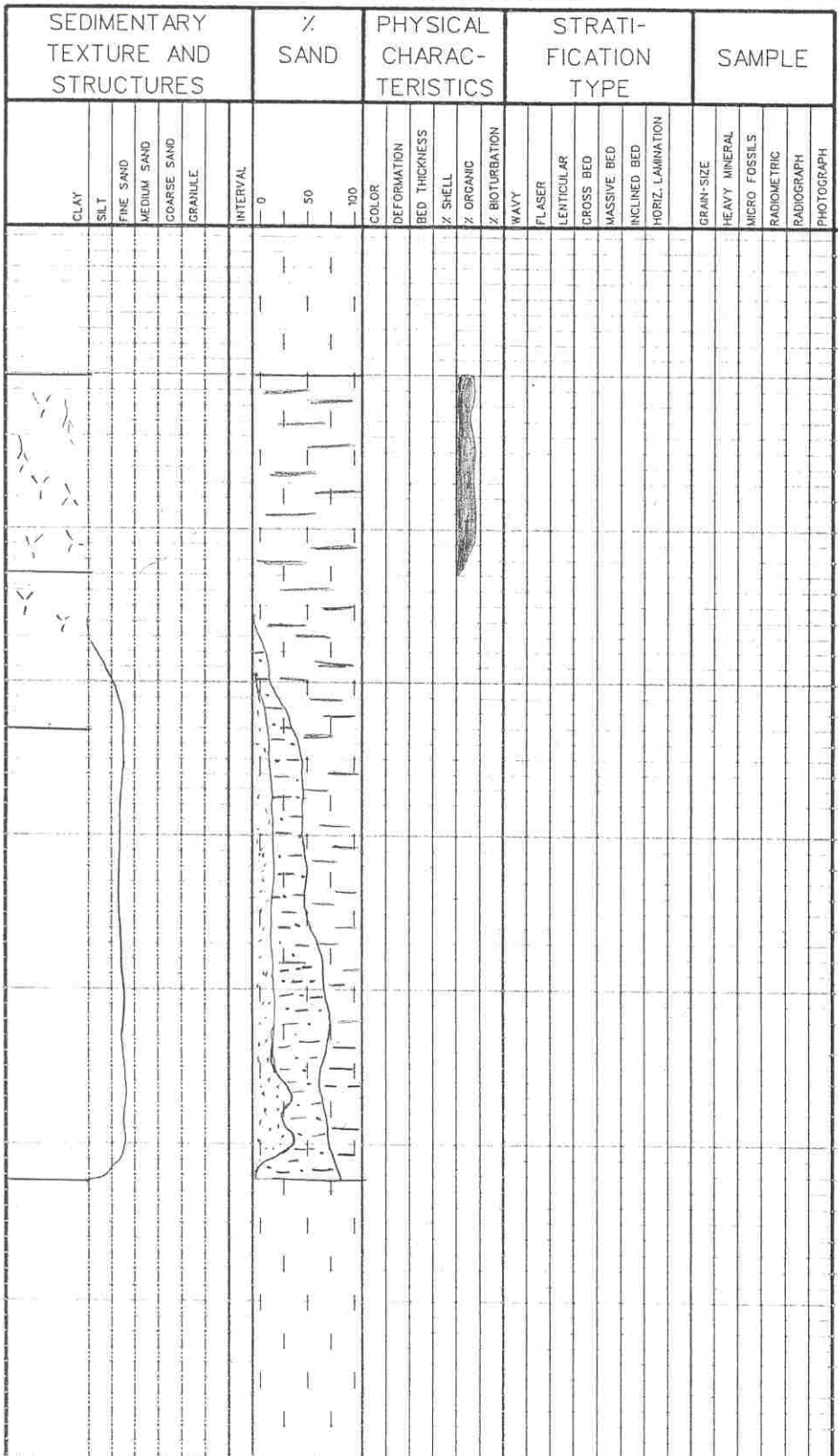

PHYSICAL DESCRIPTION

0-128 cm

Near marsh surface, olive black (5Y 2/1), sparse in situ rooting, bulk of unit unconsolidated organic material, clay lamina (3-4cm, 12-14, 19-21, 57-59, 67-74, 86-89, 97-104), gradational contact,

128-230 cm

clay, dark yellowish brown (10YR 4/2), organic fragments (136, 159), silt stringer 164-166, red clay lamina 208, gradational contact

230-bottom

Silty clay with sandy to silty stringers, dark yellowish brown (10YR 4/2) silty stringers (230-240, 250, 284, 294, 306, 349-356, 398-415, 429-444, 457-460), sandy stringers (470-474, 507, 510-514),

UNIVERSITY OF NEW ORLEANS

DEPARTMENT OF GEOLOGY AND GEOPHYSICS

VIBRACORE DESCRIPTION SHEET

CORE ID: 03-CH-07 DATE: 11-12-03 DESCRIBED BY: Liz

ELEVATION: LOCATION: Caillou Bay Headland

CORE LENGTH: 4.24 m LAT/LONG: 706141, 3237396

TOTAL DEPTH: 4.68 m COMPACTION: .75 m

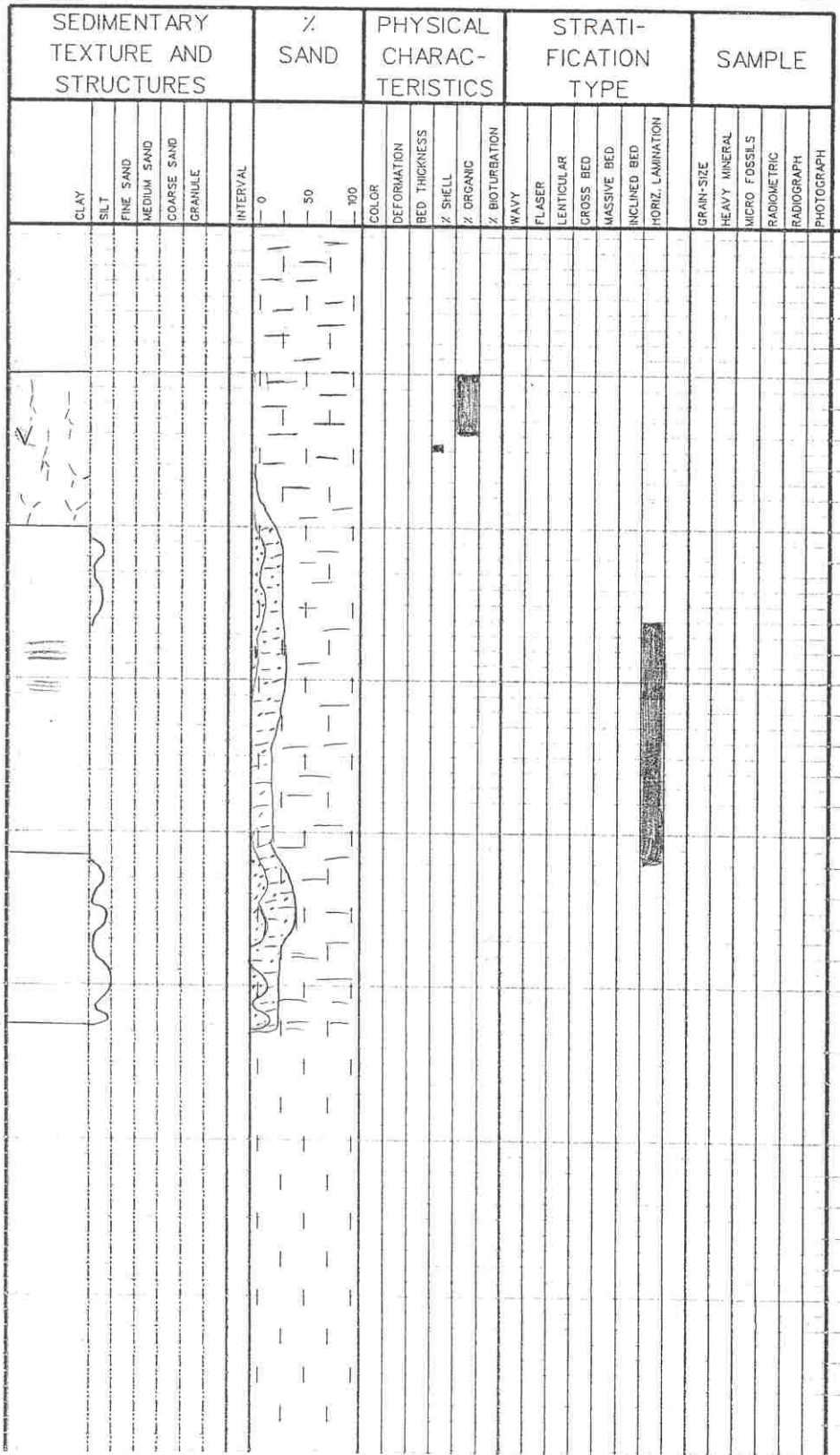

PHYSICAL DESCRIPTION

0-101

0-39 cm, near marsh surface, brownish black (5YR 2/1), unconsolidated organics with moderate in situ rooting, Mussel shells 38-39 cm, gradational contact.

39-101 cm, clay, brownish black (5YR 2/1), unconsolidated organics, sparse in situ rooting, sharp contact.

101-315

101-159, clay, light olive gray (5Y 6/1), Gradational contact

159-235, clay, pale yellowish brown (10YR 6/2), horizontal laminations, red laminations (236, 254, 276, 301), gradational contact

315-424

315-354, silty to sandy clay, dark yellowish brown (10YR 4/2), gradational contact.

354-424, Clay, moderate brown (5YR 3/4), Sand beds (362-367, 383-408, 419-424 cm)

UNIVERSITY OF NEW ORLEANS

DEPARTMENT OF GEOLOGY AND GEOPHYSICS

VIBRACORE DESCRIPTION SHEET

CORE ID: 03-CH-09 DATE: 11-13-03 DESCRIBED BY: Liz

ELEVATION: LOCATION: Caillou Bay Headland

CORE LENGTH: 4.71 m LAT/LONG: 706518, 3231224

TOTAL DEPTH: 5.84 m COMPACTION: 1.15m

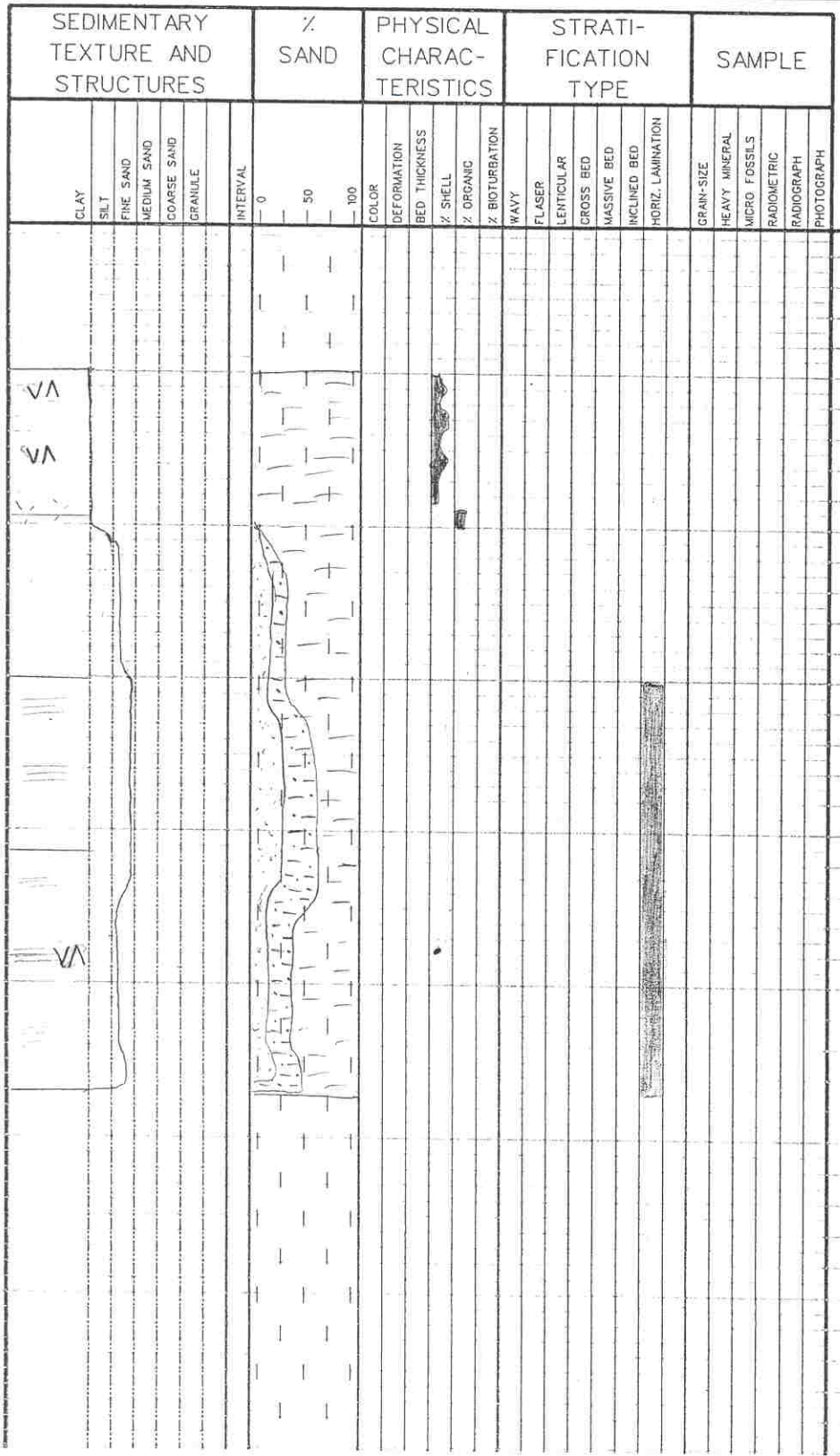

PHYSICAL DESCRIPTION

0-93 cm

clay, dusky brown (5YR 2/2) shell hash beds (17-20, 30-37, 43-44, 60-67, 83-84), unconsolidated organic matter 90-93cm, Gradual Contact.

93-200 cm

clay, pale brown (5YR 2/2), Organic Fragments (101, 108cm), large wood Fragments 114-122 cm, Gradual Contact

200-470cm

200-313cm, Sandy clay, pale yellowish brown (10YR 6/2), Trace organics (238, 292) Gradational Contact

313-470cm, clay, pale yellowish brown (10YR 6/2), horizontal lamination, Sand stringers (327-332, 343-345, 361-362, 385-389, 423-424, 431-432, 467-470cm), Rangia Clam Shell 379 cm.

UNIVERSITY OF NEW ORLEANS

DEPARTMENT OF GEOLOGY AND GEOPHYSICS

VIBRACORE DESCRIPTION SHEET

CORE ID: 03-CLT-10 DATE: 11-09-03 DESCRIBED BY: Liz

ELEVATION: LOCATION: Caillou Bay Headland

CORE LENGTH: 4.73m LAT/LONG: 706157, 3227999

TOTAL DEPTH: 5.74 m COMPACTION: .21m

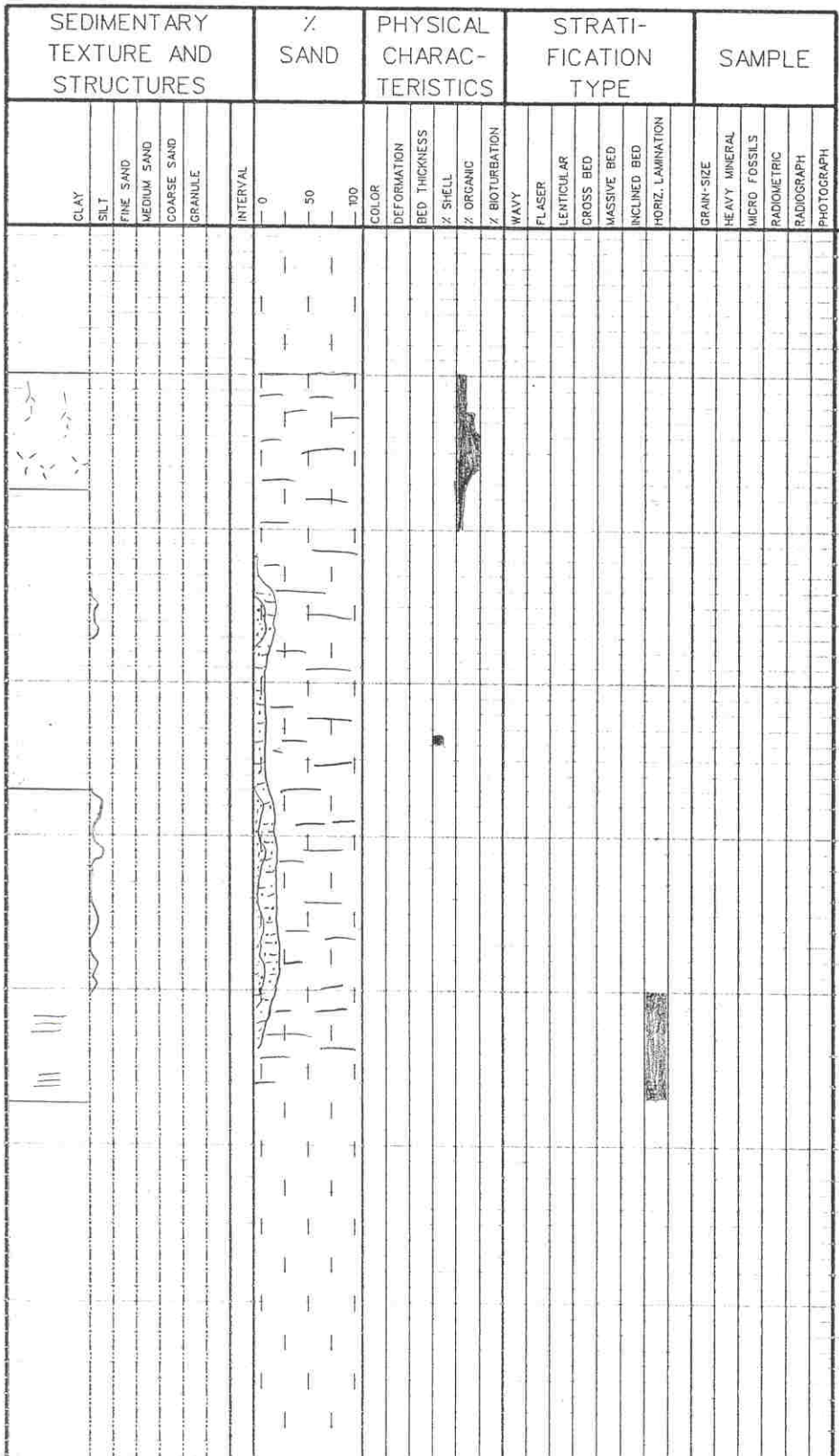

PHYSICAL DESCRIPTION

0-76 cm

0-25cm, clay, olive gray (5Y 3/2), moderate in situ rooting, gradational contact

25-76cm, near marsh surface, greenish black (5G 2/1), unconsolidated organic matter, sparse in situ rooting, clay lamina (39-41, 69), Gradational contact.

76-270cm

76-144, Clay, Olive gray (5Y 4/1), sparse organics and in situ rooting, gradational contact.

144-166 cm, clay, olive gray (5Y 4/1), silt stringers (144-146, 163-166, gradational contact,

166-270, Clay, olive gray (5Y 4/1), Massively bedded clay, snail shell 239cm, gradational contact.

270-473 cm

270-400, Silty to Sandy clay olive gray (5Y 4/1), Sandy beds beds (270-273, 310-314, 322-324, 330-333, 350-354, 373-375, 382-386(cm) gradational contact

400-473, clay, light olive gray (5y 4/1), horizontal laminations

UNIVERSITY OF NEW ORLEANS

DEPARTMENT OF GEOLOGY AND GEOPHYSICS

VIBRACORE DESCRIPTION SHEET

CORE ID: 03-CH-11 DATE: 11-09-03 DESCRIBED BY: Liz

ELEVATION: LOCATION: Caillou Bay Headland

CORE LENGTH: 5.041 m LAT/LONG: 706840, 3224692

TOTAL DEPTH: 5.44 m COMPACTION: .32cm

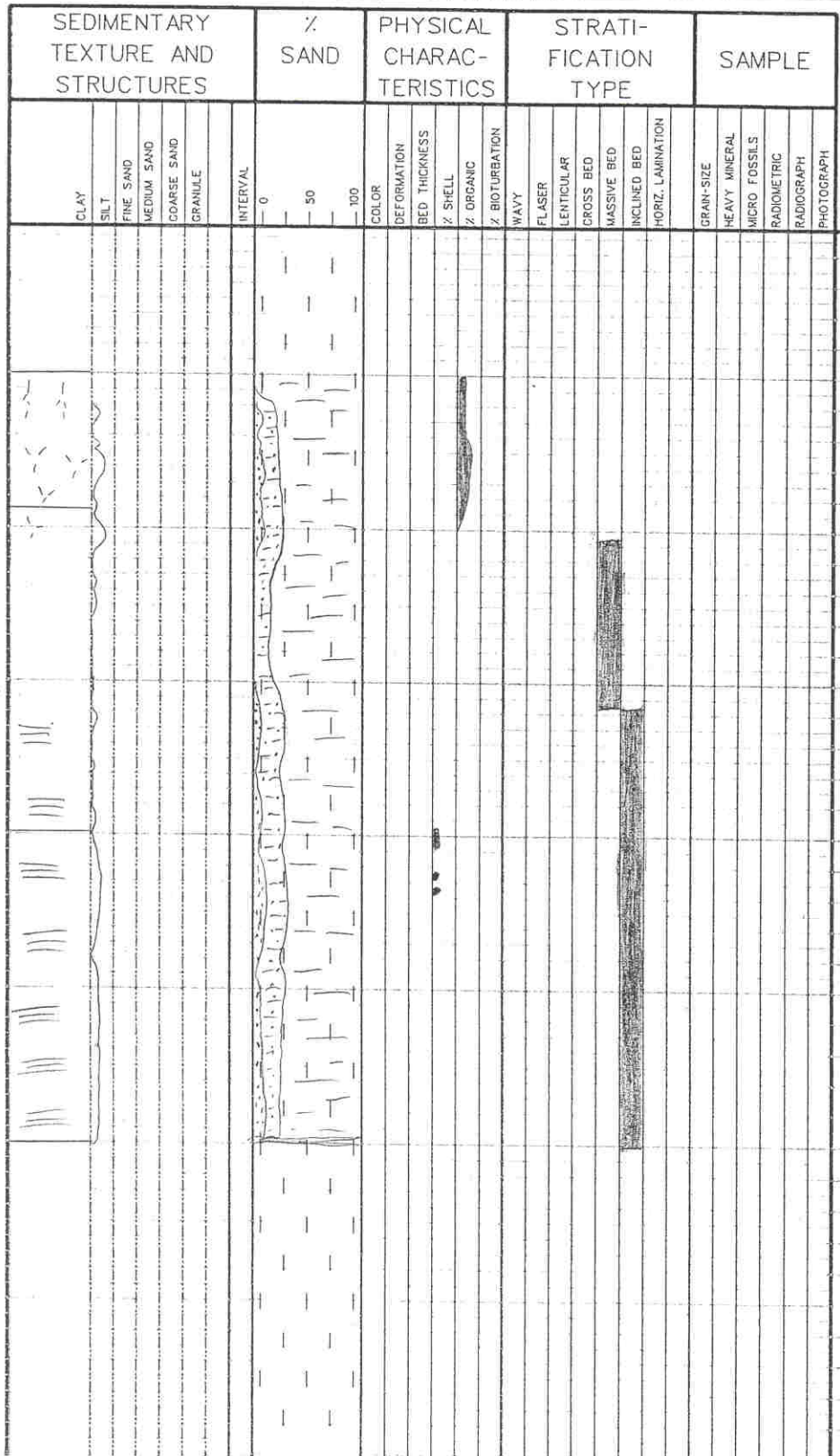

PHYSICAL DESCRIPTION

0-86 cm

0-31 cm, near marsh surface, clay with moderate in situ rooting, dusky yellowish brown (10YR 2/2) gradational contact,

31-86, unconsolidated organic matter with sparse in situ rooting, dusky brown (5Y 2/2), interbedded silty clay (35, 46-49 57-68, 81-83), gradational contact,

86-299

86-104, Silty clay, olive gray (5Y 5/2), trace organics, gradational contact,

104-299, clay, light olive gray (5Y 5/2), silt stringers (130, 153, 223, 251, 287, 289), yellow clay inclusions at 258 cm, red lamina (257, 267, 278), gradational contact

299-504

299-365, Sandy clay, olive gray (5Y 3/2), rare shell fragments (299-308, 323, 335), red laminations (336, 347, 349, 368-370, 374-379, 387).

365-504, Clay, light olive gray (5Y 3/2), horizontal laminations, silt stringers (371-373, 382, 387, 406, 412, 435, 484, 491).

UNIVERSITY OF NEW ORLEANS

DEPARTMENT OF GEOLOGY AND GEOPHYSICS

VIBRACORE DESCRIPTION SHEET

CORE ID: 03-CH-12 DATE: 11-13-03 DESCRIBED BY: liz

ELEVATION: _____ LOCATION: Caillou Bay Headland

CORE LENGTH: 2.45 m LAT/LONG: 725665, 3239154

TOTAL DEPTH: 3.36 m COMPACTION: .59m

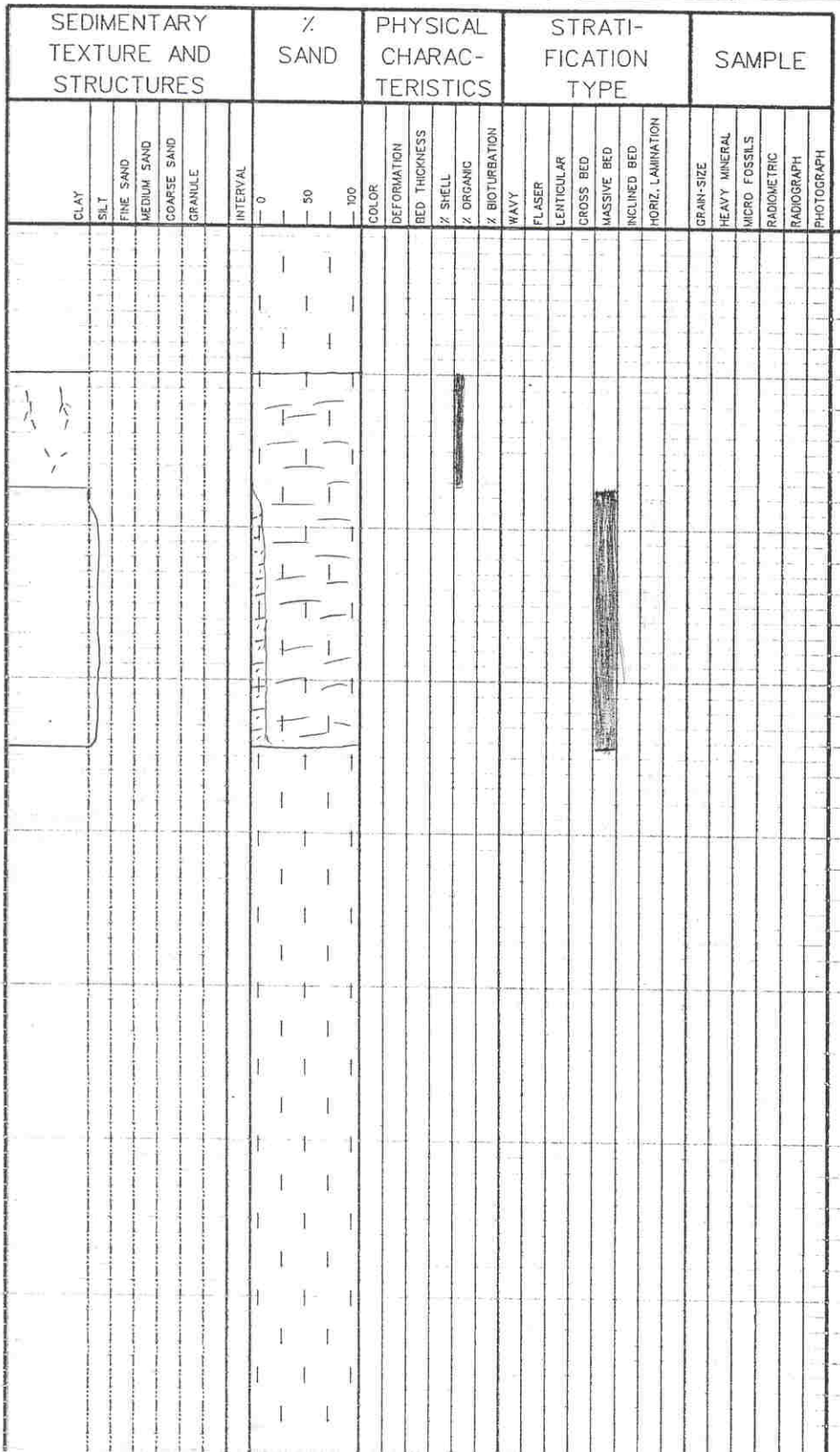

PHYSICAL DESCRIPTION

0-73cm
clay, brownish black (5YR 2/1), moderate in situ rooting and sparse unconsolidated organic matter, Gradational contact

73-245cm
clay, dark yellowish brown, (10YR 4/2), massively bedded.

UNIVERSITY OF NEW ORLEANS

DEPARTMENT OF GEOLOGY AND GEOPHYSICS

VIBRACORE DESCRIPTION SHEET

CORE ID: 03-C11-13 DATE: 11-13-03 DESCRIBED BY: Liz

ELEVATION: LOCATION: Caillou Bay Headland

CORE LENGTH: 2.45 m LAT/LONG: 730710, 3236763

TOTAL DEPTH: 2.74 m COMPACTION: 0.85 m

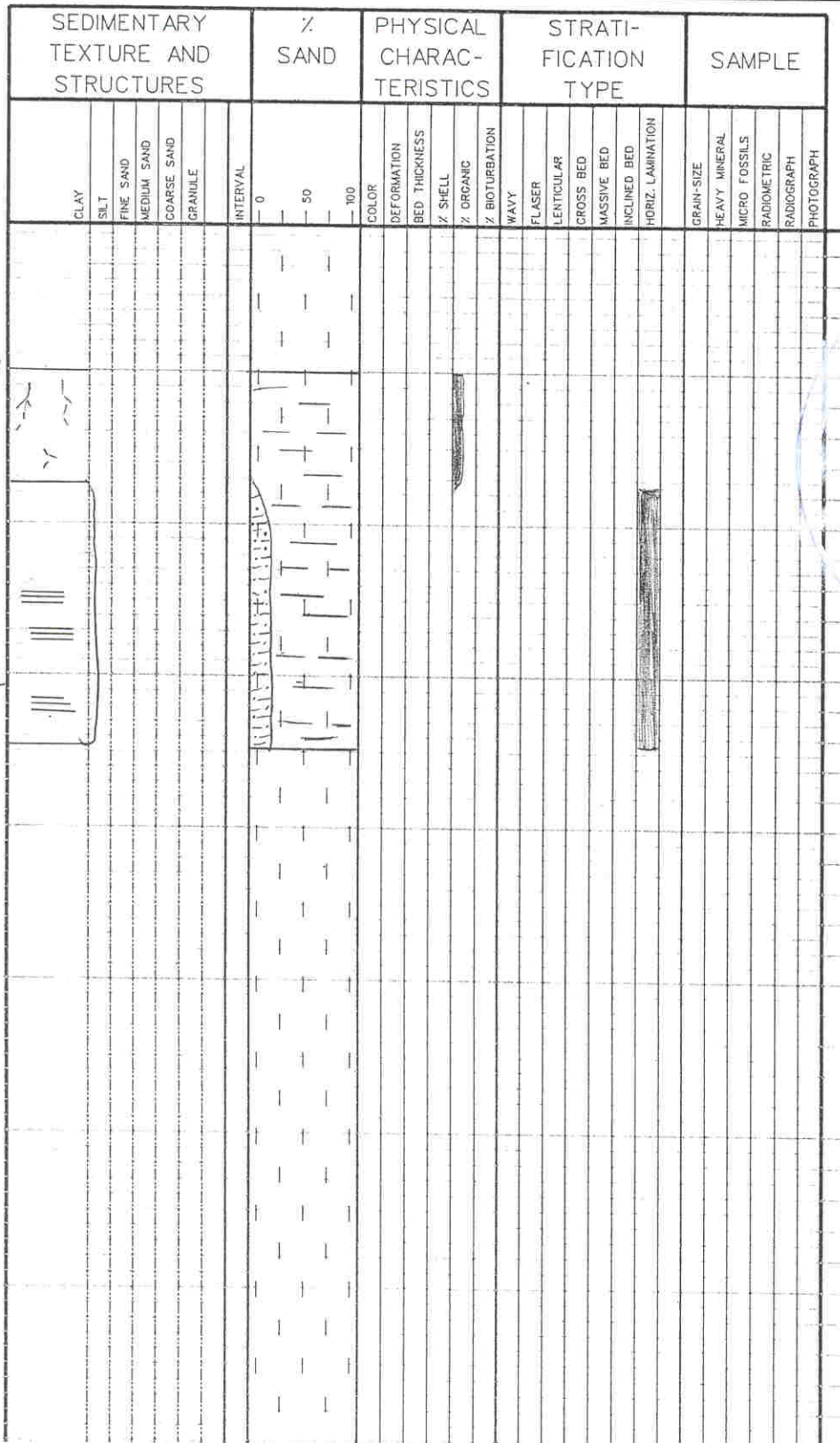

PHYSICAL DESCRIPTION

0-73 cm

clay, brownish-black (5YR 2/1), moderate in situ rooting and sparse unconsolidated organic matter, gradational contact;

73-245 cm

clay, dark yellowish brown (10YR 4/2), horizontal laminations.

UNIVERSITY OF NEW ORLEANS

DEPARTMENT OF GEOLOGY AND GEOPHYSICS

VIBRACORE DESCRIPTION SHEET

CORE ID: 035C02_01 DATE: 11-20-03 DESCRIBED BY: hiz

ELEVATION: _____ LOCATION: Caillou Bay, Headland

CORE LENGTH: 4.99 LAT/LONG: 729719, 3227800

TOTAL DEPTH: 7.42 COMPACTION: _____

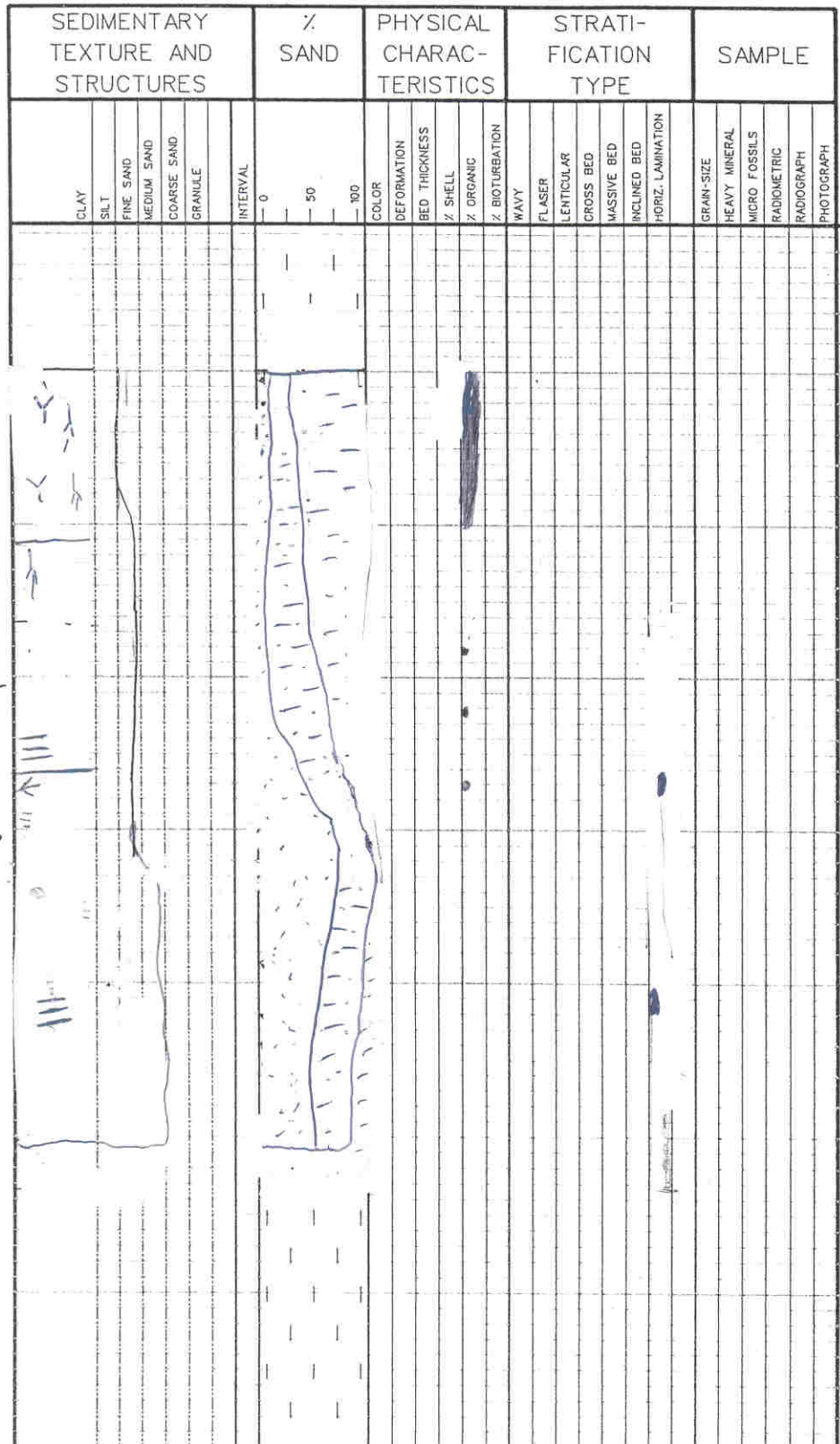

PHYSICAL DESCRIPTION

0 - 110

0-110cm, near marsh surface, organic material with sparse rooting, dusky yellow brown (10YR 2/2)

110 - 270 cm

clay, olive gray (5Y 5/2), trace organics and sparse in situ rooting, horizontal laminations at base of unit.

270 - 499

270-499 cm Sandy clay (olive gray (5Y 3/2), sparse organic fragments at top of unit, horizontal lamination near base of unit.

UNIVERSITY OF NEW ORLEANS

DEPARTMENT OF GEOLOGY AND GEOPHYSICS

VIBRACORE DESCRIPTION SHEET

CORE ID: 03SCC02-02 DATE: 11-15-03 DESCRIBED BY: liz

ELEVATION: _____ LOCATION: Caillou Bay Headland

CORE LENGTH: 5.20 LAT/LONG: 230485, 3225712

TOTAL DEPTH: 8.40 COMPACTION: _____

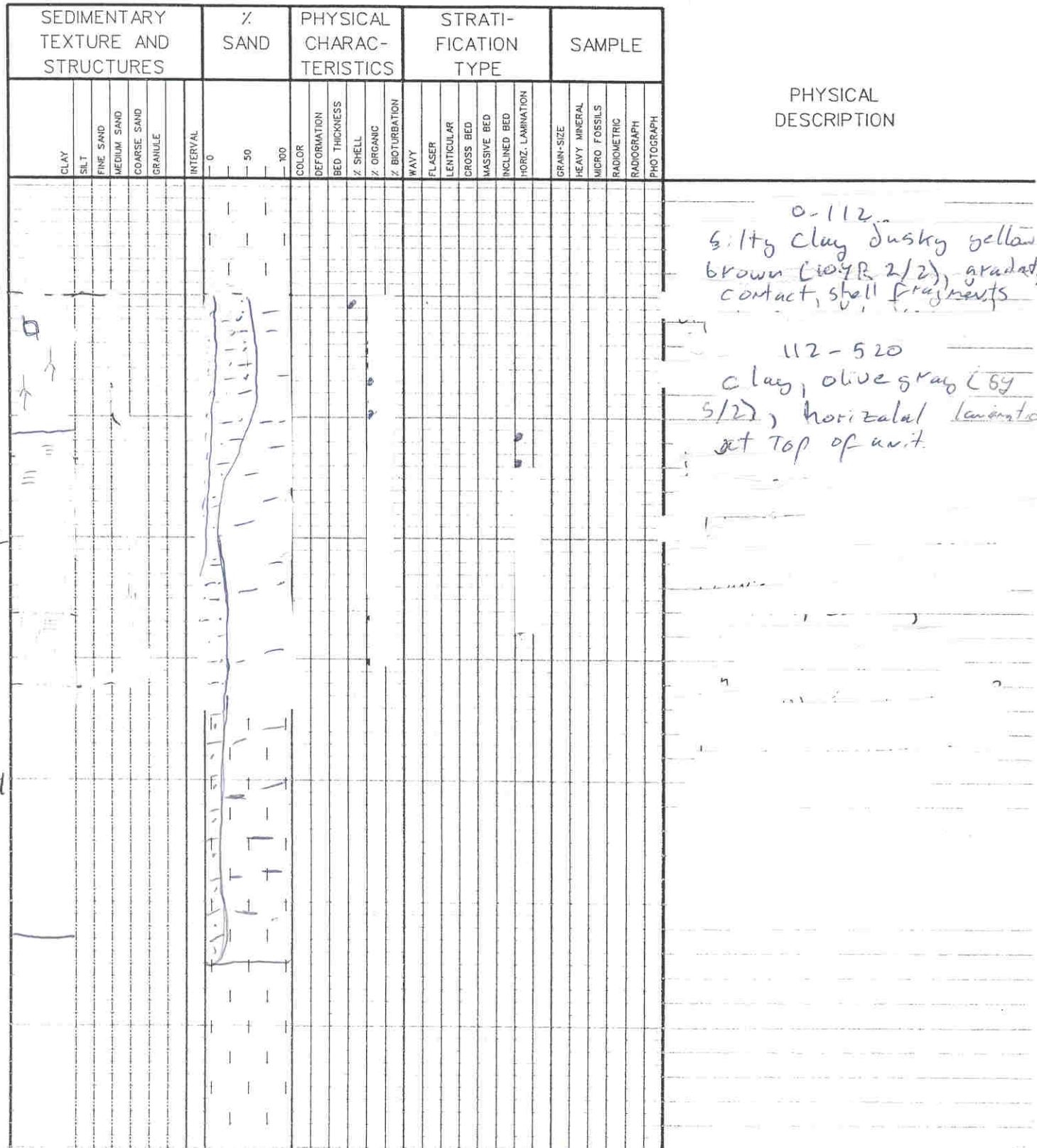

0-112

silty clay dusky yellow brown (10YR 2/2), gradational contact, shell fragments

112-520

clay, olive gray (5Y 5/2), horizalal lamination at top of unit

UNIVERSITY OF NEW ORLEANS

DEPARTMENT OF GEOLOGY AND GEOPHYSICS

VIBRACORE DESCRIPTION SHEET

CORE ID: 03SCC02-04 DATE: 10-20-03 DESCRIBED BY: Liz

ELEVATION: LOCATION: Caillou Bay Headland

CORE LENGTH: 5.25 LAT/LONG: 745248, 3227753

TOTAL DEPTH: 6.25 COMPACTION:

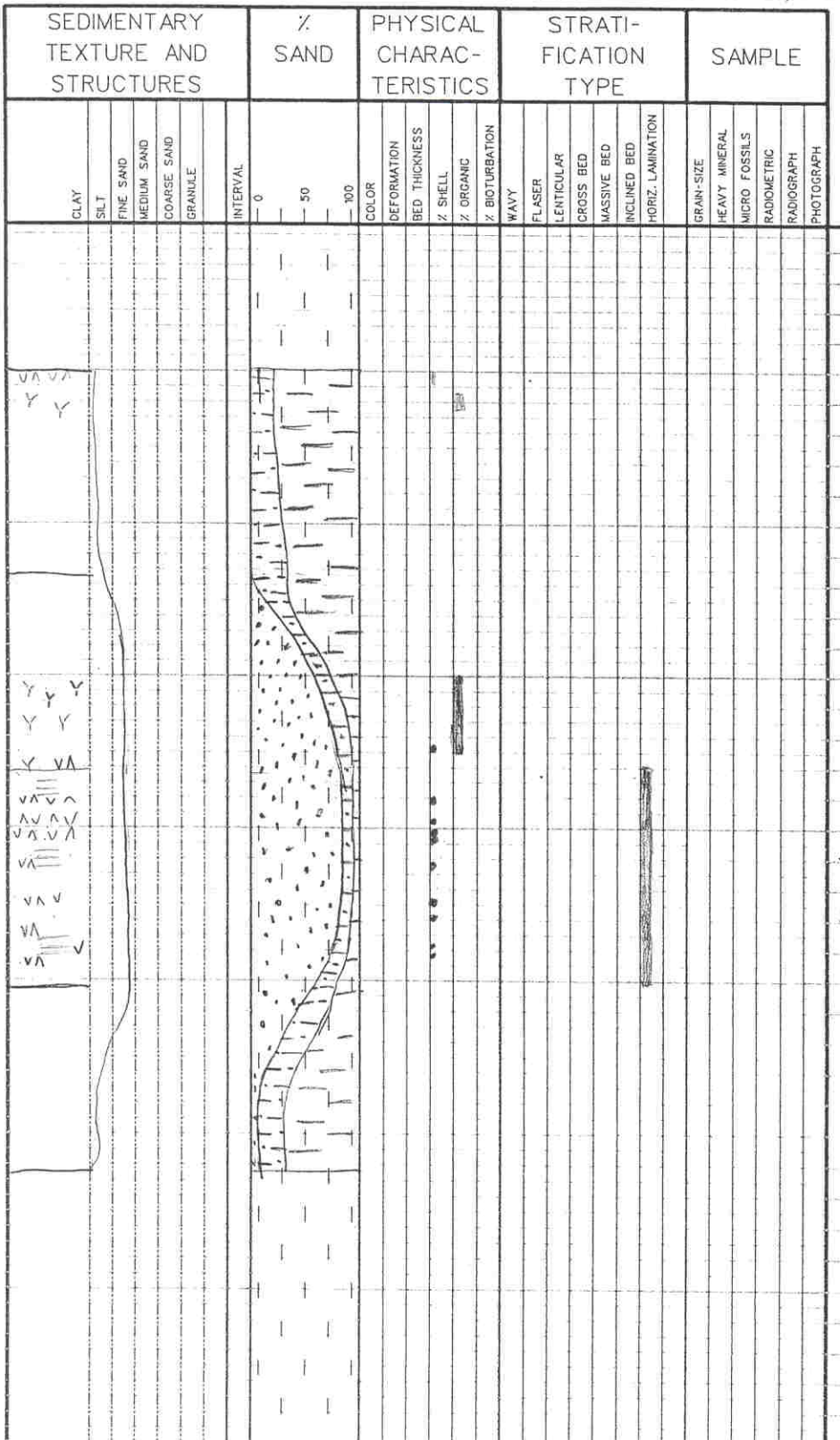

PHYSICAL DESCRIPTION

0-133cm

silty to sandy clay, dusky yellow brown (10YR 2/2), fine shell hash (0-7cm), fine organic material (15-29cm), gradational contact,

133-262cm

clayey sand, pale brown (5YR 5/2), clay layer (149-157cm), organic fragments (208, 212, 218, 219, 260cm), thin organic layer (237-239cm), shell fragment (261cm), gradational contact,

262-406cm

silty clay, dark yellowish brown (10YR 4/2), sand stringers (304-305, 354, 374-380, 400-405cm), shell hash stringers (281-282, 293, 300-302, 313, 327, 355, 366, 373, 384cm) gradational contact,

406-526cm

clay, dusky brown (5Y 2/2), sand inclusions (429, 485, 488, 500, 505, 516).

UNIVERSITY OF NEW ORLEANS

DEPARTMENT OF GEOLOGY AND GEOPHYSICS

VIBRACORE DESCRIPTION SHEET

CORE ID: 035CC02-05 DATE: 10-15-03 DESCRIBED BY: L. Z

ELEVATION: LOCATION: Caillou Bay Headland

CORE LENGTH: 5.20 m LAT/LONG: 738993, 3231267

TOTAL DEPTH: 6.50 m COMPACTION:

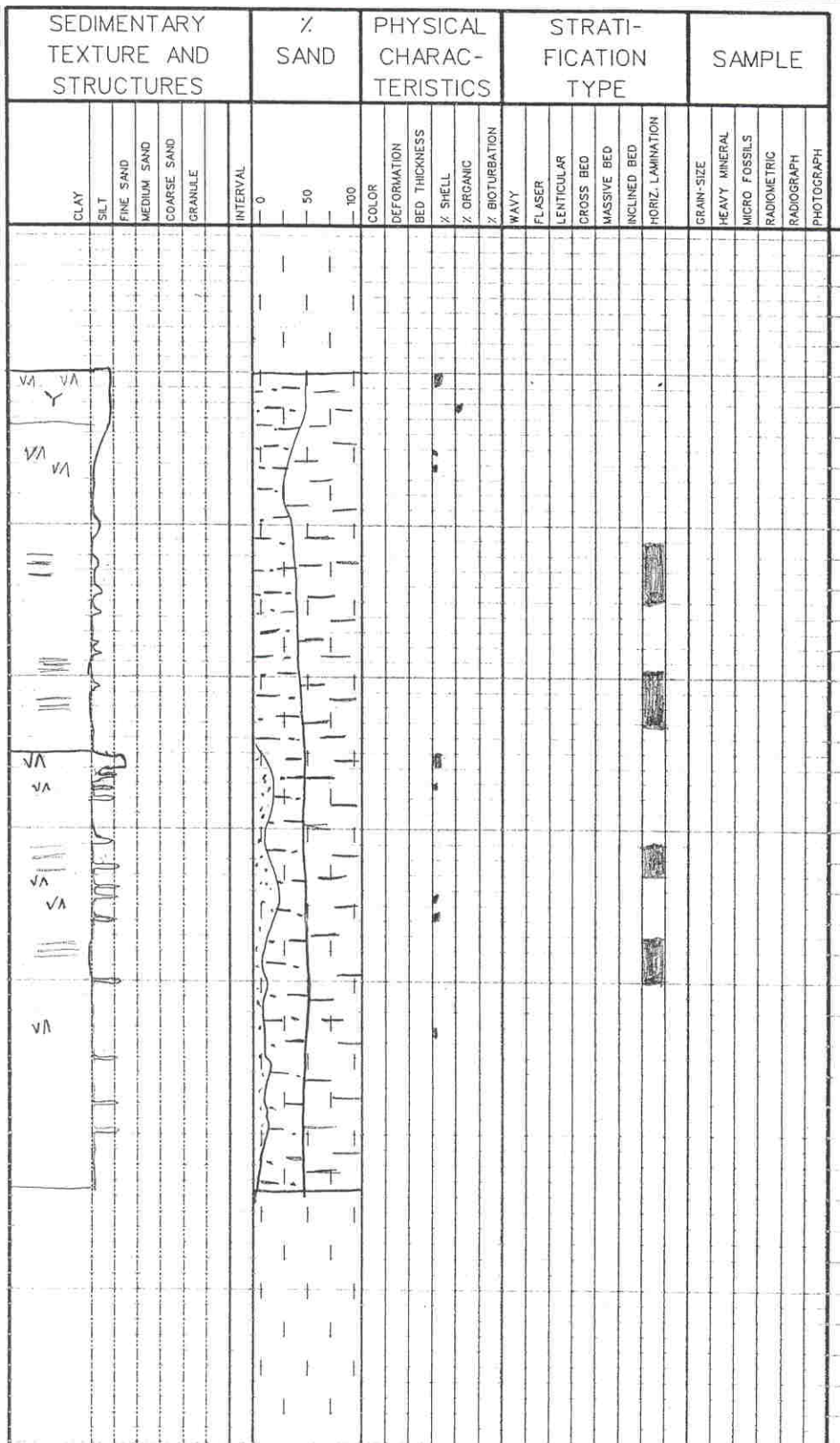

PHYSICAL DESCRIPTION

0-34cm
silty clay, dusky yellowish brown (10YR 2/2), fine shell hash (0-9cm), organic fragments (20-21cm), gradational contact,

34-250
clay, dark yellowish brown (10YR 4/2), pale brown clay lamina (64, 209, 242 cm), shell fragments (51, 60cm), silt lamina (94-96, 102-103, 122-123, 127-130, 140-143, 155-158, 178, 194, 186, 188, 190, 207cm) gradational contact,

250-534
clay, pale yellowish brown (10YR 6/2), fine shell hash (250-259cm), shell fragments (271, 344, 346, 357-359, 430 cm), sand layer (250-259, 264, 270-272, 281-283, 309-310, 324-326, 339, 345, 358-360, 400, 403, 451, 481, 497cm).

UNIVERSITY OF NEW ORLEANS

DEPARTMENT OF GEOLOGY AND GEOPHYSICS

VIBRACORE DESCRIPTION SHEET

CORE ID: 035CC02-06 DATE: 11-15-03 DESCRIBED BY: Liz

ELEVATION: LOCATION: Caillou Bay Headland

CORE LENGTH: 4.30 LAT/LONG: 734885, 3237 55

TOTAL DEPTH: 6.10 COMPACTION:

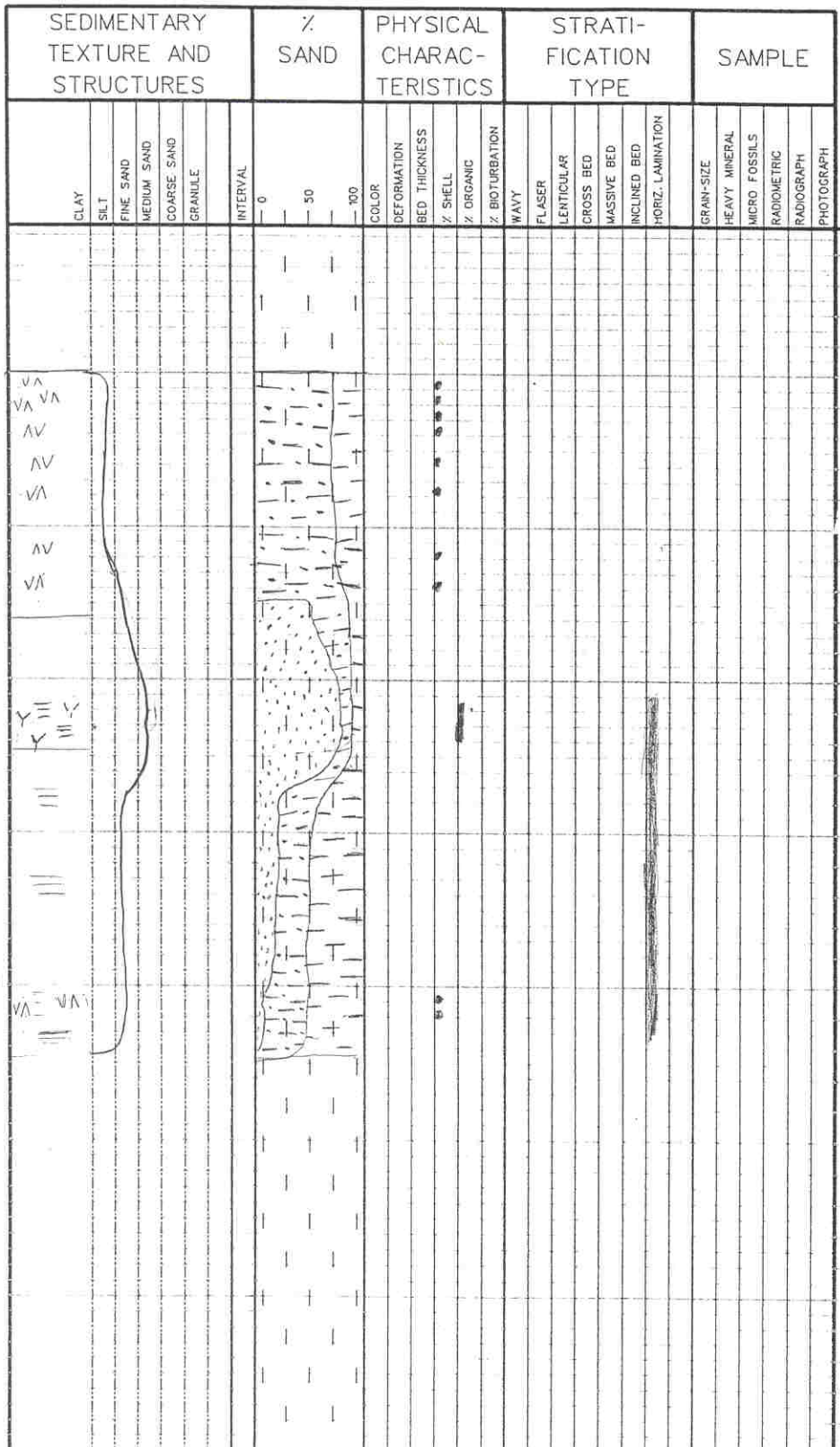

PHYSICAL DESCRIPTION

0-160 cm

silty clay, dusky yellowish brown (10YR 2/2) fine shell fragments (8-29 cm, 40-43, 60, 89, 117, 146-154 cm), sharp contact,

160 - 244 cm

Clayey Sand, light olive gray (5Y 6/1), sand fines upwards, thin interbedded clay lamina (209-239 cm), organic fragments (223, 225 cm), organic "coffee grain" layer (240 - 244 cm), Gradational contact,

244 - 446

Clay, Pale yellowish brown (10 YR 6/2), sand lamina (310 - 321, 327, 332 - 340, 382 - 385, 415 - 420 cm), silt lamina (241 - 250, 260 - 262, 277, 293 - 297, 360, 365 - 370, 376, 380, 430, 432 cm) Fine shell fragments (412, 414 cm).

UNIVERSITY OF NEW ORLEANS

DEPARTMENT OF GEOLOGY AND GEOPHYSICS

VIBRACORE DESCRIPTION SHEET

CORE ID: 035CC02-07 DATE: 10-30-03 DESCRIBED BY: Liz

ELEVATION: LOCATION: Caillou Bay Headland

CORE LENGTH: 5.15 LAT/LONG: 707092, 3219631

TOTAL DEPTH: 7.60 COMPACTION:

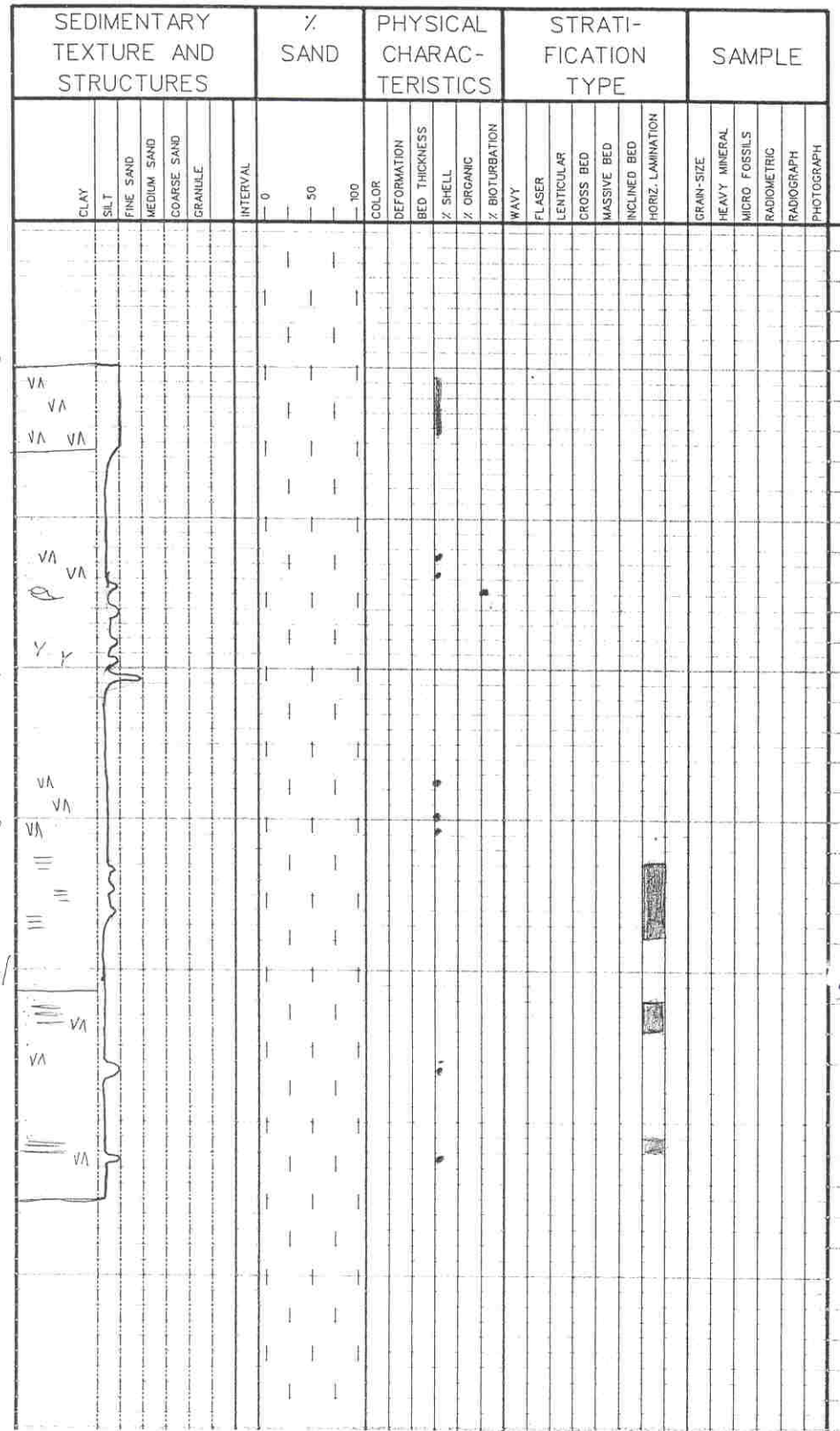

PHYSICAL DESCRIPTION

0-56

silt, dusky yellowish brown (10YR 2/2), fine shell hash (6-42cm), gradational contact,

56-415

clay, dark yellowish brown (10YR 4/2), horizontal laminations (320-380cm), burrow (151 cm), organic fragments (187, 190-192cm), shell fragments (125, 137, 275, 295, 308cm), red clay lamina (276-278, 295-299, 324, 339, 354 cm), silt lamina (140-144, 160-166, 182-185, 192, 334, 340-343, 362 cm), silt stringers (208-265, 294-308, 359, 366, 369, 373, 376, 389, 394-397, 402, 405cm), Sand layer (204-208cm), gradational contact

415-451

Sandy clay dark yellowish brown (10YR 4/2), clam shell (429 cm), shell hash (466-471, 522-525 cm) silt stringers (415-460 cm), Sand lamina (466-471, 504-505, 522-525cm).

UNIVERSITY OF NEW ORLEANS

DEPARTMENT OF GEOLOGY AND GEOPHYSICS

VIBRACORE DESCRIPTION SHEET

CORE ID: 03SCC02-08 DATE: 11-15-03 DESCRIBED BY: Liz

ELEVATION: LOCATION: Caillou Bay Headland

CORE LENGTH: 5.12 LAT/LONG: 706957, 3217772

TOTAL DEPTH: 6.45 COMPACTION:

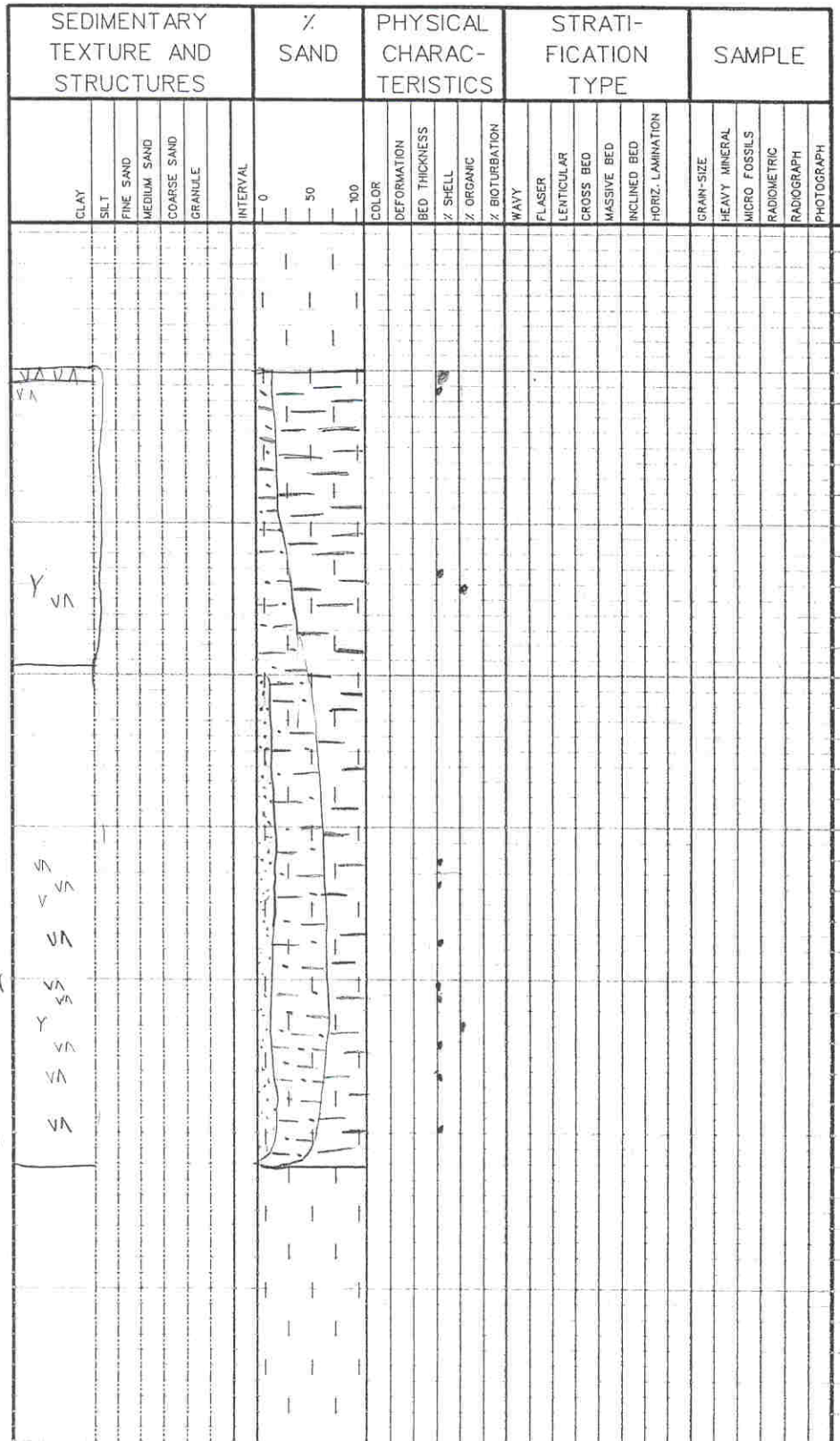

PHYSICAL DESCRIPTION

0-8cm

Clayey Sand, dark yellowish brown (10YR 4/2), extremely fine shell hash throughout, gradational contact,

8-196cm

Clay, dark yellowish brown (10YR 4/2), silt stringers (148-175cm), shell hash (10-19, 140-142cm), clam shell (57cm), woodlike organic material (133-135cm), gradational contact,

196-520cm

Sandy clay dark yellowish brown (10YR 4/2), sand stringers (196-211, 227-236, 250-254, 273-279, 317-341, 361-365, 439-445cm), shell fragments (328, 339-341, 357, 375, 407-408, 412-413, 441-446, 463, 498-501cm), woodlike organic material (433cm)

UNIVERSITY OF NEW ORLEANS

DEPARTMENT OF GEOLOGY AND GEOPHYSICS

VIBRACORE DESCRIPTION SHEET

CORE ID: 035CC02-10 DATE: 10-22-03 DESCRIBED BY: Liz

ELEVATION: LOCATION: Caillou Bay Headland

CORE LENGTH: 4.70 LAT/LONG: 691380, 3229115

TOTAL DEPTH: 6.52 COMPACTION:

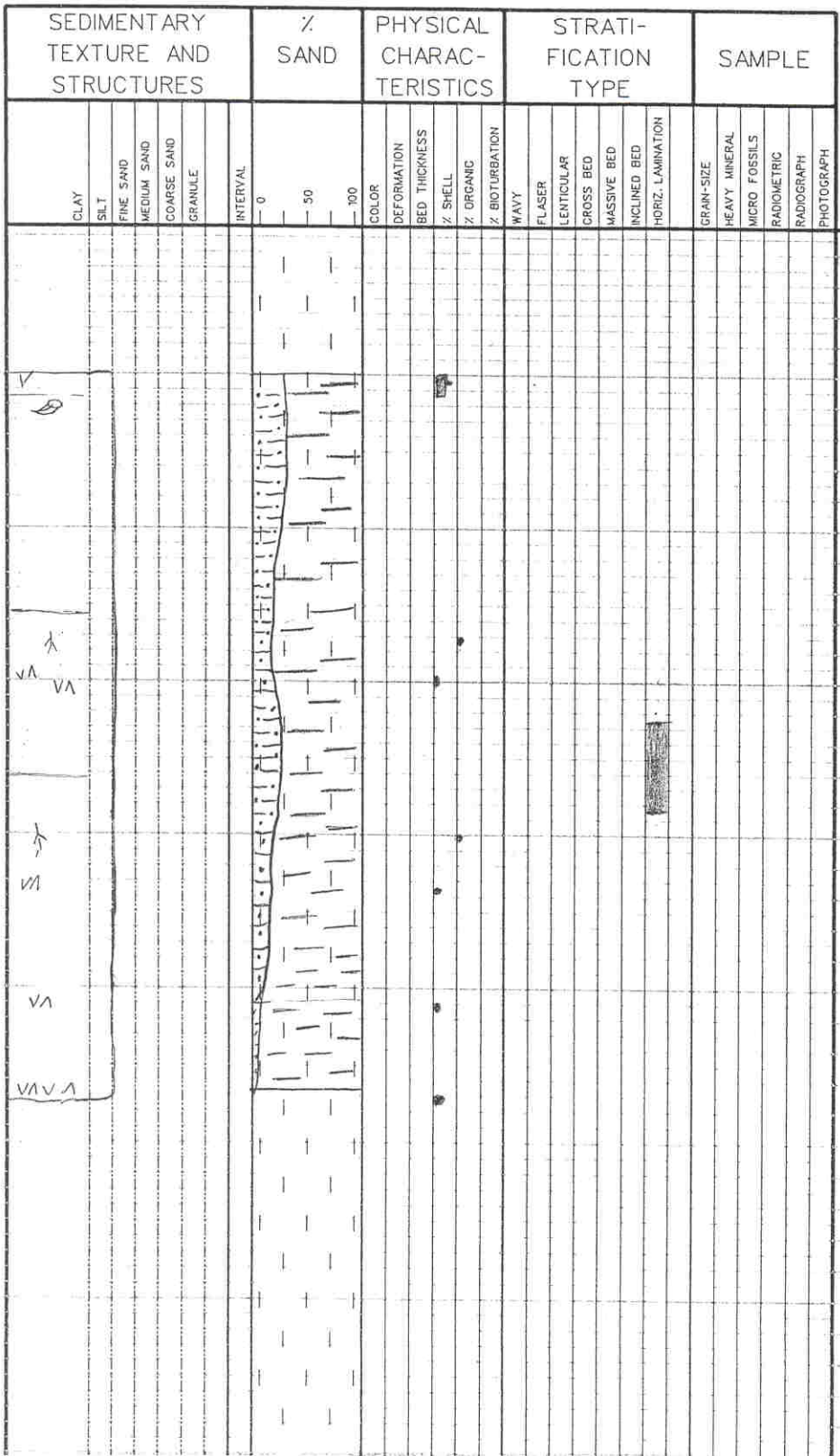

PHYSICAL DESCRIPTION

0-13 cm

Silt, olive gray (5Y 3/2), fine shell hash throughout unit, clam shell (3 cm), sharp contact,

13-114 cm

Silty clay, light olive gray (5Y 5/2), red clay lamina (57, 107 cm), burrow (18-24 cm) infilled w/ silty clay & shell hash, silty lamina (52-57, 78-81, 94-96, 111-113), gradational contact,

114-223 cm

clay, light olive gray (5Y 5/2), red clay lamina (117 cm), shell hash (199, 200-202 cm), rooting (173 cm), gradational contact,

223-472 cm

223-282 cm, Silty clay, Moderate Brown (5YR 4/4), horizontally laminated, interbedded silt & clay laminae, gradational contact,

282-472, clay, light olive gray (5YR 5/2), rooting (300 cm), silt stringers (282, 313, 318, 325, 333-336, 340-342, 349-350), sand stringers (351-358, 371, 376, 390, 406 cm), shell hash (336, 412, 470-472 cm), oyster shell (418 cm).

UNIVERSITY OF NEW ORLEANS

DEPARTMENT OF GEOLOGY AND GEOPHYSICS

VIBRACORE DESCRIPTION SHEET

CORE ID: 03SCC02-11 DATE: 11-22-03 DESCRIBED BY: L. Z

ELEVATION: LOCATION: Gaillou Bay Headland

CORE LENGTH: 3.98 LAT/LONG: 686467, 3227995

TOTAL DEPTH: 4.77 COMPACTION:

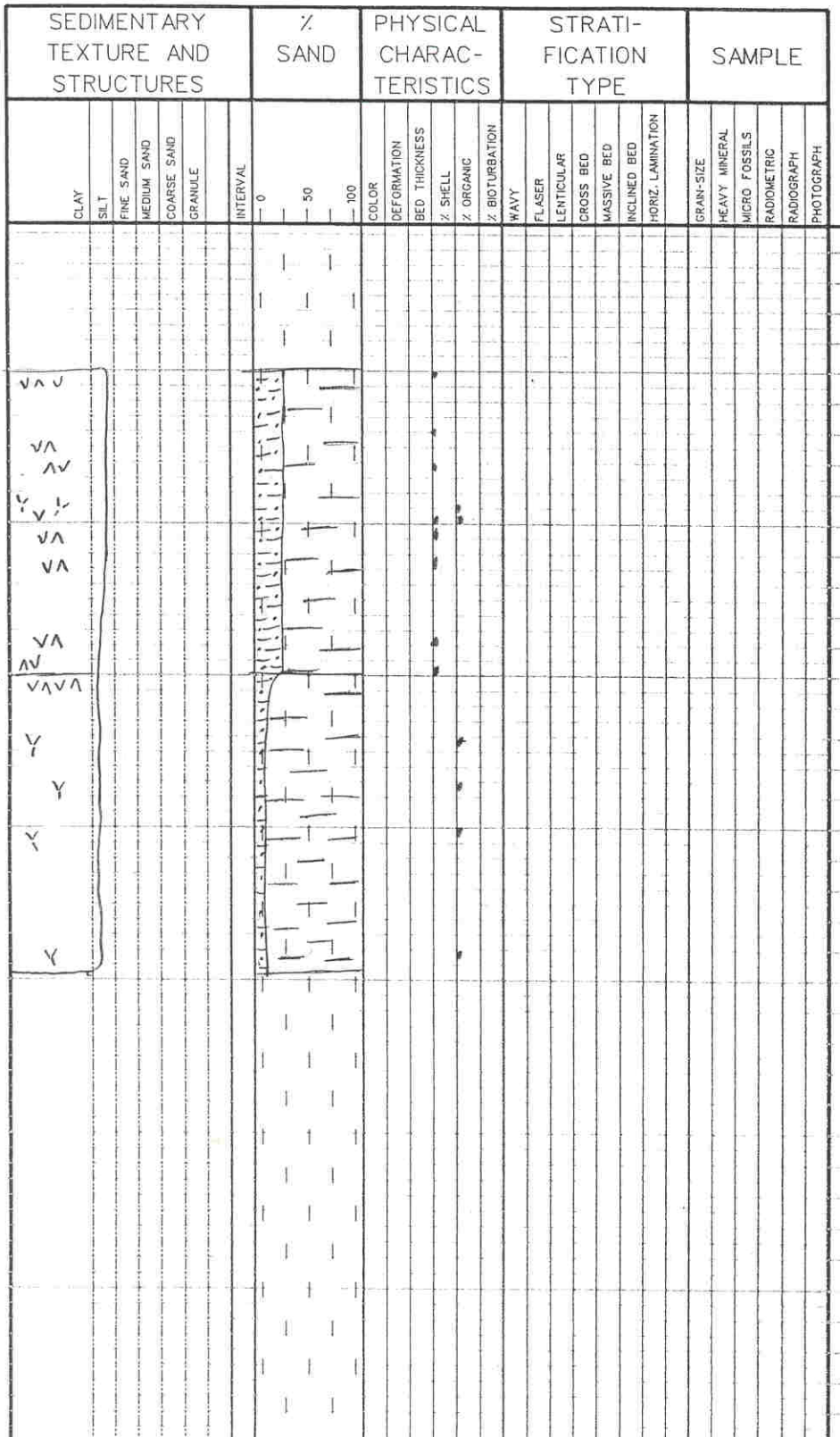

PHYSICAL DESCRIPTION

0-200cm

silty clay, dusky brown (5YR 2/2) silty lamina (19, 41-44, 48-52, 106-108, 140, 182 cm), organic fragments (84-86 cm), shell hash (0-9, 52, 60-63, 106, 130-133, 175-177, 189-192 cm), Broken oyster shell (98 cm), gradational contact

200-395 cm

clay, dusky brown (5Y 2/2), shell hash (200-207 cm), Organic fragments (246, 277, 304, 389 cm).

UNIVERSITY OF NEW ORLEANS

DEPARTMENT OF GEOLOGY AND GEOPHYSICS

VIBRACORE DESCRIPTION SHEET

CORE ID: SCC02-12 DATE: 11-12-03 DESCRIBED BY: Liz

ELEVATION: ____ LOCATION: Caillou Bay Headland

CORE LENGTH: 4.01 LAT/LONG: 721954, 3222773

TOTAL DEPTH: 6.01 COMPACTION: ____

SEDIMENTARY TEXTURE AND STRUCTURES	% SAND	PHYSICAL CHARAC-TERISTICS	STRATI-FICATION TYPE	SAMPLE	PHYSICAL DESCRIPTION
CLAY, SILT, FINE SAND, MEDIUM SAND, COARSE SAND, GRANULE, INTERVAL	0 — 50 — 100	COLOR, DEFORMATION, BED THICKNESS, % SHELL, % ORGANIC, % BIOTURBATION	WAVY, FLASER, LENTICULAR, CROSS BED, MASSIVE BED, INCLINED BED, HORIZ. LAMINATION	GRAIN-SIZE, HEAVY MINERAL, MICRO FOSSILS, RADIOMETRIC, RADIOGRAPH, PHOTOGRAPH	

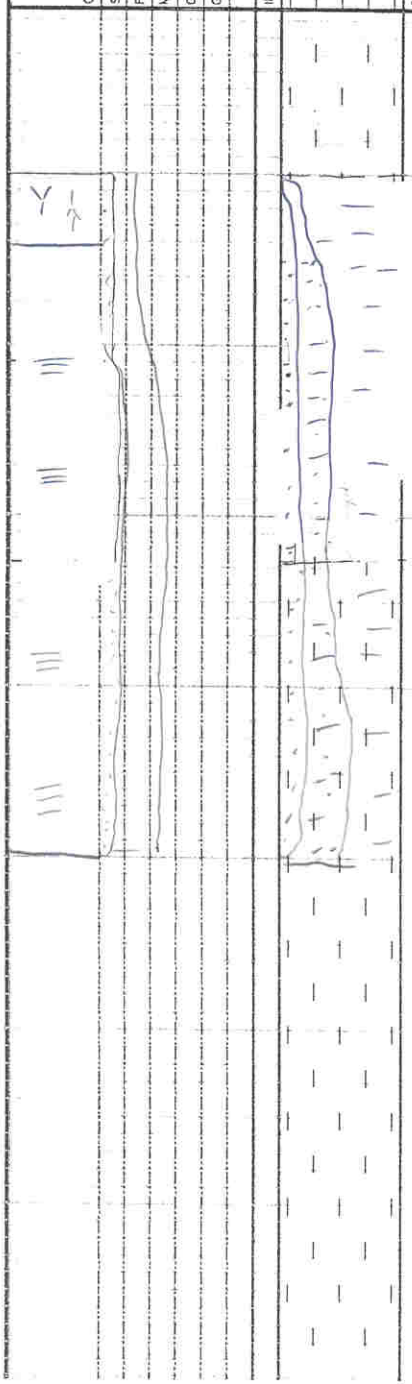

0 - 49cm

0-49cm, Near marsh surface, clay with organics an root fragments, olive gray (5Y 5/2)

49cm - 401

49-401cm silty clay olive gray (5Y 5/2), shell fragments with horizontal laminations throughout.

VITA

Elizabeth M. Petro was born in Philadelphia, Pennsylvania on January 10, 1980. She graduated from Norristown Area High School in 1998. Following high school she attended LaSalle University and graduated cum laude in December of 2002 with a dual major in Geology and Environmental Science. Upon graduation from the University of New Orleans she will be beginning her career at ChevronTexaco in New Orleans.